Metabolic Studies on *Schizosaccharomyces pombe* for improved Protein Secretion

Dissertation

zur Erlangung des Grades

des Doktors der Naturwissenschaften

der Naturwissenschaftlich-Technischen Fakultät III

Chemie, Pharmazie, Bio- und Werkstoffwissenschaften

der Universität des Saarlandes

von

Tobias Klein

Saarbrücken, August 2013

"It's not worth doing something unless someone, somewhere, would much rather you weren't doing it."

- Terry Pratchett

"Reality continues to ruin my life."

- Calvin & Hobbs

„Es gibt nichts Gutes, außer man tut es."

- Erich Kästner

Danksagung

Bei meinen Freunden und meiner Familie möchte ich mich ebenfalls für ihre Unterstützung bedanken:

Bei meinen Mitbewohnern und Freunden bedanke ich mich für die schöne Zeit, die wir zusammen hatten und die höchst notwendige Ablenkung am Wochenende, was mich stets gestärkt und munter in die neue Woche starten ließ.

Ein großer Dank gebührt auch meiner Familie, meinen Eltern Hans-Joachim und Renate Klein und meinem Bruder Martin. Ohne ihre unbedingte und immerwährende Unterstützung, Hilfe und ab und an auch mal Geduld und Nachsicht wäre ich heute sicherlich nicht da, wo ich bin.

Meiner Freundin Moni möchte ich dafür danken, dass sie während dieser Zeit immer für mich da war, mir zugehört hat, wenn es wichtig war und mich auf den Boden zurückgeholt hat, wenn es nötig war. Ich glaube nicht, dass ich das alles ohne dich und das Vertrauen und den Rückhalt den Du mir gibst geschafft hätte.

Table of contents

List of abbreviations

The following abbreviations are used throughout this thesis. In addition, amino acids are referred to by their common 3 letter codes.

Metabolites

3-PG	3-phosphoglycerate
Ac	acetate
ATP	adenosine triphosphate
DHAP	dihydroxyacetonephosphate
Fru	fructose
GAP	glyceraldehyde-3-phosphate
Glc	glucose
Glt	gluconate
Gly	glycerol
NAD+/NADH	nicotinamide adenine dinucleotide (ox/red)
NADP+/NADPH	nicotinamide adenine dinucleotide phosphate (ox/red
OAA	oxaloacetate
OMP	orotidine-5-phosphate
PEP	phosphoenolpyruvate

Enzymes and pathways

AADH	acetaldehyde dehydrogenase
ADH	alcohol dehydrogenase
FBPase	fructose-1,6-bisphosphatase
G6PDH	glucose-6-phosphate dehydrogenase
GlyDH	glycerol dehydrogenase
PDC	pyruvate decarboxylase
PFK	phosphofructokinase
PPP	pentose phosphate pathway
PYC	pyruvate carboxylase
TCA cycle	Tricarboxylic acid cycle

Rates and units

CDW	cell dry weight [$g\ L^{-1}$]
CPR	carbon dioxide production rate [$mmol\ L^{-1}\ h^{-1}$]
$k_L a$	oxygen transfer rate [h^{-1}]
OD	optical density
OUR	oxygen uptake rate [$mmol\ L^{-1}\ h^{-1}$]
q_{Ac}	specific acetate uptake rate [$mmol\ g\ CDW^{-1}\ h^{-1}$]
q_{CO2}	specific carbon dioxide uptake rate [$mmol\ g\ CDW^{-1}\ h^{-1}$]
q_{Glc}	specific glucose uptake rate [$mmol\ g\ CDW^{-1}\ h^{-1}$]
q_{Gly}	specific glycerol uptake rate [$mmol\ g\ CDW^{-1}\ h^{-1}$]
q_{O2}	specific oxygen uptake rate [$mmol\ g\ CDW^{-1}\ h^{-1}$]
q_s	specific substrate uptake rate [$mmol\ g\ CDW^{-1}\ h^{-1}$]
$Y_{X/S}$	biomass yield [$g\ CDW\ mol\ substrate^{-1}$]

Others

AMM	atom mapping matrix
Amp	ampicilin
CB4-1-scFv-GFP	GFP-coupled single chain antibody fragment
DO	dissolved oxygen
GC	gas chromatography
GFP	green fluorescent protein
HPLC	high performance liquid chromatography
LEU1	gene coding isopropyl maltase isomerase from *S. cerevisiae*
IMM	isotopomer mapping matrix
MDV	mass distribution vector
MFA	metabolic flux analysis
MS	mass spectrometry
nat	nourseothricin acetyltransferase
natMX	*nat* gene flanked by TEF promoter and TEF terminator
NCYC	National Collection of Yeast Cultures
nmt1	*"no message from thiamine"* gene
ura4	gene coding OMP decarboxylase gene from *S. pombe*

Abstract

The fission yeast *Schizosaccharomyces pombe* is an attractive host for heterologous protein secretion but currently still too little developed to compete against industrial cell factories like *Pichia pastoris* and *Saccharomyces cerevisiae*. Thus, the present work aimed at increasing the understanding of the metabolism of *S. pombe* and the metabolic burden associated with protein secretion in order to derive metabolic engineering strategies for improving recombinant protein production.

In the first part a system of small-scale parallel bioreactors was constructed to perform studies in continuous culture. This system was used for quantitative metabolic analyses applying ^{13}C-based metabolic flux analysis to *S. pombe* grown on mixtures of glycerol and acetate compared to respiratory growth on glucose as sole carbon source. Next the metabolic burden of protein secretion was investigated, using strains secreting the model protein maltase in varying amounts up to 27 mg per g cells. Quantitative analysis of the metabolic fluxes and the macromolecular cell composition revealed that lipid biosynthesis, TCA cycle and supply of mitochondrial NADPH as bottlenecks in protein secretion. From these data, a feeding strategy was derived for supplementing the media with acetate and glycerol, which enabled the cells to overcome these limitations. The results were transferred to heterologous secretion of GFP and a single-chain antibody fragment, increasing yields 2-fold and 4-fold, respectively.

Zusammenfassung

Die Spalthefe *Schizosaccharomyces pombe* stellt ein attraktives System zur heterologen Proteinsekretion dar, kann derzeit aber noch nicht mit Zellfabriken wie *Pichia pastoris und Saccharomyces cerevisiae* konkurrieren. Diese Arbeit sollte daher das Verständnis des Metabolismus von *S. pombe* und dessen Belastung durch Sekretion von Proteinen vergrößern, um Strategien für das *Metabolic Engineering* abzuleiten, welche die rekombinanten Proteinproduktion verbessern.

Zunächst wurde ein System paralleler Bioreaktoren aufgebaut, um Studien in kontinuierlicher Kultur durchzuführen. In diesem System wurden quantitative metabolische Analysen an *S. pombe* mittels ^{13}C basierter metabolischer Flussanalyse auf Gemischen aus Glycerin und Acetat durchgeführt und mit dem respirativen Wachstum auf Glucose verglichen. Weiter wurde die Belastung des Metabolismus durch Sekretion des Modellproteins Maltase untersucht. Eine quantitative Analyse der metabolischen Flüsse und der makromolekularen Zellzusammensetzung zeigte, dass die Lipid-Biosynthese, der Citratzyklus und die Bereitstellung von mitochondriellem NADPH Engpässe in der Proteinsekretion darstellen. Hieraus wurden Fütterungsstrategien abgeleitet und das Medium mit Acetat und Glycerin supplementiert, wodurch diese Limitierungen überwunden werden konnten. Diese Strategien wurden auf die heterologe Sekretion von GFP und einem Antikörper-Fragment übertragen, wodurch deren Ausbeuten um das 2-fache und 4-fache gesteigert werden konnten.

CHAPTER I

General Introduction and Theoretical Background

1 Yeasts in Biotechnology

The application of yeasts in biotechnological processes reaches back for thousands of years when these microorganisms were first used for baking bread and fermentation of beverages. It comes as no surprise that also nowadays yeasts are among the most widely used microorganisms in biotechnology.

1.1 Production of metabolites with yeasts

The advent of recombinant DNA technology and the subsequent sequencing campaigns allowed extensive genetic manipulations of yeasts, broadening the spectrum of applications for the production of metabolites in these organisms. The product spectrum ranges from bulk chemicals, foremost bioethanol and other biofuels produced with *Saccharomyces cerevisiae* (Rude and Schirmer 2009)*,* to organic acids as well as plant and fungal secondary metabolites derived from the sterol and terpenoid metabolism (Kim et al. 2012). The produced metabolites find their application as food additives and flavors, as pharmaceutical precursors or in the production of bioplastics (Kim et al. 2012; Porro et al. 2011).

1.2 Recombinant protein production in yeasts

Apart from small molecules, yeasts are extensively used for the production of recombinant proteins. The majority of these proteins are secreted into the media, since secretion of recombinant proteins is an efficient means to facilitate downstream processing and thus to significantly reduce the associated costs. The production of recombinant human insulin in *S. cerevisiae* by Novo Nordisk A/S is one of the most prominent examples. Up till now, more than 20 % of all recombinant proteins on the market are produced with *S. cerevisiae* (Ferrer-Miralles et al. 2009). Over the last two decades other yeast expression systems have emerged, with *Hansenula polymorpha* and *Kluyveromyces lactis* as well-known examples and with *Pichia pastoris* as the leading competitor to *S. cerevisiae* (Damasceno et al. 2012; Mattanovich et al. 2012). The methylotrophic yeast can be cultivated to high cell densities up to 200 g L^{-1} allowing product titers up to 20 g/L (Heyland et al. 2010; Morrow 2007). Until recently the *P. pastoris* expression system was patented through Research Cooperation Technologies making it expensive and difficult for academia and small enterprises to work with this system (Celik and

Calik 2011). With the expiration of this patent and the genome sequencing project with publicly available genome browsers (Mattanovich et al. 2009) application and engineering of this expression system has strongly picked up speed. In 2009 the first therapeutic polypeptide, ecallantide, produced with *P. pastoris* was successfully introduced to the market.

One of the major aspects that must be considered when choosing an expression host is its ability to perform post-translational modifications. Glycosylation is the most abundant modification of secreted proteins, influencing folding, stability and *in vivo* activity of the product (Mariño et al. 2010). Proteins produced in *S. cerevisiae* may carry a strong hyperglycosylation, which can cause misfolding and a reduced secretion rates (Celik and Calik 2011). Moreover, the high content of mannosyl residues which are highly immunogenic can be a major drawback in the production of therapeutic proteins. One way to circumvent this problem is the use of glyco-engineered yeasts. Here, *P. pastoris* is the most famous example, where designer strains are available producing proteins with completely humanized glycosylation patterns (Bretthauer 2003; Hamilton and Gerngross 2007).

Another way is the utilization of yeasts that produce more mammalian-like glycosylation patterns. The fission yeast *Schizosaccharomyces pombe* shares several important properties with higher eukaryotes such as regulation of cell cycle, chromosomal organization and regulation of transcription and translation. Glycoslyation patterns as well as quality control and folding of glycoproteins is considered closer to mammalian cells than in other yeast species (Parodi 1999). Due to its resemblance to higher eukaryotes, *S. pombe* has been a well-known model organism for molecular and cell biology for decades. However, various examples can be found in literature also describing the application of *S. pombe* for the heterologous production of proteins, especially for the production of mammalian proteins. Whole cells approaches using recombinant *S. pombe* for biotransformations, e.g. for steroid production using human cytochrom P_{450} enzymes (Drăgan et al. 2005; Neunzig et al. 2012) have been reported. But also the secretion of the protein of interest into the culture supernatant has been the topic of several studies. The production of human transferring and human growth hormone has been reported from Ashai Glass Company (Idiris et al. 2006a; Mukaiyama et al. 2009b) and recently the heterologous secretion of a single-chain antibody fragment up to 5 mg/L using *S. pombe* has been demonstrated (Naumann et al. 2010). Nonetheless, the *S. pombe* expression system is currently still too little developed in terms of both molecular engineering and process design to find its way into the industrial application but with further optimization of strains and production processes this organism may emerge as a serious competitor to cell factories like *S. cerevisiae* and *P. pastoris*.

2 The fission yeast *Schizosaccharomyces pombe*

2.1 History of *Schizosaccharomyces pombe*

The fission yeast *Schizosaccharomyces pombe* is a unicellular eukaryote belonging to the kingdom of fungi to the phylum ascomycota. It has been isolated from African millet beer in 1893 but most laboratory strains go back to an isolate of French grape juice from A. Osterwalder in 1921. These isolates were first characterized by Leupold et al. in the late 1940s, yielding the wild type strains 975 h$^+$ and 972 h$^-$ (Hall 1993).
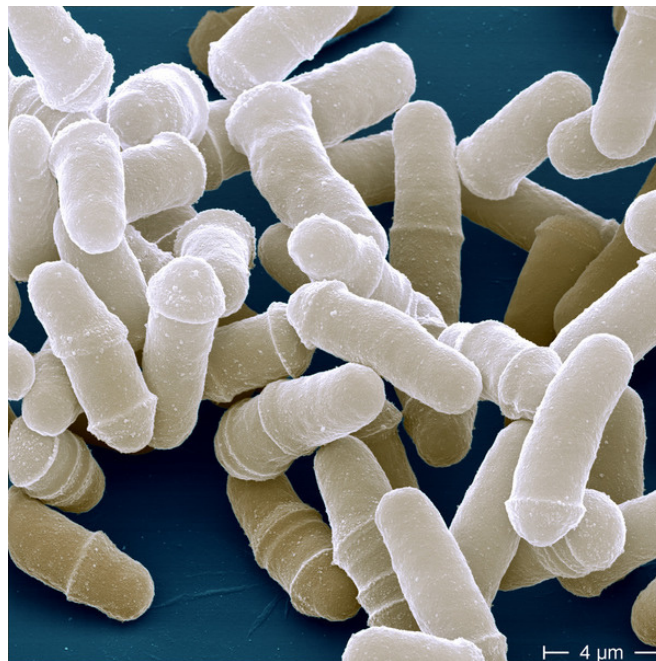
Figure I-1: Electron microscopic photograph of *Schizosaccharomyces pombe cells* at different stages of cell cycle. Picture taken from http://www.mpg.de/4354890/zoom.jpg.

S. pombe has a cylindrical shape, with a length between 7 to 14 µm and a diameter of 2 to 3 µm (Figure I-1). Cells growing vegetatively are normally haploid. Only upon nutritional depletion, especially of a nitrogen source, zygotes are formed resulting in a diploid strain. Cell division takes place along a central septum formed in the early M-Phase of the cell cycle and ends with the separation of the cell into two even-sized daughter cells. This mode of cell division gave *S. pombe* its trivial name fission yeast and is in contrast to other well characterized yeasts like

S. cerevisiae, where cell division takes place by budding. It is optically and also on the molecular level highly similar to higher eukaryotes (Russell and Nurse 1986; Simanis 1995). Murdoch Mitchison recognized this unique potential of fission yeast for studies of cell division and growth in the early 1950s (Egel 2003). Along with the genetic approaches by Urs Leupold and Paul Nurse this made *S. pombe* one of the most famous and most important model organisms for studies on cell cycle and cell division, resulting in the Nobel Prize Award in 2001 for Hartwell, Hunt and Nurse (Nurse 2002). Until today, *S. pombe* is one of the most important model organisms for basic questions of cell and molecular biology.

2.2 Heterologous protein secretion in *Schizosaccharomyces pombe*

Secretion of recombinant proteins in yeast is an efficient means to facilitate product purification in the downstream processing, thus significantly reducing the cost of the bioprocess. There are many examples in the literature for successful production of recombinant proteins with yeast cells, summarized in recent reviews by Graf et al. (2009) and Mattanovich et al. (2012).

Currently the yeasts *S. cerevisiae* and *P. pastoris* are both used in industrial processes for the production of recombinant proteins (Mattanovich et al. 2012). While this is not true for *S. pombe*, secretion of several recombinant proteins, mostly from mammalian sources, has been achieved over the years with this yeast. In Table I-1 several examples are listed for the successful secretion of recombinant proteins with *S. pombe*.

Table I-1: Examples for heterologous secretion of proteins using *S. pombe* as host strain

Protein	Reference
green fluorescent protein (GFP)	(Eiden-Plach et al. 2004)
human tumor necrosis factor α (hTNFα)	(Kjaerulff and Jensen 2005)
human growth hormone (hGH)	(Idiris et al. 2006a)
human transferrin	(Mukaiyama et al. 2009b)
human interleukin-6	(Giga-Hama and Kumagai 1998)
CB4-1-scFv-GFP fusion protein	(Naumann et al. 2010)

Despite low production titers between 0.1 and 10 mg/L, these examples indicate the potential use of *S. pombe* as a versatile production host for recombinant production of mammalian proteins.

While secretion yields can differ severely between different yeast species, the mechanisms of protein processing and secretion are highly conserved in yeasts and also in higher eukaryotes. The majority of secreted proteins follows the secretory pathway from the endoplasmic reticulum (ER) over the Golgi apparatus and subsequent secretion of the mature proteins (Figure I-2). This secretory route, the underlying mechanisms and examples for engineering of this route to improve recombinant protein production will be discussed in the following paragraphs.
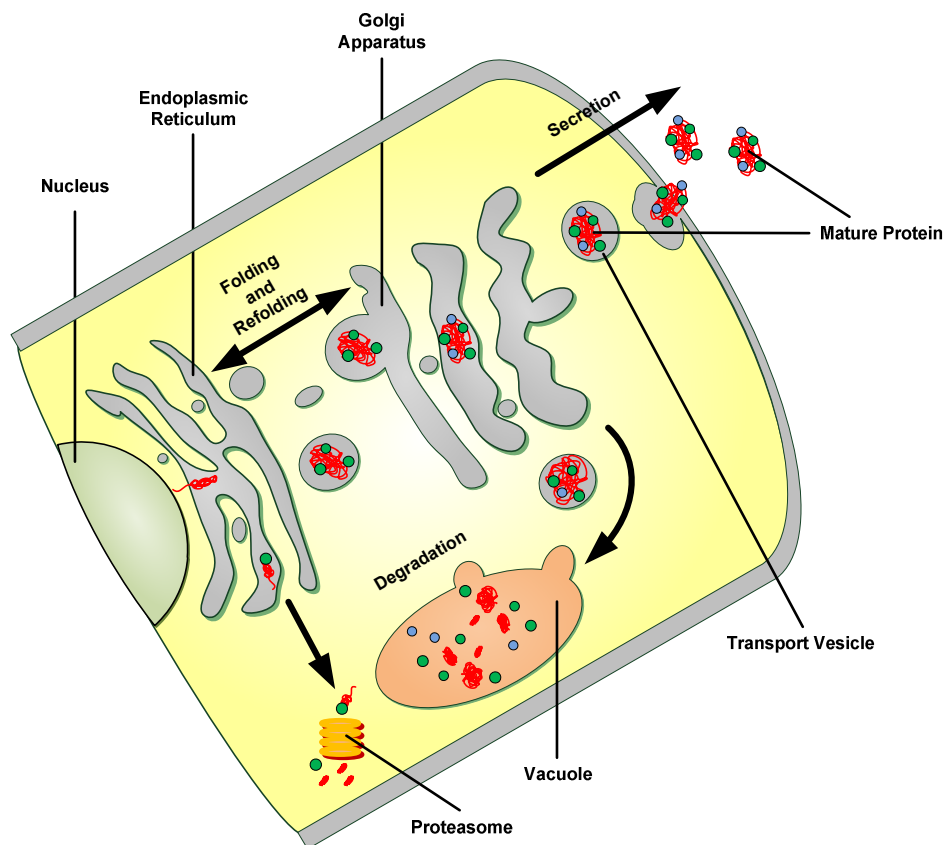
Figure I-2: Schematic overview of yeast secretory pathway: The polypeptide chain (red line) is co- or post-translationally imported into the ER, where folding and N-glycosylation (green dots) takes place. The processed protein is then transported to the Golgi apparatus for O-glycosylation (blue dots) and maturation of the N-glycosylation. Misfolded proteins can be rerouted back to the ER for refolding or towards the vacuole for degradation. Misfolded proteins in the ER are transported towards the vacuole or relocated in the cytosol where degradation via the proteasome complex takes place. Properly folded, mature proteins are transported to the plasma membrane, where fusion of transport vesicles with the membrane leads to secretion of the mature proteins into the extracellular environment.

2.2.1 Endoplasmic reticulum import and processing

For efficient targeting of the secreted proteins to the ER, an N-terminal leader peptide is necessary. These peptides range from 15-50 amino acids, with a varying hydrophobicity at the central region that determines the way of ER import (Martoglio and Dobberstein 1998). Proteins with a highly hydrophilic signal peptide are translated in the cytoplasm and post-translationally transported into the ER. The second route uses a highly hydrophobic signal peptide which allows co-translational ER import. The translated signal peptide interacts with a signal recognition particle, which causes a stop of translation. The complex is then directed towards the Sec61 transport complex, which is located in the ER membrane and allows translation of the protein into the ER-lumen (Hebert and Molinari 2007). As a third option, a weakly hydrophobic secretion signal allow synthesis of the protein in the cytosol in an unfolded shape and subsequent folding of the protein into the ER lumen via Sec61 and Sec62/63 complexes (Hebert and Molinari 2007). For heterologous secretion of proteins, a multitude of signal peptides are described which are either directly adapted from natively strongly secreted proteins or which are artificially designed to further improve secretion. The *S. cerevisiae* α-factor signal peptide is surely the most famous example (Bitter 1984). For *S. pombe* the most commonly used signal peptides nowadays are either P3 and its derivates or the Cpy1 signal peptide (Giga-Hama and Kumagai 1998; Kjaerulff and Jensen 2005) but also the secretion leader of the viral K28 toxin could efficiently promote GFP secretion in this yeast (Eiden-Plach et al. 2004).

Once the protein has entered the ER, the maturation process will start. For soluble proteins, the signal peptide is removed and chaperones assist the proper folding of the protein (Martoglio and Dobberstein 1998; Nishikawa et al. 2005). Overexpression of ER chaperones has been shown to tremendously improve secretion of recombinant proteins in various yeasts species (Idiris et al. 2010). In *S. pombe* production of human transferrin could be improved by a factor of 30 by overexpressing protein disulfide isomerase genes (Mukaiyama et al. 2009b).

N- and O-linked glycosylation of secreted proteins takes place in the ER lumen (Herscovics and Orlean 1993). *S. cerevisiae* is known to produce large mannan structures, which can influence protein half-life and cause immunogenic reactions in humans. This can become problematic in the production of therapeutics (Celik and Calik 2011; Idiris et al. 2010). *S. pombe* on the other hand starts N-glycosylation with a D-mannose backbone decorated with D-galactose residues, which can be additionally pyruvylated. These structures resemble the mammalian glycosylation much more than glycosylation patterns of other yeasts, indicating the potential of *S. pombe* as host for recombinant mammalian protein production (Celik and Calik 2011).

2.2.2 Processing in the Golgi apparatus and exocytosis

The Golgi apparatus is the second organelle involved in transport and maturation of secretory proteins in yeast. While the Golgi apparatus of *S. cerevisiae* is dispersed over the cell in cisternae structures, the *S. pombe* Golgi apparatus is organized in stacks as in higher eukaryotes (Celik and Calik 2011). It can be roughly separated into three sub-compartments: the cis-site, facing the ER, the medial Golgi and the trans-site, which is oriented towards the plasma membrane (Suda and Nakano 2012). After processing in the ER, proteins are transported via membrane vesicles to the Golgi. Maturation of the glycan structures take place in this compartment, while the protein is transported from the cis-site to the trans-site (Suda and Nakano 2012). When maturation of glycan-structures and protein folding has been finished successfully, the mature protein is transported to the plasma membrane. The transport vesicles fuse with the membrane, releasing the proteins into the extracellular environment. Efficient transport through the Golgi apparatus as well as between the organelles and the plasma membrane is a must for the successful secretion of proteins. Recently, a transcriptomic-based approach to identify targets for improved heterologous protein secretion in *P. pastoris* reported upregulation of several mRNAs coding for proteins involved in vesicular protein transport (Gasser et al. 2007). Further, overexpression of *S. cerevisiae* Sec1p and Sly1p, both involved in vesicular transport from ER to Golgi and Golgi to plasma membrane respectively, could enhance α-amylase secretion in this yeast 1.6-fold (Hou et al. 2012).

Once the protein of interest has been secreted into the media, it is often subject to degradation by extracellular proteases. This can be partially avoided by addition of a complex, protein containing component e.g. peptone, to saturate these proteases (Kjaerulff and Jensen 2005). However, this can complicate the further product purification. In bacteria and yeast, construction of protease-deficient strains is a common strategy to improve product yields (Gleeson et al. 1998). The construction of a multiprotease-deficient *S. pombe* strain has been described and secretion of human growth hormone could be increased 30-fold in this strain compared to a wild-type control (Idiris et al. 2006a; Idiris et al. 2006b).

2.2.3 The fate of misfolded proteins

High level expression of recombinant proteins can cause an accumulation of misfolded proteins in the ER and the Golgi apparatus. This leads to the induction of the unfolded protein reponse (UPR), resulting in the increased expression of chaperones located in ER and Golgi apparatus as well as proteins of the proteasome complex (Patil and Walter 2001). When misfolded proteins

are recognized, they can be cycled between the ER and the Golgi apparatus in order to refold them in a proper way (Caldwell et al. 2001). In the ER either proper refolding of the protein is reached or ubiquitination takes place, marking the protein as target for the ER associated protein degradation (ERAD). These proteins are prevented from progressing along the secretory pathway. ER-resident factors direct those proteins to the translocon for retrotranslocation into the cytosol, where they undergo ubiquitin- and proteasome-dependent degradation (Patil and Walter 2001). In yeast there is a second route of protein degradation. Misfolded proteins are packed in transport vesicles and redirected towards the vacuole, which acts a primary lysosome and degradates these proteins quickly (Hong et al. 1996).

Improving protein folding and turnover has been shown to improve recombinant protein secretion. In *S. cerevisiae* and *P. pastoris*, overexpression of inducers of the unfolded protein response, e.g. Hac1p, could effectively increase secretion of several recombinant proteins (Guerfal et al. 2010; Idiris et al. 2010). Regarding *S. pombe*, deletion of *vsp10*, a gene involved in vacuolar protein sorting improved secretion of human growth hormone by a factor of 2 (Idiris et al. 2009).

2.3 Influence of host physiology on recombinant protein production

The choice of the producer organism can severely influence the efficiency of recombinant protein secretion as well as the quality of the product. In this context host physiology plays a major role, strongly influencing product titers and space time yields (Mattanovich et al. 2012; Porro et al. 2005). Cellular stress responses, protein folding and secretion, or genetic stability can strongly depend on the metabolic activity of the host and vice versa heavily influence the metabolism of the producing strains (Merten et al. 2001; Sevastsyanovich et al. 2009). For years extensive physiological characterization was carried out, describing basic metabolic features of various yeasts like *S. cerevisiae* and *P. pastoris and* investigating the influence of environmental factors and carbon sources.

The production of recombinant proteins themselves poses a significant burden on the cellular metabolism and in recent years its influence on the metabolism of producer strains has been the topic of various studies. Several research articles deal with the influence of intracellular production of recombinant proteins as well as secretion of these proteins on the central carbon metabolism of the yeasts *S. cerevisiae* and *P. pastoris*, revealing major metabolic flux redistributions in catabolic pathways and precursor supply (Heyland et al. 2011; Jordà et al.

2012; van Rensburg et al. 2012). Approaches to solve difficulties in protein production involve the cooperation between process development and strain improvement which is crucial for the optimization of both the production strain and the process (Merten et al. 2001). Successful metabolic engineering approaches for improving recombinant protein production have been described for *E. coli* (Aristidou et al. 1995) and the eukaryotic fungi *Aspergillus niger* (Driouch et al. 2011; Driouch et al. 2010). Further, the physiological response to variation of process parameters during cultivations of the yeasts *S. cerevisiae* and *P. pastoris* has come into the focus of attention and has been a topic of research for the last years (Baumann et al. 2010; Holmes et al. 2009; Sevastsyanovich et al. 2009).

Only few studies are available dealing with the physiology of *S. pombe*, mostly describing utilization of different carbon sources like ethanol or malate (de Jong-Gubbels et al. 1996; De Queiroz and Pareilleux 1990). Publications concerning quantitative analysis of the metabolic flux distributions were so far limited to a functionalized *S. pombe* strain applied in whole-cell-biocytalysis (Dragan et al. 2006). Comparable studies have not been performed for *S. pombe* strains secreting recombinant proteins yet. However, several studies describe improvement of product titers by optimization of media composition and cultivation conditions using different carbon sources and addition of surfactants (Matsuzawa et al. 2010; Mukaiyama et al. 2009a). In 2006, Jansen et al. described the production of homologous α-glucosidase in *S. pombe*. By applying an evolutionary engineering approach and respiratory growth conditions, product titers of 1.7 g/L could be reached in a fed-batch process. This was the first study to show that *S. pombe* can be used for high-level secretion of proteins and further that the choice of the right process conditions can tremendously improve protein secretion in this organism. Accordingly, detailed knowledge of the physiology and the metabolic response to changes in process conditions and the burden of recombinant protein secretion can be used to improve *S. pombe* strains and process conditions to establish this organism as a possible alternative host besides the commonly applied yeasts.

3 Physiology of *Schizosaccharomyces pombe*

The fission yeast *Schizosaccharomyces pombe* belongs to the group of facultative fermentative yeasts like e.g. *S. cerevisiae* (Walker 1998). Carbohydrates are the carbon source of choice and with glucose as sole carbon source maximum growth rates μ_{max} up to 0.25 h^{-1} in minimal media can be achieved (de Jong-Gubbels et al. 1996). Such a μ_{max} is rather low compared to *S. cerevisiae* where maximum growth rates over 0.4 h^{-1} have been described (Frick and Wittmann 2005; Gombert et al. 2001). Depending on the environmental conditions and the specific growth rate, metabolization of carbohydrates takes place either in a respiratory or a fermentative way or a mixture of both. In the following chapters the different physiologies and specific features of the central carbon metabolism of *S. pombe* will be discussed in detail.

3.1 Respiratory and fermentative growth

The majority of yeasts are facultative fermenters, which means that carbohydrates are either metabolized via respiratory or fermentative pathways. The switch between both catabolic pathways is often a response to changes in environmental conditions and substrate concentrations, most drastically to changes in sugar and oxygen levels. Regarding the response to variations in carbohydrate concentrations, two groups of yeast can be distinguished: Crabtree-positive and Crabtree-negative yeasts. The Crabtree-positive yeasts show fermentative growth even under aerobic culture conditions with CO_2 and ethanol as the main fermentative product. The Crabtree effect can be separated into two distinct phases: a short-term effect, which takes place when aerobically growing sugar-limited cultures are exposed to sugar excess. Fast uptake and metabolization of carbohydrates exceed the capacity of the respiratory system resulting in an overflow metabolism of pyruvate and cytosolic regeneration of redox equivalents by fermentative pathways (Rieger et al. 1983; Van Urk et al. 1990). This is followed by a long-term effect, in which the cells adapt to the excess conditions and repression of respiratory enzymes takes place as a global cellular response to catabolite repression even under sugar-limiting conditions (Eraso and Gancedo 1984; van Urk et al. 1989).

S. pombe belongs to the Crabtree-positive yeasts (van Urk et al. 1989) but both respiratory and fermentative growth are only possible in the presence of oxygen (Walker 1998). The main fermentative byproduct is ethanol but also glycerol is produced in significant amounts. Further

small amounts of the organic acids pyruvate, succinate and acetate are also secreted into the media (de Jong-Gubbels et al. 1996). The growth rate at which the shift between respiratory and fermentative metabolism takes place is characteristic for an organism and can be observed in chemostat experiments. At low growth rates, a completely respiratory metabolization of carbohydrates is possible for both *S. cerevisiae* and *S. pombe* (Frick and Wittmann 2005; de Jong-Gubbels et al. 1996). Above a critical dilution rate D_{crit} the onset of fermentative metabolism occurs, characterized by the production of ethanol, a reduction of the oxygen uptake rate and an increased CO_2 production rate (de Jong-Gubbels et al. 1996). For *S. cerevisiae* strains D_{crit} has been determined at dilution rates above 0.2 h^{-1} (Frick and Wittmann 2005). Growth of *S. pombe* is slower than growth of *S. cerevisiae* and also the critical dilution rate of *S. pombe* is lower in comparison, with $D_{crit} = 0.16\ h^{-1}$. An extension of D_{crit} could be achieved by using a pulsed-feeding approach in chemostat experiments of S. *cerevisiae* (Heinzle et al. 1985). A comparable experiment has not been described for *S. pombe* but might achieve similar results.

3.2 The central carbon metabolism of *S. pombe*

The central carbon metabolism consists of a network of complex chemical reactions, which are highly conserved from bacteria to mammalian cells. It provides the cell with carbon precursors as well as redox equivalents and ATP for anabolic pathways and synthesis of the cellular macromolecules. Only 12 different chemical compounds serve as precursors necessary to produce the multitude of different chemical compounds found in a cell (Figure I-3). Dealing with variations in the cellular demand as well as available carbon and energy sources requires a very flexible network of metabolic reactions, allowing major redistributions as well as fine-tuning of the metabolic fluxes. As a consequence, even slight environmental changes can result in a strong metabolic response, which makes the central metabolism a very sensitive indicator for all kinds of intra- and extracellular perturbations.

The central carbon metabolism of *S. pombe* comprises the known and essential pathways to provide all necessary precursors for biosynthesis: glycolysis and the pentose phosphate pathway (PPP), the tricarboxylic acid cycle (TCA) and anaplerosis to refill the TCA cycle (Figure I-3). As fermentative yeast, *S. pombe* further possesses fermentative pathways for the production of ethanol, acetate and glycerol, allowing the cell the regeneration of NAD^+ without the need for a respiratory chain. These pathways as well as special metabolic features of *S. pombe* will be discussed in detail in the following paragraphs.
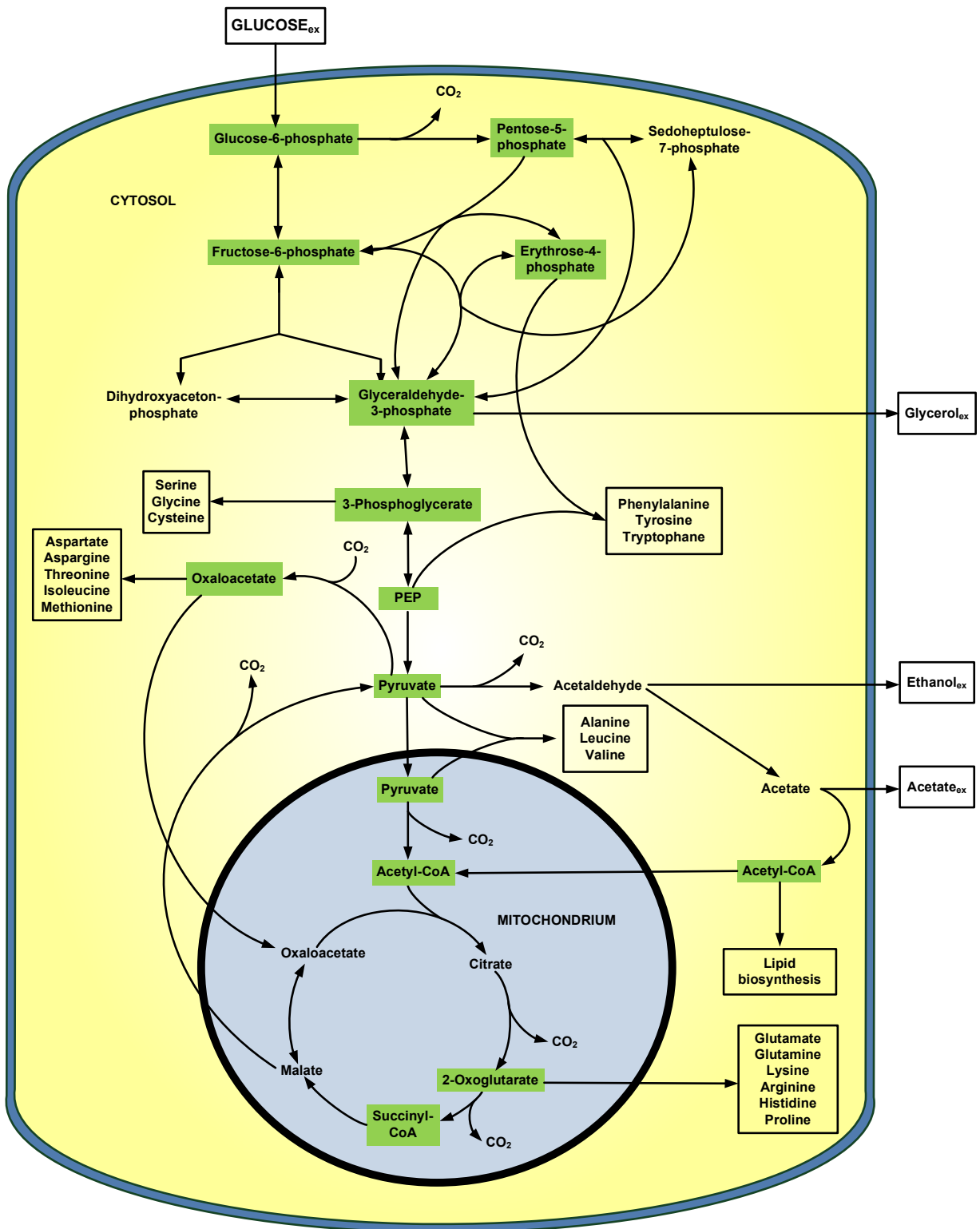
Figure I-3: Central carbon metabolism of *Schizosaccharomyces pombe*. Shown are glycolysis, pentose phosphate pathway and tricarboxylic acid cycle as well as anaplerosis and the fermentative pathways producing glycerol, ethanol and acetate. The 12 precursor metabolites are highlighted in green. Glucose, ethanol, glycerol and acetate are labeled as extracellular metabolites.

3.2.1 Glyoxylate cycle and gluconeogenesis

The glyoxylate cycle allows the cells to produce the C_4 units succinate and malate from the condensation of two C_2 units of acetyl-CoA. The first steps follow the TCA cycle: oxaloacetate and a first acetyl-CoA unit are condensed to citrate by the citrate synthase (EC 2.3.3.1), which is further converted to isocitrate by the aconitase (EC 4.2.1.3). Isocitrate is then cleaved into succinate and glyoxylate by the isocitrat lyase (EC 4.1.3.1), circumventing the decarboxylating reactions of the TCA cycle. In the last step, glyoxylate is condensed with a second acetyl-CoA unit to form malate via the enzyme malate synthase (EC 2.3.3.9).

In contrast to other yeasts like *S. cerevisiae*, no functional glyoxylate cycle has been found in *S. pombe* (de Jong-Gubbels et al. 1996; Tsai et al. 1987). No gene for maltase synthase has been annotated up to now (http://www.pombase.org/) and although there is sequence similarity data for the existence of a isocitrate lyase gene, its localization and thus its function is contradictory (Matsuyama et al. 2006). Finally no enzymatic activity for both enzymes could be demonstrated and cultivation studies have shown that *S. pombe* is unable to grow on C_2 bodies like acetate or ethanol as sole carbon and energy source (Matsuzawa et al. 2010; Tsai et al. 1987).

A further restriction in the metabolism of *S. pombe* is the absence of the enzyme PEP-carboxylase (PEPCK) (EC 4.1.1.31) (de Jong-Gubbels et al. 1996; Rhind et al. 2011). This enzyme catalyzes the formation of PEP from oxaloacetate, the first step in the gluconeogenesis. While *S. pombe* expresses a transporter for uptake of organic acids like malate, it cannot use them as sole source for carbon and energy due to this limitation (Camarasa et al. 2001; Taillandier and Strehaiano 1991). The second enzyme of the gluconeogenesis, fructose-6-bisphosphatase (EC 3.1.3.11), is needed to overcome the irreversible phosphorylation of fructose-6-phosphate to 1,6-fructose-bisphopshate. This enzyme is encoded by the *S. pombe* gene *fb1*. The gene is subject to glucose catabolite repression and further an inducer like ethanol or 2-propanol is necessary for its expression (Matsuzawa et al. 2012).

3.2.2 Fermentative pathways and the pyruvate dehydrogenase bypass

Fermentatively growing yeasts can produce a variety of products, ranging from alcohols and polyols to mono-, di- and tricarbolic acids (Van Dijken and Scheffers 1986). Formation of these products is necessary for the cells to counter imbalances in their redox state. Excess NADH is produced during the fast glycolytic breakdown of glucose, resulting in an accumulation of cytosolic NADH, which has to be regenerated via fermentative pathways (Van Dijken and

Scheffers 1986; Vemuri et al. 2007). In *S. pombe* the range of byproducts can differ, depending on the cultivation conditions and carbon sources. While organic acids like acetate, pyruvate or succinate may or may not be produced during growth under glucose-excess conditions, the main byproduct by far is ethanol, followed by glycerol (de Jong-Gubbels et al. 1996; Kunicka-Styczynska 2009). Both pathways serve as main NAD^+ regeneration systems during fermentative growth of *S. pombe* on sugars.

Glycerol production takes place to reoxidize NADH formed in the anabolism (Verduyn et al. 1990) starting with the reduction of dihydroxyacetone-phosphate to glycerol-3-phosphate by glycerol-3-phosphate dehydrogenase (GPDH) and subsequent glycerol secretion. In *S. pombe*, three isoenzymes of glycerol-3-phosphate dehydrogenase are annotated, encoded by the genes SPAC23D3.04c, SPCC1223.03c and SPBC215.05. While SPBC215.05 is induced in response to osmotic stress, SPAC23D3.04c expression seems constitutive (Degols et al. 1996; Ohmiya et al. 1995). However, few is understood up to now, concerning the distinct roles of the gene products in the different pathways.

A fast glycolytic flux results in an accumulation of pyruvate. This is either directly secreted in the media or converted to ethanol (Benito et al. 2012; Vemuri et al. 2007). The first reaction is the decarboxylation of pyruvate to acetaldehyde via the pyruvate decarboxylase (PDC). In *S. pombe* no less than four genes are annotated to encode isoenzymes of the PDC: SPAC13A11.06, SPAC186.09, SPAC1F8.07c and SPAC3G6.11c. Acetaldehyde is further converted to ethanol via alcohol dehydrogenase (ADH). There are again four genes encoding isoenzymes of the ADH: SPAC5H10.06c, SPBC1539.07c, SPBC13B11.01 and SPBC13B11.04c. De Jong-Gubbels et al. (1996) reported activity of ADH even in cells grown under respiratory, carbon limiting conditions, where no ethanol was observable in the culture supernatants. At least some of the ADH genes must be expressed constitutively, allowing the cell a fast and efficient adaption to a substrate pulse and the consequent increased glycolytic flux. The amount of isoenzymes for GPDH, PDC and ADH as well as the constitutive expression of these genes clearly indicate the importance of these fermentative pathways as the main regulators of the cellular redox homeostasis in *S. pombe*.

The pathway from pyruvate over acetaldehyde to acetyl-CoA is known as pyruvate dehydrogenase bypass and is essential for the cellular supply of cytosolic acetyl-CoA in yeasts. Acetaldehyde is converted via acetaldehyde dehydrogenase (AADH), producing acetate, which is further converted to acetyl-CoA via the acetyl-CoA synthetase (EC 6.2.1.1). It has been shown that *S. cerevisiae* cannot transport acetyl-CoA from the mitochondria into the cytosol

(Flikweert et al. 1996). Consequently the formation of cytosolic acetyl-CoA, which is mainly used as precursor for lipid biosynthesis has to take place via this pathway (Flikweert et al. 1996; Remize et al. 2000). In *S. pombe* two isoenzymes are described for AADH, which are both located in the cytosol and can use NAD^+ and $NADP^+$ as cofactors (de Jong-Gubbels et al. 1996; Matsuyama et al. 2006). Thus, acetate formation can further serve as second source for cytosolic NADPH besides the oxidative reactions of the PPP, and is involved in the cellular redox homeostasis. Little information is available on the transport between cytosol and mitochondria in *S. pombe* but one can assume that the PDH bypass has a similar function as described for *S. cerevisiae*.

3.3 Growth on different carbon sources

S. pombe can grow on a variety of substrates like carbohydrates, organic acids, glycerol or ethanol (Matsuzawa et al. 2010; Mayer and Temperli 1963). Carbohydrates are the preferred source for carbon and energy and when cells are grown in media containing high concentrations of glucose, uptake of other substrates is repressed. This is known as glucose catabolite repression and has been described for various yeasts (Gancedo 1998).

3.3.1 Growth on carbohydrates and carbohydrate acids

Six hexose transporters with varying affinities for glucose are describe for *S. pombe*, mediating efficient glucose uptake in the presence of high and low concentrations of glucose in the media (Heiland et al. 2000). Fructose uptake takes place via the same transporters, although with lower affinity than glucose uptake. In contrast to *S. cerevisiae*, no growth on galactose has been describe for *S. pombe* wild type but only for a mutant strain isolated from an evolutionary engineering experiment (Matsuzawa et al. 2011a).

Another interesting carbon source for *S. pombe* is gluconic acid (Hoever et al. 1992). While growth of *S. cerevisiae* on gluconate is poor, *S. pombe* can grow efficiently on this substrate (Caspari and Urlinger 1996). Uptake takes place via the hexose transporter ght3 as H^+ symport, causing a strong basification of the media (Caspari and Urlinger 1996; Heiland et al. 2000). Recently, also the application of *S. pombe* mutants defect in glucose but not gluconate uptake has been discussed for efficient deacidifcation of grape musts and wines (Benito et al. 2012; Peinado et al. 2005).

3.3.2 Growth on organic acids and glycerol

S. pombe expresses transporters for various carboxylic acids as well as six amino acid permeases (Grobler et al. 1995; Matsumoto et al. 2002). While metabolization of several mono- and dicarboxylic acids has been demonstrated (Mayer and Temperli 1963), none of them can serve as sole carbon source, due to the lack of the PEPCK enzyme (de Jong-Gubbels et al. 1996; Rhind et al. 2011). Growth on C_2 bodies as sole carbon source is further limited due to the lack of a functional glyoxylate cycle (de Jong-Gubbels et al. 1996) but growth on mixtures containing glucose and ethanol or glucose and malate has been described in the past (de Jong-Gubbels et al. 1996; Uribelarrea et al. 1997).

Glycerol is a promising future substrate for microbial bioprocesses (Dobson et al. 2012). However, when applying glycerol as sole carbon source, growth of *S. pombe* has only been observed in combination with glucose or C_2 bodies like ethanol or acetate (Klement et al. 2011; Matsuzawa et al. 2010). The inability of *S. pombe* to grow on glycerol as sole carbon source is not fully understood yet. On the one hand the expression of important key enzymes of glycerol degrading pathways like glycerol-dehydrogenase (*gld1*) and fructose-1,6-bisphosphatase (*fbp1*) is not induced in the presence of glycerol. Both genes are subjected to glucose catabolite repression (Matsuzawa et al. 2011b) and additionally *fbp1* expression has to be induced by small organic acids and alcohols like ethanol, 2-propanol and acetate (Klein et al. 2013; Matsuzawa et al. 2012). Moreover, overexpression of *gld1*, the dihydroxyacetone kinase coding genes *dak1* and *dak2* as well as *fbp1* did not allow growth of *S. pombe* on glycerol alone (Matsuzawa et al. 2012; Matsuzawa et al. 2010). Thus, further restrictions must exist. An imbalance of the intracellular redox state might be one possible explanation, as has been reported for growth of *S. cerevisiae* strains on xylose (Verho et al. 2003). However, few data is available concerning the physiology of *S. pombe* grown on glycerol and studies giving a detailed insight into glycerol metabolization by this organism still have to be performed.

4 Quantitative analysis of metabolic networks

The physiology of a production host can have tremendous influence on its productivity. In this context it is important to perform not only a qualitative description of the existing metabolic pathways in a cell but also to quantify the *in vivo* metabolic fluxes through each of these pathways under defined conditions. The detailed knowledge gained in such studies can be used to efficiently increase product yields by metabolic engineering of the organism and optimization of the process conditions.

4.1 Metabolite balancing

By measuring the extracellular metabolic fluxes, including substrate uptake, biomass and product formation as well as respiratory rates, a stoichiometric balancing of the intracellular flux can be performed (metabolite balancing). Unknown fluxes are calculated using a stoichiometric model of the metabolism and material balances of the measured extracellular metabolites (Stephanopoulos 1998; Wittmann and Heinzle 1999). For proper estimation of the intracellular fluxes, a metabolic steady state is necessary, where the sum of production rates of metabolites is equal to the sum of their consumption rates. Due to the mathematical background the applied matrices must not be underdetermined for proper estimation of the intracellular metabolic flux distributions. Thus this method is only applicable to simple networks or networks with a great number of extracellular fluxes, as shown for mammalian cell cultures (Niklas et al. 2010). Moreover, quantification of cyclic pathways, reaction reversibilities and separation of alternative pathways is not possible. Thus no proper balancing of redox equivalents and ATP formation can be performed with this method (Christensen and Nielsen 2000).

4.2 ^{13}C based metabolic flux analysis

To overcome the disadvantages of metabolite balancing, the ^{13}C based metabolic flux analysis was developed. By using labeled substrates carrying one or more ^{13}C isotopes instead of naturally occurring ^{12}C isotopes, the isotopomer distribution of certain metabolites in the central carbon metabolism can be determined and used for additional balancing. Since only the isotopomer distributions of the carbon atoms are of interest, the measured fragments have to be corrected for all other naturally occurring isotops (van Winden et al. 2002; Yang et al. 2009).

The natural isotope abundances of the biologically relevant elements C, H, O, and S and of Si, as important component of the derivatizing agent for GC-MS derivatization are shown in Table I-2.

Table I-2: Natural isotopic composition of elements relevant for the ^{13}C based metabolic flux analysis (Rosman and Taylor 1998)

element	monoisotopic mass [Da]	[m+0]	[m+1]	[m+2]
H	1	0,999885	0,000115	
C	12	0,9893	0,0107	
N	14	0,99632	0,00368	
O	16	0,099757	0,00038	0,00205
Si	28	0,922297	0,046832	0,030872
S	32	0,09493	0,0076	0,0429

4.2.1 Mathematical definition of metabolite labeling

In case of carbon, two relevant isotopes have to be considered, ^{12}C and ^{13}C. Each carbon atom can have a mass of either 12 or 13 Da. For a molecule consisting of n carbon atoms this results in 2^n positional isotopomers (Wiechert 2001). These are depicted in an isotopomer distribution vector (IDV), containing their relative abundances (Wittmann and Heinzle 1999). Since mass spectrometry cannot distinguish between different positional isotopomers with the same mass, those are instead summed up in n+1 mass isotopomers (Figure I-4). The relative abundances of the mass isotopomers are then depicted in a mass distribution vector (MDV) (Wittmann 2002).
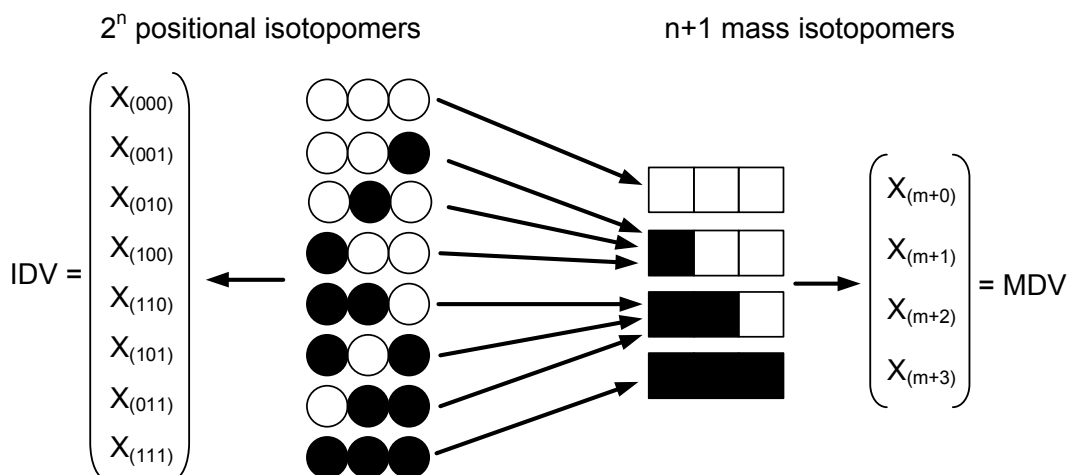
Figure I-4: Positional and mass isotopomers and the corresponding IDV and MDV of a molecule with 3 carbon atoms.

4.2.2 Mathematical definition of carbon and isotope transfer

The transition of carbon atoms between the reactants and products of a metabolic reaction is defined in atom mapping matrices (AMM) (Zupke and Stephanopoulos 1994). These matrices have the form n x m, where n is the number of carbon atoms in the product and m the number of carbon atoms in the reactant. By analogy with these AMMs, the transition of isotopomers can be described in isotopomer mapping matrices (IMM). These matrices define where each positional isotopomer of the reactant is transferred to in the product. In the case of carbon with the isotopes ^{12}C and ^{13}C, an IMM has the dimensions 2^m x 2^n, where n is again the number of carbon atoms in the product and m the number of carbon atoms in the reactant.

Using the IMMs and the IDVs of the reactant, the IDVs of the product can be calculated. In the following example, carbon and isotope transfer in a condensation reaction is shown:

$$IDV_{Product} = (IMM_{reactant\ 1 \rightarrow product} \times IDV_{reactant\ 1}) \otimes (IMM_{reactant\ 2 \rightarrow product} \times IDV_{reactant\ 2})$$

In an isotopic steady state, the sum of the production rates of all isotopomers is equal to the sum of their consumption rates. $\otimes$ refers to the pairwise multiplication of the elements of both matrices. A metabolic steady state is imperative to reach an isotopic steady state.

4.2.3 Isotopomer balancing

As a continuation of the metabolite balancing, also balances for each isotopomer of a metabolite can be formulated. The concept of cumulated isotopomers was introduced in 1999 by Wiechert et al. for efficient solving of isotopomer balances. To further facilitate the highly complex balances resulting from complex networks, in 2007 the concept of elementary metabolite units (EMU) was introduced. EMUs use the minimal information necessary for simulating the isotopomers of a metabolic network (Antoniewicz et al. 2007) thus reducing the number of balances to be solved by at least a magnitude.

The concept of EMUs was also used in this work to perform ^{13}C based metabolic flux analysis. The balances are solved using an iterative, hybrid algorithm, minimizing the deviation between measured and simulated MDVs by varying the free fluxes (Yang et al. 2008). For statistical coverage, 100 independent Monte Carlo simulations are performed (Wittmann 2002; Yang et al. 2008). The variation of the starting values was calculated from the measured MDVs and extracellular metabolite rates, assuming a normal distribution of the values. After 100 runs, the mean values and their respective standard deviations were determined for each calculated flux.

4.3 Experimental setup for quantitative network analysis

As mentioned above, a metabolic and isotopic steady state is the basic requirement to perform any of the described network analysis. The metabolic steady state can be reached by performing continuous cultivation experiments, where the cells quickly approach a steady state, with constant rates for biomass formation, substrate uptake and product formation (Hoskisson and Hobbs 2005). The big advantage of such a setup is that various process parameters can be easily influenced and the cells can be kept in this state for a theoretically infinite span of time. In batch cultivations, a so called pseudo-steady state can be reached during the exponential growth phase. While substrate and product concentrations change during this exponential growth phase, the specific rates for uptake and production of metabolites are constant, as long as no nutrient limitation or product inhibition occurs. Thus, the cells are constantly growing with the maximum possible rate in a steady-state like way.

Under these metabolic steady-state conditions, cells are cultivated on the ^{13}C labeled substrate of choice. The ^{13}C carbon is spread throughout the central carbon metabolism, depending on the activity of the different pathways. After a certain number of cell divisions, an isotopic steady state is reached and the ^{13}C enrichment of the different metabolites can be quantified. There are

several analytical methods to determine the labeling distribution: by nuclear magnetic resonance spectroscopy (NMR) or by mass spectrometry (MS), coupled either to a liquid chromatograpy (LC-MS) or a gas chromatography (GC-MS) system (van Winden et al. 2005). The enrichment can be quantified in intracellular free metabolites as well as hydrolysates of macromolecules from biomass, where in the latter reaching an isotopically stationary enrichment takes much longer (Frick and Wittmann 2005; van Winden et al. 2005).

After the measurement, the data are corrected for the naturally occurring isotopes and the MDVs are calculated (Yang et al. 2009). These experimental data are further used as starting values for the ^{13}C based metabolic flux analysis as described above. In this work, enrichment of ^{13}C labeling was measured in protein and lipid hydrolysates from biomass via GC-MS and the corrected MDVs were used to perform the computational simulation of the metabolic flux distributions. To validate the accuracy of the flux analysis, the simulated data are compared to the measured labeling distributions. A schematic workflow is given in Figure I-5.
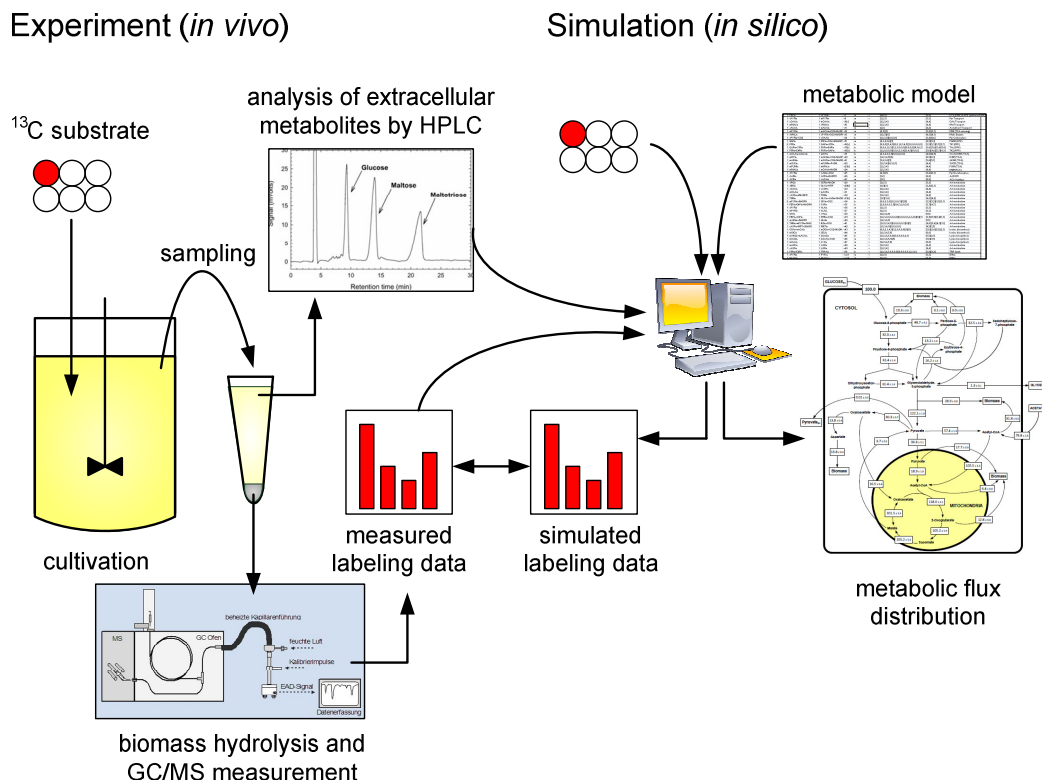

Figure I-5: Schematic workflow of the experimental part and the computational simulation part of the ^{13}C based metabolic flux analysis as performed in this work.

5 Aims and Scope

The aim of this work was to increase the understanding of the complex metabolic network of the fission yeast *Schizosaccharomyces pombe* with special emphasis on the metabolic burden of elevated protein secretion. Most experiments were performed as continuous cultivations to guarantee steady-state conditions in a defined environment and ^{13}C metabolic flux analysis allowed a quantitative estimation of *in vivo* metabolic flux distributions. In order to perform a large number of experiments with different strains, a system of 10 mL scale bioreactors was established allowing the performance of up to 8 parallel continuous cultivation experiments. To monitor process conditions, online measurement of dissolved oxygen via fluorescent dyes and mass spectrometric analysis of culture off gas for carbon balancing were implemented into the system.

Metabolic studies on the wild type strain 972 h⁻ were performed to investigate the shift from respiratory to fermentative metabolism on glucose. Further utilization of glucose compared to other carbon sources was studied, including substrate mixtures of glycerol and acetate. On these mixtures, quantitative analyses of the metabolism were performed and compared to results obtained for cells grown respiratorily on glucose. The results gave information on the metabolic flexibility of *S. pombe* as well as redox homeostasis on different substrates.

The second part of this work aimed at understanding the influence of high level protein secretion on the metabolism of *S. pombe*. While several publications on this topic are available for the yeast *S. cerevisiae* and *P. pastoris*, no research on this issue has been performed with *S. pombe* up to now. The α-glucosidase maltase was chosen as model protein and a number of strains were constructed secreting maltase in varying amounts. Chemostat cultivations using glucose as sole carbon source were performed and ^{13}C based metabolic flux analysis was applied to determine flux redistributions in the central carbon metabolism of *S. pombe* in response to elevated protein secretion. On the basis of these findings, cultivations on two substrate mixtures were performed to overcome metabolic bottlenecks limiting protein secretion. In order to examine if the applied feeding strategies for improved protein secretion were specific for maltase or rather related to high level protein secretion in general, the results of these analyses were transferred to strains secreting GFP and a single-chain antibody fragment to improve the secretion of these proteins likewise.

6 References

Antoniewicz MR, Kelleher JK, Stephanopoulos G (2007) Elementary metabolite units (EMU): a novel framework for modeling isotopic distributions. Metab Eng 9:68–86.

Aristidou AA, San KY, Bennett GN (1995) Metabolic engineering of *Escherichia coli* to enhance recombinant protein production through acetate reduction. Biotechnol Prog 11:475–478.

Baumann K, Carnicer M, Dragosits M, Graf AB, Stadlmann J, Jouhten P, Maaheimo H, Gasser B, Albiol J, Mattanovich D, Ferrer P (2010) A multi-level study of recombinant *Pichia pastoris* in different oxygen conditions. BMC Syst Biol 4:141.

Benito S, Palomero F, Morata A, Calderón F, Suárez-Lepe JA (2012) New applications for *Schizosaccharomyces pombe* in the alcoholic fermentation of red wines. Int J Food Sci Tech 47:2101–2108.

Bitter GA (1984) Secretion of Foreign Proteins from *Saccharomyces cerevisiae* directed by alpha -Factor Gene Fusions. PNAS 81:5330–5334.

Bretthauer RK (2003) Genetic engineering of *Pichia pastoris* to humanize N-glycosylation of proteins. Trends Biotechnol 21:459–462.

Caldwell SR, Hill KJ, Cooper AA (2001) Degradation of endoplasmic reticulum (ER) quality control substrates requires transport between the ER and Golgi. J Biol Chem 276:23296–303.

Camarasa C, Bidard F, Bony M, Barre P, Dequin S (2001) Characterization of *Schizosaccharomyces pombe* malate permease by expression in Saccharomyces cerevisiae. Appl Environ Microbiol 67:4144–4151.

Caspari T, Urlinger S (1996) The activity of the gluconate-H+ symporter of *Schizosaccharomyces pombe* cells is down-regulated by D-glucose and exogenous cAMP. FEBS Lett 395:272–276.

Celik E, Calik P (2011) Production of recombinant proteins by yeast cells. Biotechnol Adv 30:1108–1118.

Christensen B, Nielsen J (2000) Metabolic network analysis. A powerful tool in metabolic engineering. Adv Biochem Eng Biot 66:209–231.

Damasceno LM, Huang C-J, Batt CA (2012) Protein secretion in *Pichia pastoris* and advances in protein production. Appl Microbiol Biotechnol 93:31–39.

Degols G, Shiozaki K, Russell P (1996) Activation and regulation of the Spc1 stress-activated protein kinase in *Schizosaccharomyces pombe*. Mol Cell Biol 16:2870–2877.

Van Dijken JP, Scheffers WA (1986) Redox balances in the metabolism of sugars by yeasts. FEMS Microbiol Lett 32:199–224.

Dobson R, Gray V, Rumbold K (2012) Microbial utilization of crude glycerol for the production of value-added products. Journal Ind Microbiol Biot 39:217–226.

Dragan CA, Blank LM, Bureik M (2006) Increased TCA cycle activity and reduced oxygen consumption during cytochrome P450-dependent biotransformation in fission yeast. Yeast 23:779–794.

Drăgan C-A, Zearo S, Hannemann F, Bernhardt R, Bureik M (2005) Efficient conversion of 11-deoxycortisol to cortisol (hydrocortisone) by recombinant fission yeast *Schizosaccharomyces pombe*. FEMS Yeast Res 5:621–625.

Driouch H, Melzer G, Wittmann C (2011) Integration of in vivo and in silico metabolic fluxes for improvement of recombinant protein production. Metab Eng 14:47–58.

Driouch H, Roth A, Dersch P, Wittmann C (2010) Optimized bioprocess for production of fructofuranosidase by recombinant *Aspergillus niger*. Appl Microbiol Biotechnol 87:2011–2024.

Egel R (2003) The molecular biology of *Schizosaccharomyces pombe*. Springer.

Eiden-Plach A, Zagorc T, Heintel T, Carius Y, Breinig F, Schmitt MJ (2004) Viral Preprotoxin Signal Sequence Allows Efficient Secretion of Green Fluorescent Protein by *Candida glabrata*, *Pichia pastoris*, *Saccharomyces cerevisiae*, and *Schizosaccharomyces pombe*. Appl Environ Microbiol 70:961–966.

Eraso P, Gancedo JM (1984) Catabolite repression in yeasts is not associated with low levels of cAMP. Eur J Biochem 141:195–198.

Ferrer-Miralles N, Domingo-Espín J, Corchero JL, Vázquez E, Villaverde A (2009) Microbial factories for recombinant pharmaceuticals. Microb Cell Fact 8:17.

Flikweert MT, Van Der Zanden L, Janssen WM, Steensma HY, Van Dijken JP, Pronk JT (1996) Pyruvate decarboxylase: an indispensable enzyme for growth of *Saccharomyces cerevisiae* on glucose. Yeast 12:247–257.

Frick O, Wittmann C (2005) Characterization of the metabolic shift between oxidative and fermentative growth in *Saccharomyces cerevisiae* by comparative 13C flux analysis. Microb Cell Fact 4:30.

Gancedo JM (1998) Yeast Carbon Catabolite Repression. Microbiol Mol Biol Rev 62:334–361.

Gasser B, Sauer M, Maurer M, Stadlmayr G, Mattanovich D (2007) Transcriptomics-based identification of novel factors enhancing heterologous protein secretion in yeasts. Appl Environ Microbiol 73:6499–6507.

Giga-Hama Y, Kumagai H (1998) Foreign gene expression in fission yeast *S. pombe*. Seikagaku 70:300–304.

Gleeson MA, White CE, Meininger DP, Komives EA (1998) Generation of protease-deficient strains and their use in heterologous protein expression. Meth Mol Biol 103:81–94.

Gombert AK, Moreira dos Santos M, Christensen B, Nielsen J (2001) Network identification and flux quantification in the central metabolism of *Saccharomyces cerevisiae* under different conditions of glucose repression. J Bacteriol 183:1441–1451.

Graf A, Dragosits M, Gasser B, Mattanovich D (2009) Yeast systems biotechnology for the production of heterologous proteins. FEMS Yeast Res 9:335–348.

Grobler J, Bauer F, Subden RE, Van Vuuren HJ (1995) The *mae1* gene of *Schizosaccharomyces pombe* encodes a permease for malate and other C4 dicarboxylic acids. Yeast 11:1485–1491.

Guerfal M, Ryckaert S, Jacobs PP, Ameloot P, Van Craenenbroeck K, Derycke R, Callewaert N (2010) The *HAC1* gene from *Pichia pastoris*: characterization and effect of its overexpression on the production of secreted, surface displayed and membrane proteins. Microb Cell Fact 9:49.

Hall MN (1993) The Early Days of Yeast Genetics. Cold Spring Harbor Laboratory Press.

Hamilton SR, Gerngross TU (2007) Glycosylation engineering in yeast: the advent of fully humanized yeast. Curr Opin Microbiol 18:387–392.

Hebert DN, Molinari M (2007) In and out of the ER: protein folding, quality control, degradation, and related human diseases. Physiol Rev 87:1377–1408.

Heiland S, Radovanovic N, Hofer M, Winderickx J, Lichtenberg H (2000) Multiple hexose transporters of *Schizosaccharomyces pombe*. J Bacteriol 182:2153–2162.

Heinzle E, Moes J, Dunn IJ (1985) The influence of cyclic glucose feeding on a continuous bakers' yeast culture. Biotechnol Lett 7:235–240.

Herscovics A, Orlean P (1993) Glycoprotein biosynthesis in yeast. FASEB J 7:540–550.

Heyland J, Fu J, Blank LM, Schmid A (2011) Carbon metabolism limits recombinant protein production in *Pichia pastoris*. Biotechnol Bioeng 108:1942–1953.

Heyland J, Fu J, Blank LM, Schmid A (2010) Quantitative physiology of *Pichia pastoris* during glucose-limited high-cell density fed-batch cultivation for recombinant protein production. Biotechnol Bioeng 107:357–368.

Hoever M, Milbradt B, Hofer M (1992) D-Gluconate is an alternative growth substrate for cultivation of Schizosaccharomyces pombe mutants. Arch Microbiol 157:191–193.

Holmes WJ, Darby RA, Wilks MD, Smith R, Bill RM (2009) Developing a scalable model of recombinant protein yield from *Pichia pastoris*: the influence of culture conditions, biomass and induction regime. Microb Cell Fact 8:35.

Hong E, Davidson AR, Kaiser CA (1996) A pathway for targeting soluble misfolded proteins to the yeast vacuole. J Cell Biol 135:623–633.

Hoskisson PA, Hobbs G (2005) Continuous culture--making a comeback? Microbiology 151:3153–3159.

Hou J, Tyo K, Liu Z, Petranovic D, Nielsen J (2012) Engineering of vesicle trafficking improves heterologous protein secretion in *Saccharomyces cerevisiae*. Metab Eng 14:120–127.

Idiris A, Bi K, Tohda H, Kumagai H, Giga-Hama Y (2006a) Construction of a protease-deficient strain set for the fission yeast *Schizosaccharomyces pombe*, useful for effective production of protease-sensitive heterologous proteins. Yeast 23:83–99.

Idiris A, Tohda H, Bi KW, Isoai A, Kumagai H, Giga-Hama Y (2006b) Enhanced productivity of protease-sensitive heterologous proteins by disruption of multiple protease genes in the fission yeast *Schizosaccharomyces pombe*. Appl Microbiol Biotechnol 73:404–420.

Idiris A, Tohda H, Kumagai H, Takegawa K (2010) Engineering of protein secretion in yeast: strategies and impact on protein production. Microb Cell Fact 86:403–417.

Idiris A, Tohda H, Sasaki M, Okada K, Kumagai H, Giga-Hama Y, Takegawa K (2009) Enhanced protein secretion from multiprotease-deficient fission yeast by modification of its vacuolar protein sorting pathway. Appl Microbiol Biotechnol 85:667-677.

Jansen ML, Krook DJ, De Graaf K, van Dijken JP, Pronk JT, de Winde JH (2006) Physiological characterization and fed-batch production of an extracellular maltase of *Schizosaccharomyces pombe* CBS 356. FEMS Yeast Res 6:888–901.

De Jong-Gubbels P, van Dijken JP, Pronk JT (1996) Metabolic fluxes in chemostat cultures of *Schizosaccharomyces pombe* grown on mixtures of glucose and ethanol. Microbiology 142 (Pt 6:1399–1407.

Jordà J, Jouhten P, Cámara E, Maaheimo H, Albiol J, Ferrer P (2012) Metabolic flux profiling of recombinant protein secreting *Pichia pastoris* growing on glucose:methanol mixtures. Microb Cell Fact 11:57.

Kim I-K, Roldão A, Siewers V, Nielsen J (2012) A systems-level approach for metabolic engineering of yeast cell factories. FEMS Yeast Res 12:228–248.

Kjaerulff S, Jensen MR (2005) Comparison of different signal peptides for secretion of heterologous proteins in fission yeast. Biochem Biophys Res Commun 336:974–982.

Klein T, Heinzle E, Schneider K (2013) Metabolic fluxes in *Schizosaccharomyces pombe* grown on glucose and mixtures of glycerol and acetate. Appl Microbiol Biotechnol 97:5013–5026.

Klement T, Dankmeyer L, Hommes R, van Solingen P, Buchs J, Büchs J (2011) Acetate-glycerol cometabolism: cultivating *Schizosaccharomyces pombe* on a non-fermentable carbon source in a defined minimal medium. J Biosci Bioeng 112:20–25.

Kunicka-Styczynska A (2009) Glucose, L-malic acid and pH effect on fermentation products in biological deacidification. Czech J Food Sci 27:319–322.

Mariño K, Bones J, Kattla JJ, Rudd PM (2010) A systematic approach to protein glycosylation analysis: a path through the maze. Nat Chem Biol 6:713–723.

Martoglio B, Dobberstein B (1998) Signal sequences: more than just greasy peptides. Trends Cell Biol 8:410–415.

Matsumoto S, Bandyopadhyay A, Kwiatkowski DJ, Maitra U, Matsumoto T (2002) Role of the Tsc1-Tsc2 Complex in Signaling and Transport Across the Cell Membrane in the Fission Yeast *Schizosaccharomyces pombe*. Genetics 161:1053–1063.

Matsuyama A, Arai R, Yashiroda Y, Shirai A, Kamata A, Sekido S, Kobayashi Y, Hashimoto A, Hamamoto M, Hiraoka Y, Horinouchi S, Yoshida M (2006) ORFeome cloning and global analysis of protein localization in the fission yeast *Schizosaccharomyces pombe*. Nat Biotechnol 24:841–847.

Matsuzawa T, Fujita Y, Tanaka N, Tohda H, Itadani A, Takegawa K (2011a) New insights into galactose metabolism by *Schizosaccharomyces pombe*: isolation and characterization of a galactose-assimilating mutant. J Biosci Bioeng 111:158–166.

Matsuzawa T, Fujita Y, Tohda H, Takegawa K (2011b) Snf1-like protein kinase Ssp2 regulates glucose derepression in *Schizosaccharomyces pombe*. Eukaryot Cell 11:159–167.

Matsuzawa T, Hara F, Tohda H, Uemura H, Takegawa K (2012) Promotion of glycerol utilization using ethanol and 1-propanol in *Schizosaccharomyces pombe*. Appl Microbiol Biotechnol 95:441–449.

Matsuzawa T, Ohashi T, Hosomi A, Tanaka N, Tohda H, Takegawa K (2010) The *gld1+* gene encoding glycerol dehydrogenase is required for glycerol metabolism in *Schizosaccharomyces pombe*. Appl Microbiol Biotechnol 87:715–727.

Mattanovich D, Branduardi P, Dato L, Gasser B, Sauer M, Porro D (2012) Recombinant protein production in yeasts. Meth Mol Biol 824:329–358.

Mattanovich D, Callewaert N, Rouzé P, Lin Y-C, Graf A, Redl A, Tiels P, Gasser B, De Schutter K (2009) Open access to sequence: browsing the *Pichia pastoris* genome. Microb Cell Fact 8:53.

Mayer K, Temperli A (1963) The Metabolism of L-Malate and Other Compounds by *Schizosaccharomyces Pombe*. Arch Mikrobiol 46:320–328.

Merten O-W, Mattanovich D, Lang C, Larsson G, Neubauer P, Porro D, Postma P, Mattos JT de, Cole JA (2001) Recombinant Protein Production with Prokaryotic and Eukaryotic Cells: A Comparitive View on Host Physiology: Selected Articles from the Meeting of the EFB Sect. Springer.

Morrow K (2007) Improving protein production processes. Gen Eng News 27.

Mukaiyama H, Giga-Hama Y, Tohda H, Takegawa K (2009a) Dextran sodium sulfate enhances secretion of recombinant human transferrin in *Schizosaccharomyces pombe*. Appl Microbiol Biotechnol 85:155–164.

Mukaiyama H, Tohda H, Takegawa K (2009b) Overexpression of protein disulfide isomerases enhances secretion of recombinant human transferrin in *Schizosaccharomyces pombe*. Appl Microbiol Biotechnol 86:1135–1143.

Naumann JM, Kuttner G, Bureik M (2010) Expression and secretion of a CB4-1 scFv-GFP fusion protein by fission yeast. Appl Biochem Biotechnol 163:80–89.

Neunzig I, Göhring A, Drăgan C-A, Zapp J, Peters FT, Maurer HH, Bureik M (2012) Production and NMR analysis of the human ibuprofen metabolite 3-hydroxyibuprofen. J Biotechnol 157:417–420.

Niklas J, Schneider K, Heinzle E (2010) Metabolic flux analysis in eukaryotes. Curr Opin Biotechnol 21:63–69.

Nishikawa S, Brodsky JL, Nakatsukasa K (2005) Roles of molecular chaperones in endoplasmic reticulum (ER) quality control and ER-associated degradation (ERAD). J Biochem 137:551–555.

Nurse P (2002) The Nobel Prize and beyond: an interview with Sir Paul Nurse. EMBO Rep 3:204–206.

Ohmiya R, Yamada H, Nakashima K, Aiba H, Mizuno T (1995) Osmoregulation of fission yeast: cloning of two distinct genes encoding glycerol-3-phosphate dehydrogenase, one of which is responsible for osmotolerance for growth. Mol Microbiol 18:963–973.

Parodi AJ (1999) Reglucosylation of glycoproteins and quality control of glycoprotein folding in the endoplasmic reticulum of yeast cells. Biochim Biophys Acta 1426:287–295.

Patil C, Walter P (2001) Intracellular signaling from the endoplasmic reticulum to the nucleus: the unfolded protein response in yeast and mammals. Curr Opin Cell Biol 13:349–355.

Peinado RA, Moreno JJ, Medina M, Mauricio JC (2005) Potential application of a glucose-transport-deficient mutant of *Schizosaccharomyces pombe* for removing gluconic acid from grape must. J Agric Food Chem 53:1017–1021.

Porro D, Gasser B, Fossati T, Maurer M, Branduardi P, Sauer M, Mattanovich D (2011) Production of recombinant proteins and metabolites in yeasts: when are these systems better than bacterial production systems? Appl Microbiol Biotechnol 89:939–948.

Porro D, Sauer M, Branduardi P, Mattanovich D (2005) Recombinant protein production in yeasts. Mol Biotechnol 31:245–259.

De Queiroz JH, Pareilleux A (1990) Growth kinetics of *Schizosaccharomyces pombe* under various culture conditions: influence of pH, malate, ethanol and oxygenation. Appl Microbiol Biotechnol 33:578–581.

Remize F, Andrieu E, Dequin S (2000) Engineering of the Pyruvate Dehydrogenase Bypass in *Saccharomyces cerevisiae*: Role of the Cytosolic Mg2+ and Mitochondrial K+ Acetaldehyde Dehydrogenases Ald6p and Ald4p in Acetate Formation during Alcoholic Fermentation. Appl Environ Microbiol 66:3151–3159.

Van Rensburg E, den Haan R, Smith J, van Zyl WH, Görgens JF (2012) The metabolic burden of cellulase expression by recombinant *Saccharomyces cerevisiae* Y294 in aerobic batch culture. Appl Microbiol Biotechnol 96:197–209.

Rhind N, Chen Z, Yassour M, Thompson DA, Haas BJ, et al. (2011) Comparative functional genomics of he fission yeasts. Science 332:930–936.

Rieger M, KAPpeli O, Fiechter A (1983) The Role Of Limited Respiration In The Incomplete Oxidation Of Glucose By *Saccharomyces Cerevisiae*. Microbiology 129:653–661.

Rosman KJR, Taylor PDP (1998) Isotopic compositions of the elements 1997 (Technical Report). Pure Appl Chem 70:217–235.

Rude MA, Schirmer A (2009) New microbial fuels: a biotech perspective. Curr Opin Microbiol 12:274–281.

Russell P, Nurse P (1986) *Schizosaccharomyces pombe* and *Saccharomyces cerevisiae*: a look at yeasts divided. Cell 45:781–782.

Sevastsyanovich Y, Alfasi S, Cole J (2009) Recombinant protein production: a comparative view on host physiology. New Biotechnol 25:175–180.

Simanis V (1995) The control of septum formation and cytokinesis in fission yeast. Sem Cell Biol 6:79–87.

Stephanopoulos G (1998) Metabolic engineering: principles and methodology. Elsevier.

Suda Y, Nakano A (2012) The yeast Golgi apparatus. Traffic 13:505–510.

Taillandier P, Strehaiano P (1991) The role of malic acid in the metabolism of *Schizosaccharomyces pombe*: substrate consumption and cell growth. Appl Microbiol Biotechnol 35:541-543.

Tsai CS, Aveledo AJ, McDonald IJ, Johnson BF (1987) Diauxic growth of the fission yeast *Schizosaccharomyces pombe* in mixtures of D -glucose and ethanol or acetate. Can J Microbiol 33:593–597.

Uribelarrea JL, De Queiroz JH, Pareilleux A (1997) Growth of *Schizosaccharomyces pombe* on glucose-malate mixtures in continuous cell-recycle cultures. Kinetics of substrate utilization. Appl Biochem Biotechnol 66:69–81.

Van Urk H, Postma E, Scheffers WA, van Dijken JP (1989) Glucose transport in crabtree-positive and crabtree-negative yeasts. J Gen Microbiol 135:2399–2406.

Van Urk H, Voll WS, Scheffers WA, Van Dijken JP (1990) Transient-State Analysis of Metabolic Fluxes in Crabtree-Positive and Crabtree-Negative Yeasts. Appl Environ Microbiol 56:281–287.

Vemuri GN, Eiteman MA, McEwen JE, Olsson L, Nielsen J (2007) Increasing NADH oxidation reduces overflow metabolism in *Saccharomyces cerevisiae*. Proc Natl Acad Sci U S A 104:2402–2407.

Verduyn C, Postma E, Scheffers WA, van Dijken JP (1990) Energetics of *Saccharomyces cerevisiae* in anaerobic glucose-limited chemostat cultures. J Gen Microbiol 136:405–412.

Verho R, Londesborough J, Penttila M, Richard P (2003) Engineering Redox Cofactor Regeneration for Improved Pentose Fermentation in *Saccharomyces cerevisiae*. Appl Environ Microbiol 69:5892–5897.

Walker GM (1998) Yeast Physiology & Biotechnology. Wiley.

Wiechert W (2001) 13C metabolic flux analysis. Metab Eng 3:195–206.

Wiechert W, Möllney M, Isermann N, Wurzel M, de Graaf AA (1999) Bidirectional reaction steps in metabolic networks: III. Explicit solution and analysis of isotopomer labeling systems. Biotechnol Bioeng 66:69–85.

Van Winden WA, van Dam JC, Ras C, Kleijn RJ, Vinke JL, van Gulik WM, Heijnen JJ (2005) Metabolic-flux analysis of *Saccharomyces cerevisiae* CEN.PK113-7D based on mass isotopomer measurements of (13)C-labeled primary metabolites. FEMS Yeast Res 5:559–568.

Van Winden WA, Wittmann C, Heinzle E, Heijnen JJ (2002) Correcting mass isotopomer distributions for naturally occurring isotopes. Biotechnol Bioeng 80:477–479.

Wittmann C (2002) Metabolic flux analysis using mass spectrometry. Adv Biochem Eng Biot 74:39–64.

Wittmann C, Heinzle E (1999) Mass spectrometry for metabolic flux analysis. Biotechnol Bioeng 62:739–750.

Yang TH, Bolten CJ, Coppi M V, Sun J, Heinzle E (2009) Numerical bias estimation for mass spectrometric mass isotopomer analysis. Anal Biochem 388:192–203.

Yang TH, Frick O, Heinzle E (2008) Hybrid optimization for 13C metabolic flux analysis using systems parametrized by compactification. BMC Syst Biol 2:29.

Zupke C, Stephanopoulos G (1994) Modeling of Isotope Distributions and Intracellular Fluxes in Metabolic Networks Using Atom Mapping Matrixes. Biotechnol Prog 10:489–498.

CHAPTER II

A system of miniaturized stirred bioreactors for parallel continuous cultivation of yeast with online measurement of dissolved oxygen and off-gas

Tobias Klein, Konstantin Schneider and Elmar Heinzle

Abstract

Chemostat cultivation is a powerful tool for physiological studies of microorganisms. We report the construction and application of a set of 8 parallel small-scale bioreactors with a working volume of 10 mL for continuous cultivation. Hungate tubes were used as culture vessels connected to multichannel-peristaltic pumps for feeding fresh media and removal of culture broth and off-gas. Water saturated air is sucked into the bioreactors by applying negative pressure and small stirrer bars inside the culture vessels allow sufficient mixing and oxygen transfer. Optical sensors are used for non-invasive on-line measurement of dissolved oxygen, which proved to be a powerful indicator of the physiological state of the cultures, particularly of steady-state conditions. Analysis of culture exhaust-gas by means of mass spectrometry enables balancing of carbon. The capacity of the developed small-scale bioreactor system was validated using the fission yeast *Schizosaccharomyces pombe*, focusing on the metabolic shift from respiratory to respiro-fermentative metabolism, as well as studies on consumption of different substrates such as glucose, fructose and gluconate.

1. Introduction

The post-genomic era provides a multitude of techniques enabling global studies on genome, proteome and metabolome of prokaryotic and eukaryotic microorganisms. This does not only increase our knowledge and understanding of these microorganisms dramatically but also allowed and accelerated the development of a number of biotechnological processes based on mutant strains created by either classical mutagenesis techniques or rational approaches for genetic and metabolic engineering. To maximize efficiency and productivity of such processes, the physiology of these microorganisms has to be examined in detail regarding important parameters like kinetics of growth and product formation as well as substrate spectra, general nutritional requirements, by-product formation and metabolic flux distribution.

Continuous cultivation is one of the most powerful tools in the research of microbial physiology. Cultivation takes place in a defined and most important constant set of physico-chemical conditions, where environmental parameters like substrate supply, pH or temperature can be controlled and influenced (Hoskisson and Hobbs, 2005). First experiments have been described more than 60 years ago by Monod (1950) and Novick and Szilard (1950). Obviously, more sophisticated technical setups evolved over the years, whereas the basic principle has not changed. Cells are kept at steady state growing with a constant rate and metabolic activity, enabling detailed study of microbial metabolism with single substrate limitation (Hoskisson and Hobbs, 2005) or with additional limitation by oxygen supply that has as strong influence on cellular metabolism but also on the existence and frequency of autonomous oscillations in cultures of *S. cerevisiae* (Furukawa et al., 1983; Heinzle et al., 1983). The major disadvantages of chemostat cultivations are the large amount of time needed to reach steady-state and the high substrate consumption, which can become problematic, if expensive substances are used, e.g. isotopically labeled substrates for ^{13}C metabolic flux analysis (Niklas et al., 2010). Several approaches to solve these problems have been made. An acceleration of experimental procedures can be achieved by using parallel reactors (Akgun et al., 2004; Weuster-Botz, 2005). Reduction of substrate consumption was achieved, decreasing working volumes to 1 ml and less (Hortsch and Weuster-Botz, 2010). However these down-scaled reaction volumes often require specialized sensors for monitoring central process parameters. Non-invasive sensors based on fluorescence dyes are highly sensitive and can be easily applied in a multiplex configuration in shake flasks (Schneider et al., 2010) as well as in microtiter plates (John et al., 2003; Velagapudi et al., 2006). Application of such sensors has been described for monitoring of dissolved oxygen (DO), pH and carbon dioxide concentrations (Berggren et al., 2011; Kusterer

et al., 2008). However small-scale bioreactors are often high-tech and their handling is in no way trivial. An interesting approach has been made by Nanchen et al. (2006), reporting the design of a simple and robust system of parallel bioreactors for continuous cultivation of *E. coli*. Hungate tubes served as cultivations vessels with 10 mL working volume. Media supply and removal of culture broth were performed by two multichannel peristaltic pumps. Aeration was carried out by applying negative pressure and mixing of the broth by rising air bubbles.

Here we report the design of parallel bioreactors inspired by the work of Nanchen et al. (2006) but equipped with online DO-measurement for monitoring culture steady state and active stirring of the culture broth for appropriate mixing and boost of oxygen supply. Online analysis of culture exhaust gas was performed by means of mass spectrometry, providing detailed information about respiratory activity of the cultures and thus allowed determination and balancing of carbon (Heinzle et al., 1990). Biological validation of the bioreactor system was carried out using the fission yeast *Schizosaccharomyces pombe*. *S. pombe* belongs to the Crabtree positive yeasts (Van Urk et al., 1989). When grown on fermentable sugars, the cells exhibit a shift from respiratory metabolism at low dilution rates to respiro-fermentative metabolism at higher dilution rates (De Jong-Gubbels et al., 1996) as observed for other yeasts like *Saccharomyces cerevisiae*. We prove steady state using online DO measurement and at the same time exclude oxygen limitation that would significantly change results (Furukawa et al., 1983). The critical dilution rate D_{crit}, at which this shift occurs and the change of concentrations in biomass and byproducts with increasing dilution rates are typical parameters investigated for such an organism and comparison of our data with the current literature was used to validate our bioreactor system.

2. Material and Methods

2.1 Strains and media

All cultivation experiments were performed with *Schizosaccharomyces pombe* wild type strain 972 h⁻. For continuous cultivation experiments a minimal media was used consisting of [g/L]: NH_4SO_4 5.0; Na_2HPO_4 1.5; KH_2PO_4 12.5; $MgCl_2$ 1.0; NaCl 1.0; $CaCl_2$ 14.0 mg/L. Vitamins and minerals were added to the following final concentrations mg/L: Calcium pantothenate 1.0; Nicotinic acid 10.0; *myo*-Inositol 10.0; Pyridoxine 0.5; Biotin 0.01; $FeSO_4$ 0.7; $ZnSO_4$ 0.8; $MnSO_4$ 0.8; Boric acid 1.0; $CoCl_2$ 1.0; $NaMoO_4$ 5.0; KI 2.0; $CuSO_4$ 0.08. Glucose, fructose and sodium gluconate were used as carbon sources in concentrations of 15 mM. To avoid foaming caused by rising air bubbles, 100 µl/L media of anti-foam reagent (Antifoam 289, Sigma-Aldrich, Taufkirchen, Germany) was added.

2.2 Bioreactor design

Standard Hungate tubes (Ø 16mm; height 125 mm) were used as culture vessels. The tubes were sealed with screw caps containing a butyl rubber septum. Through this septum, three needles with 1 mm inner diameter were inserted into the reaction vessel. An 8-channel peristaltic pump (205U multi-channel cassette pump with CA8 pump head, Watson Marlow Pumps Group, Rommerskirchen, Germany) was used for pumping fresh media into the culture vessel through one of the needles, fixed at middle height of the culture broth. Different dilution rates at the same pumping rate were achieved by using tubes with varying inner diameters. A second peristaltic pump (IsmatecEcoline VC-ground unit with cassette head MS/CA 8-6, Ismatec Laboratoriumstechnik GmbH, Wertheim, Germany) was used for constant removal of culture broth via the second needle. This needle was fixed at a defined height to keep the culture volume at 10 mL. The efflux pump rate was far in excess of the feeding rate, generating a slight negative pressure inside the culture vessel. The pressure difference between culture vessel and atmospheric pressure was 11.3 ± 0.5 mmH₂0 (0.01% difference). This negative pressure was used for passive aeration of the bioreactor. Pharmed BPT tubes (Ismatec Laboratoriumstechnik GmbH, Wertheim, Germany) with an inner diameter of 1.30 mm were used. The gas flow rate was determined for different pump rates using a positive displacement unit consisting of a pipette, a tee connector and a soap solution reservoir connected to the gas outlet during cultivation. A linear correlation between pump rate and gas flow rate was obtained. The aeration rate differed by 0.24% during the course of one cultivation. When an aeration rate of

10 mL/min was applied, the aeration rate differed by 1.3% between the bioreactors. Variation was determined from three independent cultivations.

Sterile, water-saturated air was sucked into the tube via the third needle leading to the bottom of the culture vessel close to the magnetic stirrer bar. Due to culture vessel dimensions a disc-like magnetic bar (Ø 9 mm, height 6 mm) was chosen for stirring (Rotilabo LT59.1, Carl Roth GmbH, Karlsruhe, Germany). The culture vessels were positioned into a tray for Hungate tubes and completely dipped into a controlled water bath to maintain 30°C cultivation temperature. Magnetic coupling of the stirrer bars was achieved by magnetic stirrers fixed at the bottom of the tray (Variomag Micro stirrer, Thermo Scientific, Braunschweig, Germany) The stirrers were controlled by a control unit (Telemodul 20C, Thermo Scientific, Braunschweig, Germany) allowing stirring rates up to 2000 rpm. A schematic drawing of a bioreactor is shown in Figure II-1. The system allowed parallel execution of 8 continuous cultivations experiments at once.
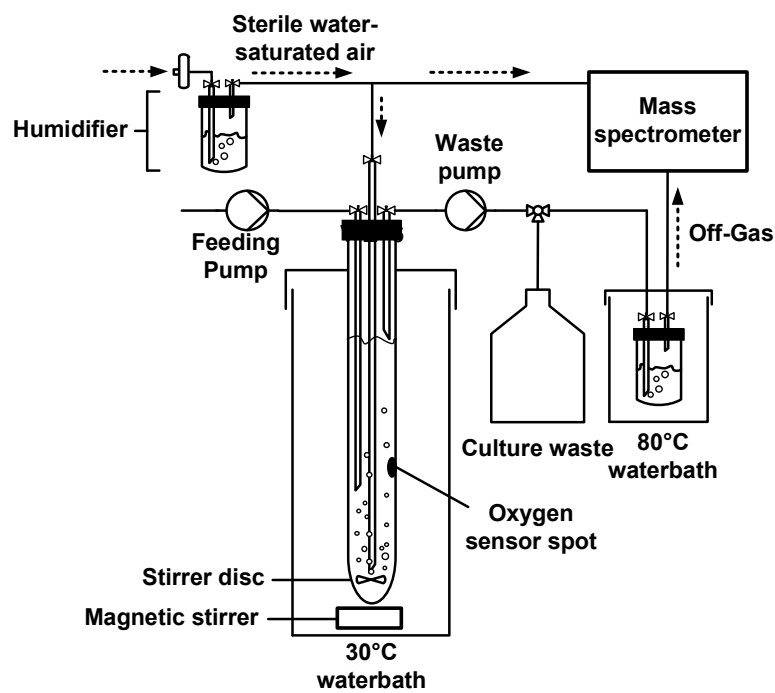
Figure II-1: Schematic setup of bioreactor. Shown is one unit out of eight.

2.3 Measurement of dissolved oxygen concentration (DO)

A O_2 fluorescent sensor spot (PreSens Precision Sensing GmbH, Regensburg, Germany) was glued on the inner surface of the tube wall. An optical fiber was attached at the outside of the culture vessel in front of the sensor spot via a rubber cuff. This cuff was constructed as cylinder exhibiting a shaft for positioning the optical fiber allowing water free positioning of the fiber at the outside of the vessel. However water between the outside of the vessel and the optical fiber did not disturb the measurements of DO. The optical waveguide connected the sensor with the oxygen meter (OXY-4-Meter, PreSens Precision Sensing GmbH, Regensburg, Germany). Data were collected and evaluated using the software OXY-4 mini ver. 2.30FB.

2.4 Determination of the volumetric mass transfer coefficient (k_La)

k_La values of the bioreactors were calculated from cultivations of *S. pombe* under respiratory conditions ($D = 0.1$ h^{-1}) using equation (1) as described previously (Mavituna and Sinclair, 1985).

$$k_L a = OUR \, (c_L{}^* - c_L)^{-1} \qquad\qquad (1)$$

Where OUR is the volumetric oxygen uptake rate [$mmolL^{-1}h^{-1}$], $c_L{}^*$ is the saturation concentration of oxygen [$mmol \, L^{-1}$] under applied conditions and c_L is the actual dissolved oxygen concentration [$mmol \, L^{-1}$]. Corrected values for Henry constants were taken from Atkinson and Mavituna (1991). Each k_La value was determined in triplicates and the propagation of error was considered (Heinzle et al., 1990).

2.5 Off-gas analysis

Exhaust gas and culture broth were removed from the culture via one single efflux tube. Therefore, culture broth and gas had to be separated prior to off-gas analysis. A 3-way-stopcock was used to switch between the main vessel for culture waste and a 50 mL bottle placed in a water bath tempered at 80°C. The bottle was filled with 25 mL water and exhibited two gastight in/outlets. Culture broth and exhaust gas were directly injected into the preheated water causing immediate inactivation of cellular metabolism. The exhaust gas was directed to the mass spectrometer via a reflux condenser to remove the high water content. Gas composition was determined with an Omnistar QMS 422 mass spectrometer (Inficon, Vaduz, Lichtenstein) as

described before (Wittmann et al., 2002). For statistical evaluation, propagation of error was calculated and considered for all measurements (Heinzle et al., 1990).

2.6 Determination of optical density (OD) and cell dry weight (CDW)

Optical density of the cultures was determined at 595 nm with a Nova Spec II Photometer (Pharmacia Biotech, Dübendorf, Switzerland). Correlation between optical density and cell dry weight was dependent on the carbon source: CDW on glucose and fructose = OD_{595} x 0.62 g L^{-1}; CDW on sodium gluconate = 0.53 g L^{-1}.

2.7 Product and substrate analysis

Composition of culture supernatant was determined by HPLC as described before (Fonseca et al., 2007). Ethanol was determined enzymatically (Ethanol UV method, Cat No 10176290035, R-Biopharm, Darmstadt, Germany). Measurements were performed at least in duplicates. For statistical evaluation confidence intervals with 95% confidence level were calculated.

3. Results and Discussion

3.1 Development of the small-scale cultivation system

The aim of this study was the development of a robust and reliable small-scale system for parallel continuous cultivation of microorganisms. Here Hungate tubes served as cultivation vessels and feeding, aeration and removal of culture broth were realized by two multi-channel peristaltic pumps as described elsewhere (Nanchen et al., 2006). Small stirrer discs guaranteed sufficient power input and boosted oxygen transfer compared to an unstirred system. Aerobic cultivation conditions were assured by online-measurement of DO concentrations.

To ensure that the working volume of the bioreactors remained constant during the course of a cultivation, a bioreactor filled with media running at $D = 0.1$ h^{-1} and an aeration rate of 1 vvm was placed on a balance for 24 h. During this time, the weight changes, corresponding to changes in the culture working volume were $\pm$ 0.14% of the working volume, thus indicating that the design applied results in bioreactors maintaining a constant working volume.

Control of pH is an important parameter in any microbial process. Conventional bioreactors therefore are equipped with a pH control system counteracting pH shifts by addition of acid or base. Implementing such a system to our small-scale bioreactors would increase the complexity severely and thereby the difficulties of handling the system. An easier approach is the choice of a strong buffer to keep pH in a suitable range throughout the entire cultivation. We used a 100 mM phosphate buffer, and confirmed in growth experiments in shake flask that the high phosphate concentration in the media had no negative influence on cellular growth (data not shown). Fission yeast is able to grow over a wide pH-range of 3-6 (De Queiroz and Pareilleux, 1990). Therefore media pH was adjusted to 5.5 for glucose and fructose cultivations and 3.8 for cultivations using gluconate. Culture broth pH was measured for all cultivations, and even at the highest cell densities reached during pure respiratory growth the pH shift was one unit at most (TableII-1). As a result we could show that 100 mM phosphate buffer is sufficient to keep pH in suited ranges within the described bioreactor system.

Table II-1: pH values of media and culture broth with a 100 mM phosphate buffer for pH control. Shown are the values for cultivation of *S. pombe* on glucose, fructose and gluconate under respiratory conditions ($D = 0.1$ h^{-1}).

substrate	media pH	pH in the bioreactor
Glucose	5.5	4.6 ± 0.05
Fructose	5.5	4.7 ± 0.08
Gluconate	3.8	4.1 ± 0.06

3.2 DO as indicator of metabolic steady state

Metabolic steady state conditions in chemostat cultivations can be characterized by constant concentrations of biomass and extracellular metabolites in the bioreactor over time as well as a steady state concerning metabolic rates, intracellular pool sizes and pathway activities (Hoskisson and Hobbs, 2005). Application of small cultivation volumes restricts sampling in terms of sample volume and frequency since large volume changes disturb the physiological steady state of the culture. It was shown earlier that DO is a very sensitive detector of metabolic steady state since even minute sustained oscillations in a culture of *S. cerevisiae* could exclusively be seen by oscillatory DO whereas other typical culture variables were constant (Heinzle et al., 1983). To verify whether dissolved oxygen (DO) can be used as reliable indicator of a steady state in this bioreactor configuration as well, continuous cultivation experiments with *S. pombe* using glucose as sole carbon source were performed at a dilution rate of 0.1 h^{-1} and an aeration rate of 1 vvm. Small samples of 50 µl (0.5% of total culture volume) for OD determination were taken by piercing the septum with a Hamilton syringe. A clear correlation between constant DO values and constant values for CDW (Figure II-2) was proving the applicability of DO as a sensitive and reliable indicator of metabolic steady state.
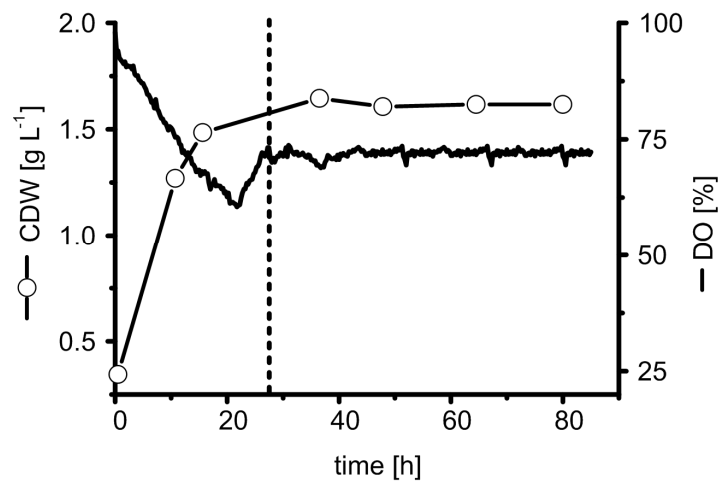
Figure II-2: Correlation between progression of in dissolved oxygen concentration (DO) and biomass (CDW) during cultivation with D = 0.1 h^{-1} and an aeration rate of 1 vvm. A clear correlation between constant biomass yield corresponding metabolic steady state of the culture and constant DO concentrations can be seen. Dotted line shows entry into steady state phase.

3.3 Influence of stirring rates on mass transfer

Non-stirred versions of the described bioreactors required aeration rates of 2.5 vvm to ensure aerobic cultivation conditions and avoid sedimentation of yeast cells (data not shown). The same applies to comparable systems using non-stirred bioreactors for cultivation of *E. coli* cells (Nanchen et al., 2006), where culture density is even more limited due to the higher specific oxygen uptake rate of *E. coli* compared to yeast. On the other hand mass transfer is significantly increased by mechanical energy input using a stirrer (Joshi et al., 1982; Kumar et al., 2004). The application of magnetic stirrers complicates reactor design only marginally. On the other hand low aeration rates are preferable for exhaust gas analysis since larger difference between inlet and off-gas concerning consumed oxygen and produced carbon dioxide are achieved that is required for accurate determination of oxygen uptake rates (Heinzle et al., 1990). Stirring of bioreactors allowed a 2.5-fold decrease of the aeration rate to 1 vvm in respiratory cultures of *S. pombe*. Comparing of DO signals from non-stirred and stirred bioreactors indicated reduced perturbations in DO time course when using the stirrer, especially during the steady state of the culture after 20 h of cultivation. Moreover the drop of DO during batch phase (first 18 h) is less pronounced, further proofing the improved oxygen transfer in case of the stirred reactor (Figure II-3).
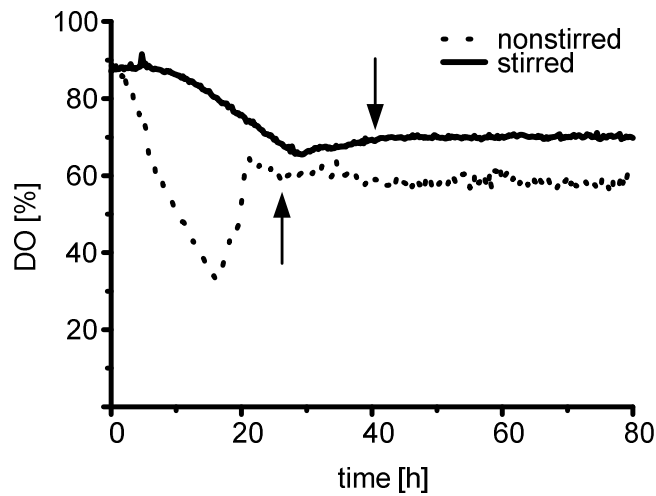
Figure II-3: Comparison of changes in dissolved oxygen concentrations during cultivation in stirred and non-stirred bioreactors applying a dilution rate of D = 0.1h $^{-1}$. The stirred bioreactor was aerated with a gas flow rate of 1 vvm, the non-stirred version with 2.5 vvm. Arrows indicate start of steady state phase.

To determine oxygen mass transfer into the liquid phase of the bioreactors, k_La values were determined applying varying stirring rates. Fission yeast was cultivated on glucose under respiratory conditions (D = 0.1 h^{-1}) with the desired aeration rate of 1 vvm. During steady state, the stirring rate was stepwise decreased from 2000 rpm to 1000 rpm and the decrease of the DO concentration was monitored (Figure II-4A). DO concentrations decreased with decreasing stirring rates but always leveled out at stable plateaus, indicating proper mixing and aerobic growth conditions for all stirring rates, since DO concentrations did not drop below 20% air saturation. k_La values were between 48.5 ± 0.2 h^{-1} at 2000 rpm and 26.8 ± 0.2 h^{-1} at 1000 rpm and increased proportionally with increasing stirrer speed (Figure II-4B). Within the used range of stirrer speed ranging from 1000 to 2000 min^{-1}, we observed a linear relationship which might change to a nonlinear one using a broader range of stirrer speed. Increasing the stirrer speed *n* should result in a corresponding increase in the k_La value with a power between 2 and 3, depending on geometry, fluid characteristics, stirrer, etc (Joshi et al., 1982). The unexpected observed linear correlation may be a result of the applied narrow range of stirrer speed.
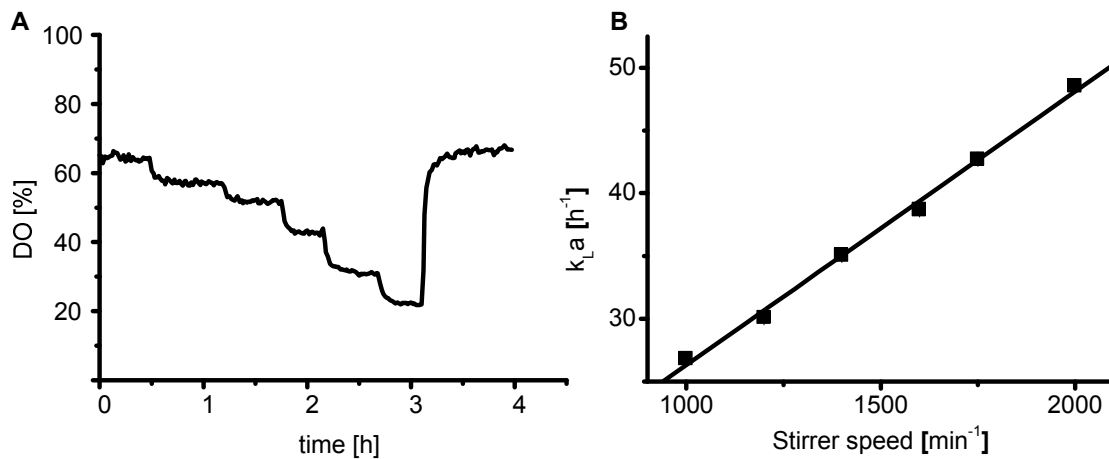
Figure II-4: A) Changes of dissolved oxygen concentration during cultivation at $D = 0.1$ h^{-1} and an aeration rate of 1 vvm while stepwise decreasing the stirrer speed; **B)** $k_L a$ values of the bioreactors at different stirrer speeds determined during cultivation of yeast cells under respiratory growth conditions $(D = 0.1$ $h^{-1})$ using equation 1.

3.4 Validation of exhaust gas analysis in the small-scale bioreactor system

S. pombe was cultivated on glucose, fructose and gluconate under respiratory conditions $(D = 0.1$ $h^{-1})$ and DO progression was monitored verifying the growth behavior of the culture. Exhaust gas analysis of each bioreactor was performed for at least 3 h before bioreactors were completely harvested to determine CDW and extracellular metabolites during stationary growth of the cultures. Proper determination of oxygen uptake rates (OUR) and carbon dioxide production rates (CPR) is dependent on the accurate determination and control of the aeration rate as well as the precise analysis of the gas composition. Therefore extracellular carbon was balanced to validate the sensitivity and accuracy of the applied analytics, especially exhaust gas analysis (Table II-2).

All analyses were performed in duplicates. For all substrates carbon recoveries over 95% were achieved, indicating that the aeration rates and CPRs were determined correctly. Concentrations of oxygen and carbon dioxide differed around 5% at most, showing that exhaust gas analysis produced reliable results with only minor deviations between parallel cultivations.

Table II-2: Carbon balances for cultivations of *S. pombe* with different substrates under respiratory growth conditions ($D = 0.1 \text{ h}^{-1}$). n.d.: not detectable.

Product	Yield [Cmol Cmol^{-1}]		
	Glucose	**Fructose**	**Gluconate**
Biomass	0.58 ± 0.0	0.57 ± 0.01	0.49 ± 0.01
CO$_2$	0.36 ± 0.02	0.40 ± 0.01	0.44 ± 0.01
Ethanol	n.d.	n.d.	n.d.
Pyruvate	0.016 ± 0.0	0.004 ± 0.0	0.026 ± 0.0
Acetate	0.002 ± 0.0	0.003 ± 0.0	0.015 ± 0.0
Glycerol	0.001 ± 0.0	0.002 ± 0.0	0.01 ± 0.0
Carbon recovery [%]	**96.4 ± 1.8**	**98.5 ± 1.0**	**97.9 ± 1.6**

3.5 Characterization of different respiratory physiologies on glucose, fructose and gluconate

With the reliability of the analytics secured, the different physiologies of *S. pombe* under respiratory growth conditions on the substrates glucose, fructose and gluconate could be investigated (Table II-3). No ethanol was detected in any of the culture supernatants. The absence of this typical fermentation product is a strong indicator for respiratory growth (De Jong-Gubbels et al., 1996). When cells were grown on glucose, small amounts of pyruvate (32 mmol mol glucose^{-1}) could be detected in the culture supernatant as well as traces of acetate and glycerol. Exhaust gas analysis yielded a carbon dioxide production rate of 2.39 ± 0.05 mmol g CDW^{-1} h^{-1} and an oxygen uptake rate of 2.34 ± 0.09 mmol g CDW^{-1} h^{-1}. The biomass yield on glucose was 90.1 ± 0.7 g CDW mol^{-1} and the respiratory quotient (RQ) was determined at 1.03 ± 0.05, indicating respiratory growth. Further cultivations were performed with fructose and gluconate, since both substrates are readily available to *S. pombe* when growing in its natural habitats (Brown et al., 2011). Especially gluconate is an interesting carbon source, since *S. pombe* is able to grow efficiently on high concentrations of this sugar acid in contrast to other yeast species e.g. *Saccharomyces cerevisiae* (Mehta et al., 1998).

Several studies concerning gluconate uptake and metabolization by *S. pombe* have been accomplished in the past but mainly addressed the topic on a biochemical level (Caspari, 1997; Caspari and Urlinger, 1996). This work rather focused on the physiological part of the metabolization of these different substrates.

As expected, growth on fructose showed only slight differences compared to growth on glucose. The yields of extracellular metabolites in the culture supernatant did not differ from the results obtained for glucose cultivations, as both sugars are metabolized in more or less the same way. Only a slight increase in specific oxygen uptake to 2.69 ± 0.11 mmol g CDW^{-1} h^{-1} and carbon dioxide production to 2.75 ± 0.04 mmol g CDW^{-1} h^{-1} compared to cultivations on glucose was observed.

However, growth on gluconate was partially different. Compared to cultivations on carbohydrates, levels of extracellular pyruvate increased 1.6 fold. Acetate and glycerol increased 5 fold and 10 fold. In contrast, the biomass yield on gluconate decreased to 76.0 ± 1.4 g/mol. The specific CO_2 production rate increased to 3.4 ± 0.08 mmol g CDW^{-1} h^{-1} while the oxygen uptake rate was determined at 2.49 ± 0.12 mmol g CDW^{-1} h^{-1}. Consequently the RQ increased to 1.37 ± 0.08. Gluconate assimilation involves conversion to 6-phosphogluconate in the first step and further decarboxylation to ribulose-5-phosphate (Mehta et al., 1998), yielding 1 mol CO_2 per mol gluconate, thus explaining the lower biomass yield due to the carbon loss accompanying gluconate metabolization and the increased RQ value compared to glucose and fructose metabolization.

Table II-3: Physiological characteristics of cultivations of glucose, fructose and gluconate under respiratory growth conditions (D = 0.1 h^{-1}).

substrate	q_s [mmol g CDW^{-1} h^{-1}]	q_{O2} [mmol g CDW^{-1} h^{-1}]	q_{CO2} [mmol g CDW^{-1} h^{-1}]	$Y_{x/s}$ [g CDW mol^{-1}]	RQ
Glucose	1.10 ± 0.05	2.34 ± 0.09	2.39 ± 0.05	90.13 ± 0.65	1.03 ± 0.05
Fructose	1.13 ± 0.04	2.69 ± 0.11	2.75 ± 0.04	88.39 ± 1.11	1.02 ± 0.06
Gluconate	1.29 ± 0.04	2.49 ± 0.12	3.40 ± 0.08	76.04 ± 1.4	1.37 ± 0.08

3.6 Characterization of metabolic shift from respiratory to respiro-fermentative metabolism

S. pombe was cultivated on glucose at different dilution rates to monitor the shift from a completely respiratory metabolism towards a respiro-fermentative metabolism (Figure II-5). For all cultivations closed carbon balances as shown above were observed.

The cells exhibited a respiratory metabolism up to a dilution rate of 0.16 h^{-1}, characterized by the absence of ethanol in the culture supernatant and a RQ close to 1. Above this critical dilution rate D_{crit}, a shift towards a respiro-fermentative metabolism occurred. This shift was characterized by the onset of ethanol production up to a maximum specific production rate q_{EtOH} of 9.24 ± 0.4 mmol g CDW^{-1} h^{-1} at a dilution rate of $D = 0.24$ h^{-1} . As a consequence the biomass yield decreased sharply, reaching a minimum of 34.3 ± 1.2 g CDW mol^{-1}. Above D_{crit} CO_2 production increased while oxygen uptake decreased at the same time, resulting in a sharply increasing RQ. The maximum RQ value at $D = 0.24$ h^{-1} was determined at 5.06 ± 0.05.
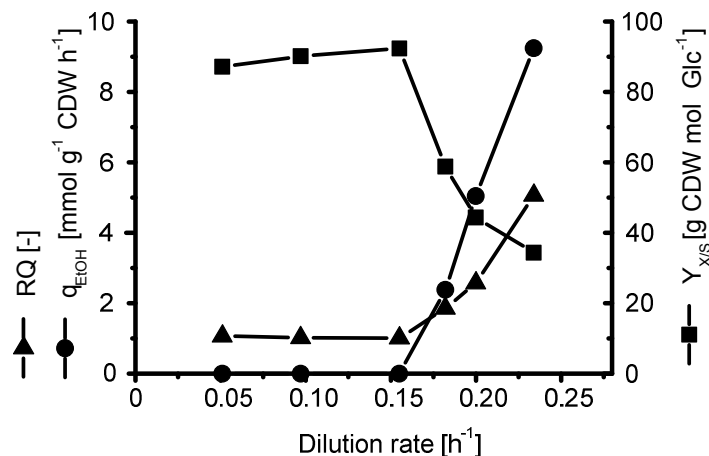
Figure II-5: Shift from respiratory metabolism to respiro-fermentative metabolism during cultivation of fission yeast on glucose at different dilution rates. For all cultivations the following parameters applied: working volume 10 mL; aeration rate: 1 vvm; stirrer speed 2000 min^{-1}.

The results obtained in this work concerning the respiratory growth on glucose as well as the shift to fermentative metabolism at dilution rates above 0.16 h^{-1} were in good accordance with data published earlier (De Jong-Gubbels et al., 1996; Uribelarrea et al., 1993). This supports the

design applied to the development of a parallel small-scale bioreactor system for continuous cultivation, especially the off gas analysis.

4. Conclusion

We present the setup and application of a system of small-scale bioreactors applicable for continuous cultivation of yeast, inspired by the work of Nanchen et al. (2006). The parallel use of 8 bioreactors allows the performance of a large range of experiments in a very short time. The design of the reactors also permits online gas analysis using mass spectrometry allowing gas balancing that is essential for a comprehensive physiological characterization of cells, for example respiratory quotient as well as carbon balancing. The small volume of 10 mL drastically decreases the working costs compared to standard fermentation units working at volumes of 100-1000 mL. This is of special importance if expensive substrates like isotopically labeled substances are used, e.g. in ^{13}C assisted metabolic flux analysis (Niklas et al., 2010; Velagapudi et al., 2007).

The obtained k_La values that are below those of well-stirred laboratory bioreactors somewhat limit the system to low cell dry weight concentrations. However, the system is well suited for physiological studies since all common experiments applied in this context can be carried out with the biomass created in the described small scale reactor system. The cell dry weight can be increased to a certain extent applying pure oxygen for aeration or by increasing the aeration rate in this system.

A number of parallel bioreactors systems for the cultivation of microorganisms operating on batch or chemostat mode has been described in literature, ranging from volumes of 200 ml to 0.1 ml (Weuster-Botz, 2005; Zhang et al., 2006b). Also the number of parallelization differs from 2 (Betts et al., 2006) up to 48 parallel running bioreactors (Puskeiler et al., 2005). A critical point with these small scale systems is process monitoring and process control. We used fluorescence sensors for non-invasive DO measurement which are an appropiate solution to the problem, allowing to monitor various process parameters (Zhang et al., 2006a).

We put special emphasis on the possibility to measure culture off gas in our bioreactor system since it is an important tool to determine crucial physiological respiration parameters like oxygen consumption and CPRs and to validate the accuracy of analytics and data consistency by carbon balancing. Various approaches for off gas analysis exist, either by mass spectrometry

(Heinzle et al., 1990), photometrically (Beuermann et al., 2011) or by means of electrochemical sensors (Van Leeuwen et al., 2010). Mass spectrometry, however, also permits the determination of isotopomers, which can be of advantage when isotopically labeled substrates are used.

However, many of the applied bioreactor techniques and sensors are very sophisticated and their use as well as the data interpretation is in no way trivial. Under this point of view, the bioreactor system described by Nanchen et al. (2006) was a straightforward yet well working approach for parallel continuous cultivation of microorganisms in small scale. The aim of this study was to develop this system further by adding small stirrers to improve mixing of the bioreactors and mass transfer into the liquid phase. The use of optical sensor for DO measurement allowed on-line monitoring of metabolic steady state of the culture without any interference and off gas analysis by mass spectrometry was a powerful tool for carbon balancing and respiration studies.

Finally, the system was kept as simple as possible in design and we put special emphasis on strict utilization of commercially available standard equipment. This should allow the possibility for other laboratories to set up a comparable system for parallel small-scale cultivation of yeast and other microorganisms.

5. Acknowledgements

6. Literature

Akgun A, Maier B, Preis D, Roth B, Klingelhofer R, Buchs J. 2004. A novel parallel shaken bioreactor system for continuous operation. *Biotechnol Prog* **20**:1718–1724.

Atkinson B, Mavituna F. 1991. Biochemical engineering and biotechnology handbook 2nd Ed. NY: Stockton Press; 1271 p.

Berggren M, Lapierre JF, Del Giorgio PA. 2011. Magnitude and regulation of bacterioplankton respiratory quotient across freshwaters environmental gradients. *ISME Journal*:1–10.

Betts JI, Doig SD, Baganz F. 2006. Characterization and application of a miniature 10 mL stirred-tank bioreactor, showing scale-down equivalence with a conventional 7 L reactor. *Biotechnol Prog* **22**:681–688.

Beuermann T, Egly D, Geoerg D, Klug KI, Storhas W, Methner FJ. 2011. On-line carbon balance of yeast fermentations using miniaturized optical sensors. *J Biosci Bioeng* **113**:399–405.

Brown WR, Liti G, Rosa C, James S, Roberts I, Robert V, Jolly N, Tang W, Baumann P, Green C, Schlegel K, Young J, Hirchaud F, Leek S, Thomas G, Blomberg A, Warringer J. 2011. A Geographically Diverse Collection of *Schizosaccharomyces pombe* Isolates Shows Limited Phenotypic Variation but Extensive Karyotypic Diversity. *G3 (Bethesda,Md.)* **1**:615–626.

Caspari T. 1997. Onset of gluconate-H+ symport in *Schizosaccharomyces pombe* is regulated by the kinases Wis1 and Pka1, and requires the gti1+ gene product. *J Cell Sci* **110**:2599–2608.

Caspari T, Urlinger S. 1996. The activity of the gluconate-H+ symporter of *Schizosaccharomyces pombe* cells is down-regulated by D-glucose and exogenous cAMP. *FEBS Lett* **395**:272–276.

Fonseca GG, Gombert AK, Heinzle E, Wittmann C. 2007. Physiology of the yeast *Kluyveromyces marxianus* during batch and chemostat cultures with glucose as the sole carbon source. *FEMS Yeast Res* **7**:422–435.

Furukawa K, Heinzle E, Dunn IJ. 1983. Influence of oxygen on the growth of *Saccharomyces cerevisiae* in continuous culture. *Biotechnol Bioeng* **25**:2293–2317.

Heinzle E, Dunn IJ, Furukawa K, Tanner RD. 1983. Modelling of sustained oscillations observed in continuous culture of *Saccharomyces cerevisiae* . *IFAC PROC SER* **31**:57–65.

Heinzle E, Oeggerli A, Dettwiler B. 1990. On-line fermentation gas analysis: error analysis and application of mass spectrometry. *Anal Chim Acta* **238**:101–115.

Hortsch R, Weuster-Botz D. 2010. Milliliter-scale stirred tank reactors for the cultivation of microorganisms. *Adv Appl Microbiol* **73**:61–82.

Hoskisson PA, Hobbs G. 2005. Continuous culture--making a comeback? *Microbiology* **151**:3153–3159.

John GT, Goelling D, Klimant I, Schneider H, Heinzle E. 2003. PH-sensing 96-well microtitre plates for the characterization of acid production by dairy starter cultures. *J Dairy Res* **70**:327–333.

De Jong-Gubbels P, Van Dijken JP, Pronk JT. 1996. Metabolic fluxes in chemostat cultures of *Schizosaccharomyces pombe* grown on mixtures of glucose and ethanol. *Microbiology* **142 (Pt 6**:1399–407.

Joshi JB, Pandit AB, Sharma MM. 1982. Mechanically agitated gas-liquid reactors. *Chem Eng Sci* **37**:813–844.

Kumar S, Wittmann C, Heinzle E. 2004. Minibioreactors. *Biotechnol Lett* **26**:1–10.

Kusterer A, Krause C, Kaufmann K, Arnold M, Weuster-Botz D. 2008. Fully automated single-use stirred-tank bioreactors for parallel microbial cultivations. *Bioprocess Biosyst Eng* **31**:207–215.

Lee KS, Boccazzi P, Sinskey AJ, Ram RJ. 2011. Microfluidic chemostat and turbidostat with flow rate, oxygen, and temperature control for dynamic continuous culture. *Lab Chip* **11**:1730–1739.

Van Leeuwen M, Krommenhoek EE, Heijnen JJ, Gardeniers H, Van der Wielen LA, Van Gulik WM. 2010. Aerobic batch cultivation in micro bioreactor with integrated electrochemical sensor array. *Biotechnol Prog* **26**:293–300.

Mavituna F, Sinclair CG. 1985. A grpaical method for the determination of critical biomass concentration for non-oxygen-limited growth. *Biotechnol Lett* **7**:69–74.

Mehta S, Velmurugan S, Lobo Z. 1998. Repression of enzymes of the pentose phosphate pathway by glucose in fission yeast. *FEBS Lett* **440**:430–433.

Monod J. 1950. Continuous culture technique: Theory and applications. *Ann. Inst. Pasteur*:390–410.

Nanchen A, Schicker A, Sauer U. 2006. Nonlinear dependency of intracellular fluxes on growth rate in miniaturized continuous cultures of *Escherichia coli*. *Appl Environ Microbiol* **72**:1164–1172.

Niklas J, Schneider K, Heinzle E. 2010. Metabolic flux analysis in eukaryotes. *Curr Opin Biotechnol* **21**:63–69.

Novick A, Szilard L. 1950. Experiments with the Chemostat on spontaneous mutations of bacteria. *Proc Natl Acad Sci U S A* **36**:708–719.

Puskeiler R, Kaufmann K, Weuster-Botz D. 2005. Development, parallelization, and automation of a gas-inducing milliliter-scale bioreactor for high-throughput bioprocess design (HTBD). *Biotechnol Bioeng* **89**:512–523.

De Queiroz JH, Pareilleux A. 1990. Growth kinetics of *Schizosaccharomyces pombe* under various culture conditions: influence of pH, malate, ethanol and oxygenation. *Appl Microbiol Biotechnol* **33**:578–581.

Schneider K, Schutz V, John GT, Heinzle E. 2010. Optical device for parallel online measurement of dissolved oxygen and pH in shake flask cultures. *Bioprocess Biosyst Eng* **33**:541–547.

Uribelarrea JL, De Queiroz H, Goma G, Pareilleux A. 1993. Carbon and energy balances in cell-recycle cultures of *Schizosaccharomyces pombe*. *Biotechnol Bioeng* **42**:729–736.

Van Urk H, Postma E, Scheffers WA, Van Dijken JP. 1989. Glucose transport in crabtree-positive and crabtree-negative yeasts. *J Gen Microbiol* **135**:2399–2406.

Velagapudi VR, Wittmann C, Lengauer T, Talwar P, Heinzle E. 2006. Metabolic Screening of *Saccharomyces cerevisiae* Single Knockout Strains Reveals Unexpected Mobilization of Metabolic Potential. *Process Biochem.* **41**:2170–2179.

Velagapudi VR, Wittmann C, Schneider K, Heinzle E. 2007. Metabolic flux screening of *Saccharomyces cerevisiae* single knockout strains on glucose and galactose supports elucidation of gene function. *J Biotechnol* **132**:395–404.

Weuster-Botz D. 2005. Parallel reactor systems for bioprocess development. *Adv Biochem Eng Biotechnol* **92**:125–143.

Wittmann C, Hans M, Bluemke W. 2002. Metabolic physiology of aroma-producing *Kluyveromyces marxianus*. *Yeast* **19**:1351–1363.

Zhang Z, Boccazzi P, Choi HG, Perozziello G, Sinskey AJ, Jensen KF. 2006a. Microchemostat-microbial continuous culture in a polymer-based, instrumented microbioreactor. *Lab Chip* **6**:906–913.

Zhang Z, Szita N, Boccazzi P, Sinskey AJ, Jensen KF. 2006b. A well-mixed, polymer-based microbioreactor with integrated optical measurements. *Biotechnol Bioeng* **93**:286–296.

CHAPTER III

Metabolic fluxes in *Schizosaccharomyces pombe* grown on glucose and mixtures of glycerol and acetate

Tobias Klein, Elmar Heinzle and Konstantin Schneider

Abstract

Growth on glycerol has already been a topic of research for several yeast species and recent publications deal with the regulatory mechanisms of glycerol assimilation by the fission yeast *Schizosaccharomyces pombe*. We investigated glycerol metabolism of *S. pombe* from a physiological point of view, characterizing growth and metabolism on a mixture of glycerol and acetate and compared it to growth on glucose under respiratory growth conditions in chemostat experiments. On glycerol/acetate mixtures the cells grew with a maximum specific growth rate of 0.11 h^{-1} where 46% of the carbon was channeled into biomass and the key fermentation product ethanol was not detectable. ^{13}C assisted metabolic flux analysis resolved substrate distributions through the central carbon metabolism, proofing that glycerol is used as precursor for glycolysis, gluconeogenesis and the pentose phosphate pathway while acetate enters the tricarboxylic acid cycle via acetyl-CoA. Considering compartmentalization between cytosol and mitochondria in the metabolic model, we found compartmentalization of biosynthesis for the amino acids aspartate and leucine. Balancing of redox cofactors revealed an abundant production of cytosolic NADPH that must be finally regenerated via the respiratory chain shown by the simulated and measured CO_2 production and oxygen consumption rates which were in good agreement.

1. Introduction

With numbers of bio-based industrial processes continuously increasing, the need for renewable feedstock is rising in order to guarantee the sustainability of these processes for the years to come. Crude glycerol, a waste product from biodiesel production, has come to attention recently as affordable and widely available carbon source for microbial bioprocesses (Rumbold et al. 2010). Various prokaryotic and eukaryotic microorganisms are able to use glycerol as carbon source (Dobson et al. 2012) and its successful application for the industrially relevant yeasts *Saccharomyces cerevisiae* and *Pichia pastoris* has been described (Ferreira et al. 2012; Yu et al. 2012). Recently, the utilization of glycerol as carbon source and the underlying regulatory network in the fission yeast *Schizosaccharomyces pombe* have come into the focus of research. In contrast to other yeasts, *S. pombe* is unable to grow on glycerol as sole carbon source (Matsuzawa et al. 2010). The first steps of glycerol metabolization in *S. pombe* involve the oxidation to dihydroxyacetone (DHA) via glycerol dehydrogenase encoded by *gld1* and further phosphorylation via DHA kinase, encoded by the genes *dak1* and *dak2,* to dihydroxyacetone phosphate (DHAP) (Matsuzawa et al. 2010). These genes as well as the gene for fructose-1,6-bisphosphatase *fbp1* are subject to glucose catabolite repression (Matsuzawa et al. 2012; Matsuzawa et al. 2011). Glycerol itself does not induce expression of these key enzymes (Matsuzawa et al. 2012), explaining to some extent the inability of *S. pombe* to grow on glycerol as sole carbon source. Instead, expression of these genes is induced by the addition of ethanol or isopropanol to the media (Matsuzawa et al. 2012). C_2 bodies like ethanol cannot serve as sole carbon source for *S. pombe* due to the absence of a functional glyoxylate cycle (de Jong-Gubbels et al. 1996) as well as phosphoenolpyruvate carboxykinase (Rhind et al. 2011), the enzyme catalyzing the first step of gluconeogenesis. However, ethanol can be metabolized in combination with another carbon source like glucose (de Jong-Gubbels et al. 1996) or glycerol (Matsuzawa et al. 2010) and growth of *S. pombe* on mixtures of glycerol and acetate has been described recently (Klement et al. 2011).

Although *S. pombe* is primarily known as model organism for molecular and cell biology, its use for production of metabolites (Hansen et al. 2009; Neunzig et al. 2012) and recombinant proteins (Celik and Calik 2011; Mukaiyama et al. 2009) has been demonstrated and *S. pombe* is regarded as a potential cell factory especially for recombinant production of mammalian proteins (Celik and Calik 2011). Thus, the efficient utilization of an affordable carbon source like glycerol is of interest. While the regulatory network of glycerol metabolism has been investigated in detail, little information is available describing this metabolism from a more

physiological point of view. In this study we cultivated *S. pombe* on a mixture of glycerol and acetate, showing that growth on this mixture is respiratory. Depending on the purpose, e.g. recombinant protein production, this can be an important advantage compared to fermentative carbon sources like glucose, since no carbon is lost via fermentative pathways. We determined important physiological parameters of growth on the glycerol/acetate mixture and compared them to respiratory growth on glucose. To get an overview of active metabolic pathways, activities of several key enzymes were determined on both glucose and a mixture of glycerol/acetate. We used ^{13}C tracer studies to get an insight into contribution of both substrates to the central carbon metabolism. Metabolic flux analysis was applied to determine the flux distributions through the central carbon metabolism in cells grown on glucose and on glycerol/acetate and allowed the differentiation between cytosolic and mitochondrial acetyl-CoA formation, while in addition pointing towards compartmentation of certain pathways of amino acid biosynthesis. Further we observed an abundant production of cytosolic NADPH on both glucose and glycerol/acetate which is eventually reoxidized via the respiratory chain by a mechanism yet unidentified.

2. Materials and Methods

2.1 Strains and media

All cultivation experiments were performed with *Schizosaccharomyces pombe* wild type strain 972h- (ATCC 24843). For growth on glycerol/acetate mixtures a minimal media was used consisting of [g/L]: glycerol 9.3; sodium acetate 4.1; NH_4SO_4 15.0; KH_2PO_4 11.0; $MgCl_2$ 1.0; NaCl 1.0; $CaCl_2$ 14.0 mg/L. Vitamins and minerals were added to the following final concentrations mg/L: calcium pantothenate 1.0; nicotinic acid 10.0; myo-inositol 10.0; pyridoxine 0.5; biotin 0.01; $FeSO_4$ 0.7; $ZnSO_4$ 0.8; $MnSO_4$ 0.8; boric acid 1.0; $CoCl_2$ 1.0; $NaMoO_4$ 5.0; KI 2.0; $CuSO_4$ 0.08. The pH of the media was set to 5.5. For chemostat cultivations on glucose a previously described medium was used (Klein et al. 2012)

2.2 Cultivation conditions

Shake flask cultivations were performed in baffled shake flasks at 30°C and 230 rpm. Fermentations were performed in a Vario 1000 bioreactor with 100 mL working volume (Meredos, Bovenden, Germany) at 30°C and a stirring rate of 1000 min^{-1}. The aeration rate was controlled at 100 mL/min using a mass flow controller (WMR Compact 4, Brooks Instruments, Veenendal, Netherlands). Temperature, stirring speed and pH were controlled by a FCE 03 control unit (FairMenTec, Wald, Switzerland). To avoid foaming, 100 µl/L media of anti-foam reagent (Antifoam 289, Sigma-Aldrich, Taufkirchen, Germany) was added. Continuous cultivation experiments with glucose were performed in the previously described system of 10 mL scale parallel bioreactors at a dilution rate D = 0.1 h^{-1} (Klein et al. 2012). For tracer studies, naturally labeled substrates were exchanged for $[1,3-^{13}C]$ glycerol, $[1,2-^{13}C]$ sodium acetate and $[1-^{13}C]$ glucose which were purchased from Cambridge Isotope Laboratories (Andover, USA). All labeled substances had a purity of 99.0 %.

2.3 Cell disruption and quantification of in vitro enzyme activities

For *in vitro* enzyme activity assays, cells were grown in 25 ml of minimal media containing glycerol and acetate and harvested in the mid-exponential phase, resulting in a biomass concentration between 1.8 to 2.4 g CDW L^{-1}. For enzyme assays from glucose chemostat cultures, the whole culture was harvested resulting in a biomass concentration of 1.2 to 1.3 g CDW L^{-1}. Preparation of cell extracts and determination of protein concentration was

performed as described previously (de Jong-Gubbels et al. 1995). Enzyme assays for pyruvate caboxylase (PYC), phosphoenolpyruvate carboxykinase (PEPCK), pyruvate decarboxylase (PDC), phosphofructokinase (PFK) and fructose-1,6-bisphosphatase (FBPase) were performed according to the method of de Jong-Gubbels et al. (1996a). Assays for dehydrogenases were performed in a 100 mM Tris-HCl buffer with pH 8.0, containing 1 mM $MgCl_2$, 1 mM of the cofactors NAD^+ or $NADP^+$ and the following substrate concentrations: glycerol 50 mM, acetaldehyde 10 mM, glucose-6-phosphate 10 mM, sodium glutamate 50 mM, isocitrate trisodium salt 10 mM. The final volume of the assays was 1 ml. Each assay contained an appropriate amount of cell extract and was started by the addition of the corresponding substrate. The progression of the absorption at 340 nm was monitored photometrically at 30°C over 15 to 30 min and the enzyme activities were calculated. All determinations were performed in triplicates.

2.4 Analytics of culture supernatants and off gas

For calculation of consumption and production rates of metabolites on glycerol/acetate, culture samples were taken during the exponential growth phase and analysis of culture supernatants and off gas was performed as described previously (Klein et al. 2012) In case of chemostat cultivations in the small scale bioreactor system, the whole reactor was harvested for analysis of culture supernatants. A correlation between cell dry weight (CDW) and optical density (OD) at 595 nm was determined to be $OD_{595} = 0.60$ g CDW L^{-1} for growth on glycerol/acetate mixtures. The correlation for growth on glucose with $OD_{595} = 0.62$ g CDW L^{-1} was taken from Klein et al. (2012).

2.5 Analysis of ^{13}C labeling in proteinogenic amino acids and fatty acids

Samples from shake flask cultures of *S. pombe* cells grown on ^{13}C labeled glycerol or acetate were taken during mid-exponentiell phase. To ensure isotopic steady state, samples were taken at three different biomass concentrations. Metabolic steady state was confirmed by constant rates for substrate uptake and product formation. In case of chemostat experiments, cells were cultured for 5 residence times after switching to [1-^{13}C] glucose. Samples were taken from the bioreactor outlets and a final sample by harvesting the bioreactor. Cells were sampled by centrifugation at 13.000 x g at 4°C for 3 min. For extraction of amino acids from the cellular protein the cell pellet was washed twice with distilled water, resuspended in 100 µL of 6 M HCl

and incubated for 24 h at 100 °C for hydrolysis of the cellular protein. GC-MS measurement of the proteinogenic amino acids was carried out as described by Frick and Wittmann (2005). For fatty acid analysis, a method was used for extraction and direct transesterification of lipogenic fatty acid from biomass (Rodríguez-Ruiz et al. 1998). GC-MS measurement of fatty acid methylesters was performed with the GC-MS method described by Schneider et al. (2009). The labeling distribution of stearic acid was analyzed and used to determine the ratio of acetyl-CoA derived from glycerol and from acetate. Table III-1 depicts the amino acid and fatty acid fragments, which were chosen for labeling determination.

Table III-1: Fragments of amino acids and fatty acids measured by GC-MS for determination of labeling patterns.

metabolite	measured fragments (m/z)	carbon atoms from precursor
alanine	260	1-2-3
glycine	246	1-2
valine	288	1-2-3-4-5
leucine	200	2-3-4-5-6
isoleucine	200	2-3-4-5-6
serine	390	1-2-3
threonine	404	1-2-3-4
phenylalanine	336	1.-2-3-4-5-6-7-8-9
aspartate	418	1-2-3-4
glutamate	432	1-2-3-4-5
stearic acid	143	2-3-4-5-6-7-8

2.6 Metabolic Network and Metabolic Flux Analysis

The metabolic network comprised glycolysis, pentose phosphate pathway and the citrate cycle as well as anabolic reactions for amino acid synthesis. The stoichiometric model and reaction reversibilities are shown in Table III-2. The anabolic demand for biomass formation was adapted from the *Saccharomyces cerevisiae* model of Gombert et al. (2001) and is shown in Table III-3. Cytosol and mitochondria were implemented as separate compartments with separate pools for pyruvate, acetyl-CoA, oxaloacetate and malate. Amino acid biosyntheses

were assumed to be carried out in one compartment, except the formation of alanine, leucine and aspartate which were allowed in both compartments. Extracellular fluxes were the substrate uptake vinpGlc for growth on glucose as well as vinpGly and vinpAc for growth on glycerol/acetate. On both substrates secretion of small amounts of pyruvate (vext1) and succinate (vext2) was considered. The model contained an unbalanced pool of methyltetrahydrofalte (MTF), allowing the transfer of C_1 bodies for glycine and methionine biosynthesis. CO_2 production rate was left variable but closed balances with a maximum error of 5% for carbon and degree of reduction were applied as constraints. Produced NAD(P)H that was not consumed for biosynthesis was regenerated via the respiratory chain with oxygen as terminal electron acceptor. For balancing of intracellular metabolite pools, the following balance equations were defined:

cytosolic metabolite pools

(1)   a) for growth on glucose: glucose-6-phosphate: $vinpGlc - v1 - v14 - vb1 = 0$

b) for growth on glycerol/acetate: glucose-6-phosphate: $v1 - v14 - vb1 = 0$

(2)   fructose-6-phosphate: $v1 - v2 + v16 + v17 = 0$

(3)   glyceraldehyde-3-phosphate: $v2 - v3 - v4 - vb4 = 0$

(4)   a) for growth on glucose: dihydroxyacetone phosphate: $v2 - v3 = 0$

b) for growth on glycerol/acetate: dihydroxyacetone phosphate: $vinpGly - v3 - v2 = 0$

(5)   3-phosphoglycerate: $v4 - v5 - v27 - vb5 = 0$

(6)   phosphoenolpyruvate: $v5 - v6 - v34 - v38 - vb6 = 0$

(7)   cytosolic pyruvate: $v6 - v7 + v12 - v13 - v24 - v35 - vext1 = 0$

(8)   acetaldehyde: $v24 - v25 + v32 = 0$

(9)   a) for growth on glucose: acetate: $v25 - v26 = 0$

b) for growth on glycerol/acetate: $v25 + vinpAc - v26 = 0$

(10)   cytosolic acetyl-CoA: $v26 - v9 - vb7 - v44 = 0$

(11)   cytosolic oxaloacetate: $v13 - v8 - v29 = 0$

(12)   cytosolic malate: $v11 - v12 = 0$

(13)   pentose phosphate: $v14 - v15 - v17 - vb2 = 0$

(14)   erythrose-4-phosphate: $v16 - v17 - v34 - vb3 = 0$

(15)   sedoheptulose-7-phosphate: $v15 - v16 = 0$

(16)   shikimate-5-phosphate: $v34 - v38 = 0$

(18)   cytosolic 2-oxoisocaproate: $v44 - v45 = 0$

(18)   glutamate: $v39 - vb10 = 0$

(19)   cytosolic aspartate: $v29 - v31 - v41 - v50 = 0$

(20)   mixed aspartate pool: $v49 + v50 - vb11 = 0$

(21)   serine: $v27 - v28 - vb12 = 0$

(22)   glycine: $v28 + v32 - vb13 = 0$

(23)   threonine: $v31 - v32 - v40 - vb14 = 0$

(24)   phenylalanine: $v38 - vb15 = 0$

(25)   valine: $v37 - vb16 = 0$

(26)   isoleucine: $v40 - vb19$

(27)   methionine: $v41 - vb18 = 0$

(28)   lysine: $v48 - vb20 = 0$

(29)   alanine: $v35 + v36 - vb9 = 0$

(30)   leucine: $v43 + v45 - vb19 = 0$

(31)   a) for growth on glucose: NAD(P)H: $v4 + v10 + v12 + v14 + v19 + v20 + v21 + v23 + v32 + v42 + v44 - v31 - v33 - v34 - v39 - v40 - v41 - vb22 = 0$

b) for growth on glycerol/acetate: NAD(P)H: $vinpGly + v4 + v10 + v12 + v14 + v19 + v20 + v21 + v23 + v32 + v42 + v44 - v31 - v33 - v34 - v39 - v40 - v41 - vb22 = 0$

mitochondrial metabolite pools

(32)   mitochondrial pyruvate: $v7 - v10 - v36 - v40 = 0$

(33)   mitochdonrial acetyl-CoA: $v9 + v10 - v18 - v42 - v46 = 0$

(34)   mitochondrial isocitrate: $v18 - v19 = 0$

(35)   mitochondrial 2-oxoglutarate: $v19 - v20 - v39 - v46 - v49 - vb8 = 0$

(36)   mitochondrial succinate: $v20 - v21 - vext2 = 0$

(37)   mitochondrial fumarate: $v21 - v22 = 0$

(38)   mitochondrial malate: $v22 - v23 - v11 = 0$

(39)   mitochondrial oxaloacetate: $v23 + v8 - v18 - v30 = 0$

(40)   mitochondrial aspartate: $v30 - v49 = 0$

(41)   mitochondrial 2-oxoisovalerate: $v33 - v37 - v42 = 0$

(42)   mitochondrial 2-oxoisocaproate: $v42 - v43 = 0$

(43)   2-oxaloglutarate: $v46 - v47 = 0$

(44)   2-oxoadiapate: $v47 - v48 = 0$

Calculation of metabolic fluxes was performed by fitting simulated mass isotopomer distributions to experimentally determined labeling distributions in amino acids of hydrolyzed cellular protein. Mathematical modeling and metabolic flux analysis were performed using Matlab Version 7.7.0 (Mathworks Inc., Nattick, USA) as described by (Yang et al. 2008). Correction of mass isotopomers for naturally occurring isotopes in the amino acid fragments and the derivatization reagent was performed as described previously (van Winden et al. 2002; Wittmann and Heinzle 1999; Yang et al. 2009). Statistical analysis was carried out applying 100 independent Monte Carlo runs.

Table III-2: Stoichiometric network used for metabolic flux analysis. cyt: cytosolic. mit: mitochondrial. ext: external. P: phosphate residue.MTF: unbalanced pool of methyltetrahydrofolate. Arrows indicate direction of reaction and reversible reactions.

name	reaction stoichiometry		
v1	glucose-6-P	←→	fructose-6-P
v2	fructose-6-P	←→	glyceraldehyde-3-P + dihydroxyacetone-P
v3	glyceraldehyde-3-P	←→	dihydroxyacetone-P
v4	glyceraldehyde-3-P	→	3-phosphoglycerate
v5	3-phosphoglycerate	→	phosphoenolpyruvate
v6	phosphoenolpyruvate	→	cyt. pyruvate
v7	cyt. pyruvate	→	mit. pyruvate
v8	cyt. oxaloacetate	←→	mit. oxaloacetate
v9	cyt. acetyl-CoA	→	mit. acetyl-CoA
v10	mit. pyruvate	→	mit. acetyl-CoA + CO_2
v11	mit. malate	→	cyt. malate
v12	cyt. malate	→	cyt. pyruvate + CO_2
v13	cyt. pyruvate	→	cyt. oxaloacetate
v14	glucose-6-P	→	pentose-P + CO_2
v15	2 pentose-P	←→	sedoheptulose-5-P + glyceraldehyde-3-P
v16	sedoheptulose-5-P + glycerolaldehyde-3-	←→	fructose-6-P + erythrose-4-P
v17	pentose-P + erythrose-4-P	←→	fructose-6-phosphate + glyceraldehyde-3-P
v18	mit. oxaloacetate + mit. acetyl-CoA	→	mit. isocitrate
v19	isocitrate	→	2-oxoglutarate + CO_2
v20	2-oxoglutarate	→	succinate + CO_2
v21	succinate	→	fumarate
v22	fumarate	→	mit. malate
v23	mit. malate	→	mit. oxaloacetate
v24	cyt. pyruvate	→	acetaldehyde
v25	acetaldehyde	→	acetate
v26	acetate	→	cyt. acetyl-CoA
v27	3-phosphoglycerate	→	serine
v28	serine	←→	glycine + MTF
v29	cyt. oxaloacetate	→	cyt. aspartate
v30	mit. oxaloacetate	→	mit. aspartate
v31	cyt. asparate	→	threonine
v32	threonine	←→	glycine + acetaldehyde
v33	mit. pyruvate	→	oxoisovalerate
v34	phosphoenolpyruvate + erythrose-4-P	→	shikimate-5-P

Table III-2 continued

v35	cyt. pyruvate	→	alanine
v36	mit. pyruvate	→	alanine
v37	2-oxisovalerate	→	valine
v38	phosphoenolpyruvate + shikimate-5-P	→	phenylalanine + CO_2
v39	2-oxoglutarate	→	glutamate
v40	threonine + mit. pyruvate	→	isoleucine + CO_2
v41	cyt. asparate + MTF	→	methionine
v42	2-oxoisovalerate + mit. acetyl-CoA	→	mit.2- oxoisocaproate + CO_2
v43	mit.2- oxoisocaproate	→	leucine
v44	2-oxoisovalerate + cyt. acetyl-CoA	→	cyt.2- oxoisocaproate + CO_2
v45	cyt.2- oxoisocaproate	→	leucine
v46	mit. 2-oxoglutarate + mit. acetyl-CoA	→	mit. oxaloglutarate
v47	mit. oxaloglutarate	→	mit. 2-oxoadipate + CO_2
v48	mit. 2-oxoadipate	→	lysine
v49	mit. aspartate	→	aspartate
v50	cyt. aspartate	→	aspartate
vext1	cyt. pyruvate	→	ext. pyruvate
vext2	mit. succinate	→	ext. succinate
vinp	ext. glucose	→	glucose-6-P
vinp	ext. glycerol	→	dihydroxyacetone-P
vinp Ac	ext. acetate	→	cyt. acetate
vb1	glucose-6-P	→	biomass
vb2	pentose-P	→	biomass
vb3	erythrose-4-P	→	biomass
vb4	glyceraldehyde-3-P	→	biomass
vb5	3-phosphoglycerate	→	biomass
vb6	phosphoenolpyruvate	→	biomass
vb7	cyt. acetyl-CoA	→	biomass
vb8	mit. 2-oxoglutarate	→	biomass
vb9	alanine	→	biomass
vb10	glutamate	→	biomass
vb11	asparate	→	biomass
vb12	serine	→	biomass
vb13	glycine	→	biomass
vb14	threonine	→	biomass
vb15	phenylalanine	→	biomass
vb16	valine	→	biomass

Table III-2 continued

vb17	isoleucine	→	biomass
vb18	methionine	→	biomass
vb19	leucine	→	biomass
vb20	lysine	→	biomass
vb21	CO_2	→	biomass
vb22	cofactor	→	biomass

Table III-3: Anabolic demand for *S. pombe* during respiratory growth (specific growth rate of 0.1 h^{-1}). Data are given in mmol g CDW^{-1} and were adapted from Gombert et. al (2001).

precursor	demand [mmol g CDW^{-1}]
glucose-6-phosphate	1.730
pentose-5-phosphate	0.163
erythrose-4-phosphate	0.153
glyceraldehyde-3-phosphate	0.077
3-phosphoglycerate	0.565
phosphoenolpyruvate	0.271
cytosolic acetyl-CoA	1.900
mitochondrial acetyl-CoA	0.290
alanine	0.354
glutamate	0.639
aspartate	0.359
serine	0.400
glycine	0.275
threonine	0.243
phenylalanine	0.130
valine	0.232
isoleucine	0.174
methionine	0.042
leucine	0.198
lysine	0.200
cytosolic NADPH	4.65
mitochondrial NADPH	4.16

3. Results

3.1 Physiology of S. pombe during growth on mixtures of glycerol and acetate and during respiratory growth on glucose

Cells of *S. pombe* were grown in minimal media containing glycerol or acetate as sole carbon source or a mixture of both, glycerol and acetate. Cell growth was only observed when cells were grown on a mixture of both substrates (Figure III-1).
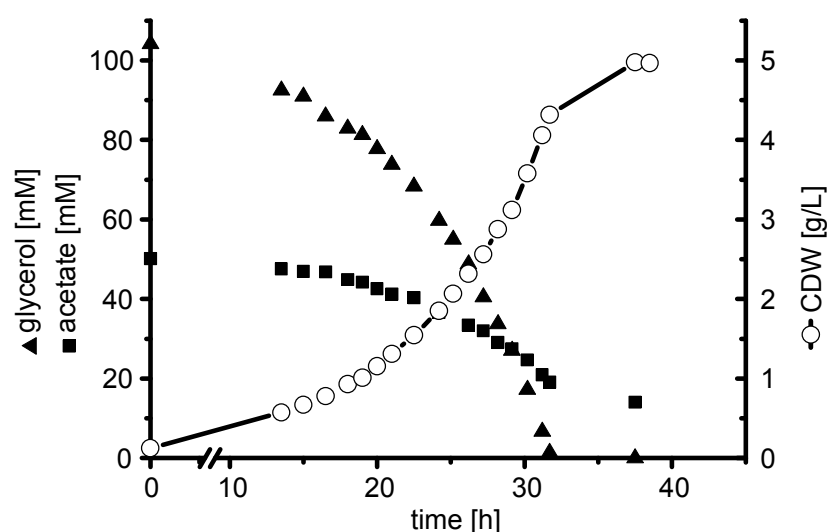
Figure III-1: Growth (circles) and substrate uptake of *Schizosaccharomyces pombe* grown in a minimal media containing glycerol (filled triangles) and acetate (filled squares) as carbon source.

Growth on this mixture was characterized by a specific growth rate μ of 0.11 ± 0.0 h^{-1} and a biomass yield of 11.39 ± 0.05 g Cmol^{-1} substrate. Glycerol and acetate were consumed simultaneously, with a specific glycerol uptake rate of 2.57 ± 0.08 mmol g CDW^{-1} h^{-1} and a specific acetate uptake rate of 0.72 ± 0.02 mmol g CDW^{-1} h^{-1} (Table III-4). Ethanol as main indicator of fermentative growth was absent and only very small amounts of pyruvate and succinate of were detected in the culture supernatants.

A specific oxygen uptake rate of 4.76 ± 0.10 mmol g CDW^{-1} h^{-1} and a specific carbon dioxide production rate of 4.81 ± 0.13 mmol g CDW^{-1} h^{-1} were determined, resulting in a respiratory quotient (RQ) of 1.01. The high biomass yield and the absence of ethanol and other reduced byproducts were strong indicators for respiratory growth of *S. pombe* on glycerol/acetate mixtures. A closed carbon balance (carbon recovery 97%) assured the consideration of all relevant extracellular carbon fluxes. Chemostat cultivations of S. *pombe* on glucose under respiratory growth conditions (D = 0.1 h^{-1}) resulted in a slightly increased biomass yield of 14.73 ± 0.19 g Cmol^{-1} substrate compared to glycerol/acetate grown cells (Table III-4). Cells grown respiratorily on glucose exhibited a reduced CO_2 production rate of 2.75 ± 0.04 mmol g CDW^{-1} h^{-1} compared to glycerol/acetate grown ones, pointing towards a significant increase of CO_2 producing fluxes during growth on the glycerol/acetate mixture. On glucose the specific oxygen consumption rate matched the specific CO_2 production rate, resulting in a RQ value of 1.02.

Table III-4: Physiological parameters of growth of *S. pombe* on a mixture of glycerol and acetate compared to cultivations on glucose under respiratory conditions (D = 0.1 h^{-1}). Stadard deviation were obtained from two parallel experiments.

Substrate	$Y_{X/S}$ [g Cmol^{-1}]	q_s [mmol g^{-1} h^{-1}]		q_{O2} [mmol g^{-1} h^{-1}]	q_{CO2} [mmol g^{-1} h^{-1}]	RQ
Glycerol/ Acetate	11.39 ± 0.05	q_{gly} 2.57 ± 0.08	q_{ac} 0.72 ± 0.02	4.76 ± 0.13	4.81 ± 0.10	1.01
Glucose	14.73 ± 0.19	1.08 ± 0.05		2.69 ± 0.11	2.75 ± 0.04	1.02

3.2 Quantification of in vitro enzyme activities on glycerol/acetate mixtures and glucose

In vitro enzyme activities of several key enzymes of the central carbon metabolism, namely glucose 6-phosphate dehydrogenase (G6PDH), phosphofructokinase (PFK), fructose 1,6-bisphosphatase (FBPase), glycerol dehydrogenase (GlyDH), pyruvate decarboxylase (PDC), pyruvate carboxylase (PYC), acetaldehyde dehydrogenase (AADH), PEP carboxykinase (PEPCK) and isocitrate dehydrogenase (IcDH) were quantified in order to set up the

stoichiometric model applied for the metabolic flux analysis. Enzyme assays were performed using cells grown on mixtures of glycerol/acetate as well as cells from glucose chemostat cultures grown at a dilution rate of 0.1 h^{-1}. Specific activities of all enyzmes were similar on both substrates except for FBPase. Cells grown on glycerol/acetate mixtures exhibited a specific enzyme activity of 0.58 ± 0.06 U mg^{-1} whereas no activity for FBPase was observed in extracts of glucose grown cells. In addition, no activity for PEPCK was detectable on both substrates. GlyDH activity was observed on both substrates with a specific enzyme activity of 0.71 ± 0.05 U mg^{-1} on the glycerol/acetate mixture and 0.50 ± 0.01 U mg^{-1} on glucose (Table III-5).

Table III-5: Specific enzyme activities [U/mg] for key enzymes of the central carbon metabolism for cells grown on glucose in chemostat at D = 0.1 h^{-1} and on the glycerol/acetate mixture. For dehydrogenases, activities were determined with both NAD$^+$ and NADP$^+$. n. d. – not detectable.

	Glucose D = 0.1 h^{-1}			**Glycerol/Acetate mixture**		
PFK	0.73 ± 0.06			0.68 ± 0.02		
FBPase	n.d.			0.58 ± 0.06		
PDC	0.21 ± 0.02			0.14 ± 0.01		
PYC	0.12 ± 0.01			0.14 ± 0.01		
PEPCK	n. d.			n. d.		
	NAD$^+$	**NADP$^+$**	**total**	**NAD$^+$**	**NADP$^+$**	**total**
G6PDH	n.d.	1.25 ± 0.12	1.25 ± 0.12	0.0	1.14 ± 0.04	1.14 ± 0.04
GlyDH	0.34 ± 0.01	0.17 ± 0.01	0.50 ± 0.01	0.51 ± 0.04	0.20 ± 0.02	0.71 ± 0.05
AADH	0.02 ± 0.0	0.08 ± 0.0	0.1 ± 0.0	0.05 ± 0.01	0.08 ± 0.01	0.13 ± 0.01
IcDH	0.07 ± 0.0	0.12 ± 0.01	0.19 ± 0.01	0.10 ± 0.02	0.56 ± 0.04	0.66 ± 0.04

3.3 Distribution of acetate throughout the central carbon metabolism

In order to verify the activity of the different central metabolic pathways and the distribution of the substrates glycerol and acetate throughout the central metabolism, especially focusing on a potential gluconeogenic flux, *S. pombe* was cultivated on ^{13}C labeled substrates. Based on the ^{13}C enrichment of proteinogenic amino acids, the distribution of the corresponding substrates was determined. Feeding universally labeled acetate resulted in a ^{13}C enrichment in glutamate, suggesting that acetate enters the TCA cycle via acetyl-CoA (Figure III-2). No enrichment of ^{13}C was observed for serine, derived from 3-phosphoglycerate (3PG) and phenylalanine derived from PEP and erythrose-4-phosphate, thus pointing towards an inactive gluconeogenic flux from oxaloacetate towards PEP under the applied growth conditions using a mixture of glycerol and acetate.
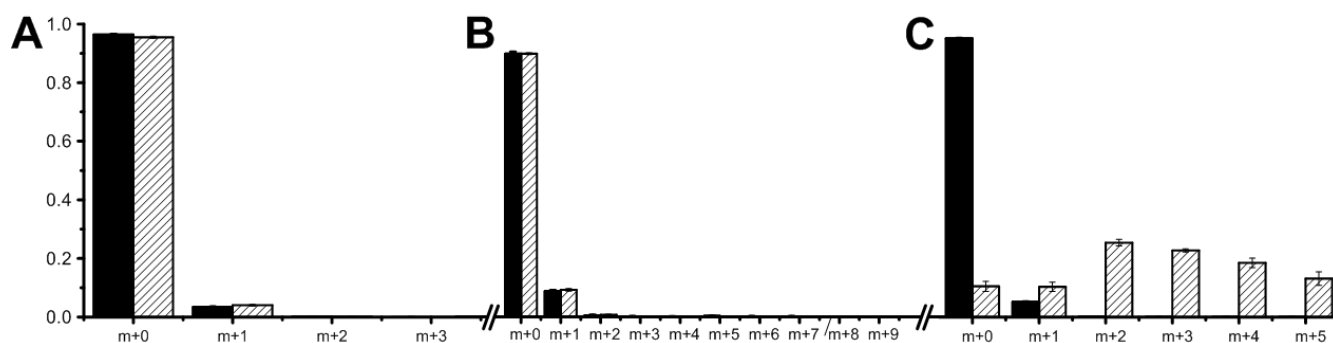
Figure III-2: Mass distribution vectors (MDVs) of selected proteinogenic amino acids from cultivations on glycerol and acetate. Filled bars show MDVs from cultivations on unlabeled substrates, dashed bars show MDVs from cultivations with [1, 2-^{13}C] acetate.A) serine; B) phenylalanine; C) glutamate. Error bars indicate standard deviations.

3.4 Metabolic flux analysis on glucose and glycerol/acetate

[1-^{13}C] glucose was used as tracer substrate in chemostat cultivations of *S. pombe*. For tracer studies on glycerol/acetate mixtures, [1,3-^{13}C] glycerol was used as well as [1,2-^{13}C] acetate. Flux simulations were performed with tracer information from [1,2-^{13}C] acetate, [1,3-^{13}C] glycerol and a combination of both tracer experiments. The combined approach consisted of two experiments (^{13}C labeled acetate/naturally labeled glycerol and vice versa) where both datasets were used in parallel to obtain the flux distribution. The flux distributions from this combined approach were used for comparison with flux distributions in glucose limited chemostats.

Metabolic fluxes during growth on glucose are depicted in Figure III-3A, corresponding fluxes during growth on the glycerol/acetate mixture are shown in Figure III-3B. A strong activity of the tricarboxylic acid cycle (TCA cycle) was observed on both substrates. Isocitrate dehydrogenase activity was identical under both cultivation conditions, exhibiting a flux of 0.79 ± 0.03 mmol g CDW^{-1} h^{-1} on glucose and 0.78 ± 0.04 mmol g CDW^{-1} h^{-1} on the glycerol/acetate mixture.

In case of the glycerol/acetate substrate mixture, measurement of the labeling pattern of stearic acid allowed a good resolution of the flux distributions around the pyruvate node. Acetate taken up from the media was the main source of cytosolic acetyl-CoA synthesized by acetyl-CoA synthethase. Only a fraction of 26.5% of cytosolic acetyl-CoA was produced by decarboxylation of cytosolic pyruvate. 0.20 mmol g CDW^{-1} h^{-1} of the cytosolic acetyl-CoA was used for lipid biosynthesis, while most of it was transported into the mitochondria. In contrast, the flux via the pyruvate dehydrogenase complex synthesizing mitochondrial acetyl-CoA form mitochondrial pyruvate was very small and therefore hard to determine precisely.

A clear compartmentation of leucine biosynthesis was observed in *S. pombe* which was found to use exclusively mitochondrial acetyl-CoA for the synthesis of leucine. The stoichiometric model involved a mitochondrial and a cytosolic biosynthetic route for leucine. However, the flux for mitochondrial leucine production was 0.017 ± 0.00 mmol g CDW^{-1} h^{-1}, whereas for cytosolic leucine a production flux of 0.00 ± 0.00 mmol g CDW^{-1} h^{-1} was determined. Further, asparatate and thus threonine were synthesized exclusively from cytosolic OAA during growth on both substrates, while no incorporation of mitochondrial OAA was observed. A compartmentation for alanine biosynthesis could not be determined but was assumed to take place in the mitochondria (s. Discussion).

On glucose and the glycerol/acetate mixture, a net flux from cytosolic oxaloacetate (OAA) to mitochondrial OAA was observed. On glycerol/acetate mixtures, the flux from cytosolic to mitochondrial OAA was 0.18 ± 0.01 mmol g CDW^{-1} h^{-1} while the reverse flux was 0.02 ± 0.00 mmol g CDW^{-1} h^{-1}, resulting in a net flux of 0.16 ± 0.01 mmol g CDW^{-1} h^{-1} with a reversibility ζ of 0.14. On glucose, the reversibility of this import could not be determined. However, the net flux from cytosolic OAA towards mitochondrial OAA was 0.34 ± 0.05 mmol g CDW^{-1} h^{-1} and thus 2 times higher compared to growth on glycerol/acetate mixtures. At the same time, the export from mitochondrial malate into the cytosol and pyruvate production from cytosolic malic enzyme were 10 times higher on glucose than on glycerol/acetate mixtures.

Glycerol is metabolized via the formation of DHAP in the first two steps, which is further converted to glycerolaldehyde 3-phosphate (GAP). At this point, GAP is either condensed with DHAP for the formation of fructose 6-phosphate or channeled into glycolysis with pyruvate as end product. During growth on glycerol/acetate mixtures the major demand for acetyl-CoA is covered by acetate supplied via the media. This demand must be completely met by the formation of acetyl-CoA from pyruvate during growth on glucose. Thus the flux from GAP to pyruvate was 1.8 times higher on glucose than on glycerol/acetate mixtures. The remaining glycerol followed the gluconeogenic route towards fructose 6-phosphate with a flux of 1.50 mmol g CDW^{-1} h^{-1}. A high flux through the non-oxidative part of the pentose-phosphate pathway (PPP), generating additional fructose 6-phosphate increased the flux towards glucose 6-phosphate to 4.07 mmol g CDW^{-1} h^{-1}. Respiratory growth on glucose lead to a flux of 0.69 mmol g CDW^{-1} h^{-1} of glucose 6-phosphate to the pentose 5-phosphates, generating 1.38 mmol g CDW^{-1} h^{-1} of cytosolic NADPH. The flux through the oxidative PPP on the glycerol/acetate mixture was 5.6 times higher (3.89 mmol g CDW^{-1} h^{-1}), generating 7.78 mmol g CDW^{-1} h^{-1} of cytosolic NADPH. The fluxes through the non-oxidative part of the PPP were increased by the same factor accordingly, generating the above mentioned high back flux towards fructose 6-phosphate. Thus, the carbon atoms of glycerol were cycled through the PPP, generating increased amounts of CO_2 which is in good agreement with the increased carbon dioxide production rate of 4.81 ± 0.10 mmol g CDW^{-1} h^{-1} observed as well as a vast increase of the cytosolic NADPH production.

3.5 Balancing of redox cofactors

Rates for production and consumption of NADH and NADPH as well as CO_2 and oxygen were calculated from the flux simulation data sets. These data were used to review the accuracy of metabolic flux analysis by comparing the calculated values with the experimental data from off gas analysis.

Cofactor specificities of the key dehydrogenases of the central carbon metabolism were determined along with the enzyme activity assays. Only G6PDH showed cofactor specificity for $NADP^+$, all other dehydrogenases tested exhibited activity with both cofactors (NAD^+/$NADP^+$) (Table III-5).

Figure III-3A: Intracellular carbon flux distributions of *S. pombe* cultivated in a chemostat under respiratory growth conditions (D = 0.1 h^{-1}) on [1-^{13}C] glucose and. Fluxes are given in mmol g CDW^{-1} h^{-1} and standard deviations are given to reflect the precision of the flux determination.. For reversible reactions, net fluxes are shown and arrows indicate the direction of the fluxes.

Figure III-3B: Intracellular carbon flux distributions of *S. pombe* cultivated on a mixture of glycerol and acetate. [1,3-^{13}C] glycerol and [1,2-^{13}C] acetate were used as tracers in independent experiments. Fluxes are given in mmol g CDW^{-1} h^{-1} and standard deviations are given to reflect the precision of the flux determination.. For reversible reactions, net fluxes are shown and arrows indicate the direction of the fluxes.

The oxidative PPP was considered as sole source of cytosolic NADPH. Considering the anabolic demand for NADPH (Table III-3) as well as NADPH consuming reactions in the metabolic model (Table III-2), the flux through the oxidative PPP produced a surplus of cytosolic NADPH of 0.66 mmol g CDW^{-1} h^{-1} on glucose and 6.96 mmol g CDW^{-1} h^{-1} on glycerol/acetate respectively. In *S. pombe*, AADH is encoded by only one gene, SPAC9E9.09c and the enzyme is localized in the cytosol (Matsuyama et al. 2006). Thus IcDH was considered as only source of mitochondrial NADPH production. Since mitochondrial IcDH exhibited activity for both NAD^+ and $NADP^+$, the NADPH production was assumed to match the mitochondrial NADPH demand. AADH was considered to produce only NADH, since the PPP already produced a surplus of cytosolic NADPH.

The NADH production rates were calculated to be 4.86 mmol g CDW^{-1} h^{-1} on glycerol/acetate and 3.14 mmol g CDW^{-1} h^{-1} on glucose respectively. Since cell growth was respiratory on both substrates, NADH reoxidation should exclusively occur via the respiratory chain with a ratio of 2 mol NADH per mol O_2. Further the surplus of cytosolic NADPH was considered to be eventually reoxidized via the respiratory chain. The calculation of a specific oxygen uptake rate as well as a CO_2 production rate from the flux data and the resulting calculated RQ values matched the experimentally determined values (Table III-6). The difference from the experimentally determined values was at most 2.6% for glucose and not more than 6.6% for glycerol/acetate respectively. These results strongly indicated direct or indirect reoxidation of the excess NADPH by the respiratory machinery.

Table III-6: Specific CO_2 production rates, pecific O_2 consumption rates [mmol g CDW^{-1} h^{-1}] and RQ values calculated from flux simulations (cal.) on glucose and the glycerol/acetate mixture compared to the experimentally determined values from off gas analyses (exp.).

Substrate	CO₂ cal.	CO₂ exp.	O₂ cal.	O₂ exp.	RQ cal.	RQ exp.
Glucose	2.81 ± 0.32	2.75 ± 0.04	$2.76\ 0.22$	2.69 ± 0.11	1.02	1.02
Glycerol/ Acetate	5.12 ± 0.22	4.81 ± 0.13	5.05 ± 0.19	4.76 ± 0.10	1.02	1.01

4. Discussion

Glycerol from biodiesel production is a readily available carbon source for microbial bioporocesses. While glycerol utilization for other yeasts has been investigated in detail, little work has been performed concerning physiology of *S. pombe* grown on glycerol. Thus our study aimed at getting an insight into the physiology of *S. pombe* grown on a mixture of glycerol and acetate and comparing the obtained results to glucose, a standard carbon source for yeast cultivations. The physiological characterization revealed that growth on the glycerol/acetate mixture was respiratory due to the absence of the key fermentative product ethanol, a RQ of 1.01 and a high biomass yield of 11.39 ± 0.05 g Cmol^{-1} substrate. Glycerol uptake was much faster than acetate uptake, with a C-mol ratio of uptake of 5.5 to 1. For chemostat cultivations with glucose/ethanol mixtures at $D = 0.1$ h^{-1} a C-mol ratio of the uptake for glucose and ethanol up to 2.3 to 1 has been described (de Jong-Gubbels et al. 1996). However, complete incorporation of ethanol into biomass was observed only for C-molar rations below 6.5 :1 (glucose to ethanol).Increasing the ethanol uptake by increased fractions of ethanol in the medium resulted in the formation of acetate. The authors described a limitation of ethanol converting enzymes alcohol dehydrogenase, acetaldehyde dehydrogenase and acetyl-CoA synthetase as reason for the limited complete utilization of ethanol and the occurring acetate production. Accordingly, such a limitation of acetate metabolization might explain the low acetate uptake rate, compared to the glycerol uptake rate. This is in agreement with the observation that increasing amounts of acetate in the media did not further increase the acetate uptake rate (date not shown).

Comparison of these results to chemostat cultivations on glucose at a dilution rate of 0.1 h^{-1} yielded comparable results with a high biomass yield of 14.73 ± 0.19 g Cmol^{-1} substrate and the absence of ethanol as well as an RQ of 1.02. The comparable degree of reduction of glucose and the glycerol/acetate mixture with an elemental composition of CH_2O for glucose and $CH_{2.6}O$ for the glycerol/acetate mixture, respectively, (based on the stoichiometry ratio of the uptake of both substrates) explains the similar RQ values on both substrates. Although the degree of reduction of the substrate mixture is increased by 15% compared to glucose, an increased biomass yield on the glycerol/ acetate mixture was not observed. This might result from an essentially altered carbon metabolism e. g. the carbon cycling through the PPP resulting in a substantial loss of carbon compared to glucose cultivations.

The *in vitro* activities of the tested enzymes of the central carbon metabolism showed similar results on both substrates. Regulation of enzyme expression in the central carbon metabolism of

S. pombe can be strongly dependent on the growth rate and the consequent physiology (de Jong-Gubbels et al. 1996). On the other hand expression of the tested enzymes of the central carbon metabolism seems much less dependent of the substrate since comparable growth rates and comparable physiologies are present on both substrates.

Glycerol dehydrogenase, the first enzyme in glycerol metabolism, was also expressed when cells were grown on glucose. Chemostat cultivation applying low dilution rates resulting in respiratory growth is comparable to the low glucose conditions described by Matsuzawa (2010) as a condition inducing *gld1* expression, explaining the activity of glycerol dehydrogenase under these conditions. However, in contrast to those results, where the glycerol dehydrogenase was described as strictly NAD^+ dependent, we detected activity with both NAD^+ and $NADP^+$. There might be strain specific isoenzymes or altered cofactor specificities, since we used the wild type strain 972h⁻ while the strain described by Matsuzawa (2010) was originally provided from Asahi Glass Co. A strong FBPase activity on glycerol/acetate in contrast to glucose grown cells was the only remarkable difference between enzyme activities on both substrates. A strong induction in the absence of glucose and addition of ethanol has been shown before on the mRNA level (Matsuzawa et al. 2012) and was confirmed by similar results in a direct assay of enzymatic activity (this work). These results suggest that glycerol dehydrogenase is target of glucose catabolite repression and expressed if this repression disappears. The *fbp1* gene on the other hand is also repressed in the presence of glucose but expression appears to take place only upon additional induction by ethanol (Matsuzawa et al. 2012) or acetate (this work). The enzyme assays confirmed that on both glycerol/acetate and glucose no activity for PEPCK could be detected which is in accordance with literature data (de Jong-Gubbels et al. 1996; Rhind et al. 2011). This result was confirmed by tracer studies with [1,2-^{13}C] acetate, showing an incorporation of ^{13}C into the amino acids derived from TCA cycle intermediates but no ^{13}C incorporation into amino acids derived from PEP or 3-phosphoglycerate. Due to the lack of PEPCK formation of PEP from oxaloacetate is not possible in *S. pombe*.

Metabolic flux analysis indicated highly similar TCA cycle fluxes during growth on glucose or glycerol/acetate. TCA cycle fluxes were independent of the carbon source, since growth on both substrates is respiratory and the growth rates were similar. One would expect a much stronger effect by applying variations of the growth rates and switching between respiratory growth and fermentative growth as shown for *S. cerevisiae* (Frick and Wittmann 2005).On glucose, a distinction between cytosolic acetyl-CoA formation via the pyruvate dehydrogenase bypass and mitochondrial acetyl-CoA formation was not possible. Thus no reliable statement can be made to the actual rate of pyruvate import into the mitochondria under these growth conditions. There

is only a minimum import that has to take place to meet the anabolic demand for mitochondrial pyruvate, since, in contrast to *S. cerevisiae*, no mitochondrial malic enzyme can replenish the mitochondrial pyruvate pool. Likewise a minimal flux via the cytosolic pyruvate dehydrogenase bypass must be active to meet the anabolic demand for cytosolic acetyl-CoA.

Additional measurement of stearic acid labeling pattern on the glycerol/acetate mixture showed that assimilated acetate was the main source of cytosolic acetyl-CoA while production from pyruvate via PDC made up only 26.5% of the cytosolic acetyl-CoA pool. Most of the cytosolic acetyl-CoA was transported to the mitochondria for metabolization via the TCA cycle and accordingly mitochondrial acetyl-CoA production from mitochondrial pyruvate was very low and hard to determine precisely. However, leucine biosynthesis was clearly shown to use exclusively mitochondrial acetyl-CoA as precursor. The clarity of this assignment shows that there must be a slight difference in the labeling pattern between cytosolic and mitochondrial acetyl-CoA and thus a small amount of mitochondrial acetyl-CoA must be formed from mitochondrial pyruvate.

The simulation of compartmented flux distributions also gave insight into the compartmentation of biosynthesis of the amino acids aspartate and threonine. Although aspartate aminotransferases are described to be located in both cytoplasm and mitochondria of *S. pombe* (Matsuyama et al. 2006), aspartate and thus threonine were both derived solely from the cytosolic OAA pool, an observation that has been made for other yeast species but not for *S. pombe* yet (Blank et al. 2005). On both substrates, a net flux from cytosolic to mitochondrial OAA was determined. On the glycerol/acetate mixture, the reversibility of the transport could be determined with $\zeta = 0.14$, while for glucose cultivations ζ could not be determined. However, the clear separation between cytosolic and mitochondrial aspartate biosynthesis is attributed to distinct labeling patterns of cytosolic and mitochondrial OAA pools and thus the exchange between both pools must be small on glucose. High exchange fluxes would result in basically identical labeling patterns of both OAA pools which would prevent a clear determination of compartmentalized biosynthesis of aspartate.

A separation of cytosolic and mitochondrial pools of pyruvate with $[1\text{-}^{13}C]$ glucose has been described for *S. cerevsiae* due to differences in the labeling pattern of cytosolic pyruvate formed in the glycolysis and mitochondrial pyruvate formed by the reaction of the mitochondrial malic enzyme (Frick and Wittmann 2005). In contrast to *S. cerevisiae*, the malic enzyme of *S. pombe* is located in the cytosol (Boles et al. 1998). Here, both pyruvate pools carry same labeling information, making it impossible to distinguish between both pools. Therefore a separation

between cytosolic and mitochondrial pyruvate pools was not possible and no information for compartmentation of alanine biosynthesis was available. Since there was no difference between the observed compartmentation of other amino acid biosyntheses in *S. pombe* and those described for *S. cerevisiae*, it seems reasonable to assume that alanine biosynthesis takes place in the mitochondria under respiratory conditions as described for baker's yeast (Frick and Wittmann 2005).

A striking difference between the two substrates was found in the CO_2 production rate. A 1.7-fold increase was observed during growth on the glycerol/acetate mixture compared to glucose grown cells. The reason for this increase was found in a drastically increased flux through the oxidative PPP. The mixture of glycerol/acetate resulted in a sufficient supply of acetyl-CoA from acetate to meet the anabolic demands in both compartments. This led to a drastically decreased glycolytic flux towards pyruvate compared to glucose grown cells. The flux from GAP towards pyruvate was decreased by a factor of 1.8. Since glycerol uptake was fast with a rate of 2.57 mmol g CDW^{-1} h^{-1}, the remaining carbon entered gluconeogenesis. This led to a cycle of the carbon atoms from glycerol through the upper part of the gluconeogenesis and the PPP, causing the observed increase in CO_2 production and raising the level of cytosolic NADPH compared to glucose cultivations. The increased carbon flux through the PPP was dictated by the ratio of glycerol and acetate derived carbon found in intermediates of the TCA cycle. Since the acetyl-CoA supplying flux from acetate is fixed, the glycolytic carbon flux form glycerol is restricted to a certain value to meet this ratio. The remaining carbon derived from glycerol uptake must be either incorporated into biomass or follow the described cycle between gluconeogenesis and PPP forming CO_2. CO_2 production rate was not used for balancing but for validation of the overall CO_2 production determined by the flux model. The good agreement between measured and simulated CO_2 production supports these findings of the carbon cycling through the PPP.

On both substrates, a surplus of cytosolic NADPH was observed, which was far more pronounced on the glycerol/acetate mixture. However, calculation of specific oxygen consumption rates and CO_2 production rates matched the experimentally determined values, if this surplus was considered to be reoxidized via the respiratory chain (Table III-6). The production of excess cytosolic NADPH and its regeneration by the enzymes of the respiratory chain has been described for other yeasts like *Kluyveromyces lactis* and *Candida utilis* (Tarrío et al. 2006; Urk et al. 1989). No information is available on *S. pombe* and it has been clearly shown that *S. cerevisiae* is unable to reoxidize NADPH this way (Urk et al. 1989). Another possible explanation would be the transport of electrons from NADPH to NADH via

transhydrogenase-like cycles. Their existence has been proposed by (Boles et al. 1993), describing a cycle of $NAD(P)^+$ dependent glutamate dehydrogenases in *S. cerevisiae*. An upregulation of exactly these glutamate dehydrogenases has been described for mutant strains of *S. cerevisiae* which showed a relocalization of the mitochondrial $NADP^+$ dependent malic enzyme to the cytosol (Moreira dos Santos et al. 2004). We determined *in vitro* activities of glutamate dehydrogenases in cells grown on the glycerol/acetate mixture and glucose and found activity for NAD^+ and $NADP^+$ dependent glutamate dehydrogenases in both cases (Figure III-4). This is no real proof for the existence of such an electron-transferring cycle in *S. pombe*, but the expression of both isoforms of glutamate dehydrogenase allows such a cycle to take place in theory at least. *S. pombe* must have some means by which surplus NADPH can be regenerated via the respiratory chain. However the mechanisms of this NADPH regeneration are yet still unclear and will be the topic of further studies.

In this study we could show that growth of *S. pombe* on a glycerol/acetate mixture is respiratory, which is an advantage compared to fermentative carbon sources like glucose in terms of reduced carbon loss and higher biomass formation. Metabolic flux analysis was used to get an insight into the metabolization of both substrates throughout the central carbon metabolism. Here the utilization of a mixture of two substrates allowed a detailed resolution of the metabolic fluxes around the pyruvate node, which is not possible with a single carbon source like glucose in *S. pombe*. The obtained results and applied techniques can be used for further physiological studies on *S. pombe* to get a better understanding of the physiology and potential of this important microorganism.
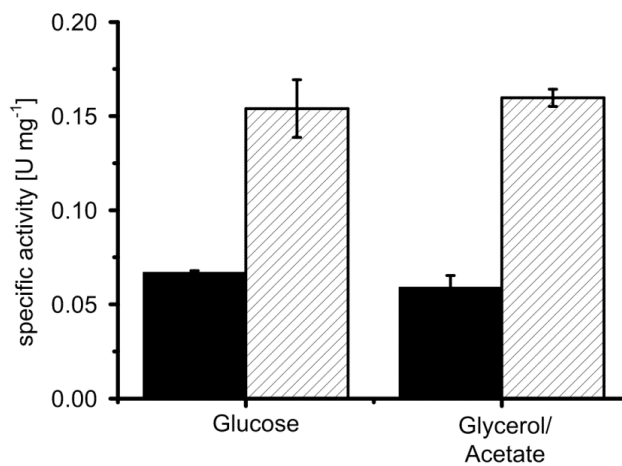
Figure III-4: Specific enzyme activities of glutamate dehydrogenases of *S. pombe* grown on glucose under respiratory growth conditions (D = 0.1 h^{-1}) and on a mixture of glycerol and acetate. Solid bars show activity with NAD^{+}, dashed bars activity with NADP^{+}.

5. Acknowledgements

6. References

Blank LM, Lehmbeck F, Sauer U (2005) Metabolic-flux and network analysis in fourteen hemiascomycetous yeasts. FEMS Yeast Res 5:545–558.

Boles E, de Jong-Gubbels P, Pronk JT (1998) Identification and characterization of *MAE1*, the *Saccharomyces cerevisiae* structural gene encoding mitochondrial malic enzyme. J Bacteriol 180:2875–2882.

Boles E, Lehnert W, Zimmermann FK (1993) The role of the NAD-dependent glutamate dehydrogenase in restoring growth on glucose of a *Saccharomyces cerevisiae* phosphoglucose isomerase mutant. Eur J Biochem 217:469–477.

Celik E, Calik P (2011) Production of recombinant proteins by yeast cells. Biotechnol Adv 30:1108–1118.

Dobson R, Gray V, Rumbold K (2012) Microbial utilization of crude glycerol for the production of value-added products. J Ind Microbiol Biotechnol 39:217–226.

Ferreira AR, Ataíde F, von Stosch M, Dias JML, Clemente JJ, Cunha AE, Oliveira R (2012) Application of adaptive DO-stat feeding control to *Pichia pastoris* X33 cultures expressing a single chain antibody fragment (scFv). Bioprocess Biosyst Eng 35:1609-1614.

Frick O, Wittmann C (2005) Characterization of the metabolic shift between oxidative and fermentative growth in *Saccharomyces cerevisiae* by comparative 13C flux analysis. Microb Cell Fact 4:30.

Gombert AK, Moreira dos Santos M, Christensen B, Nielsen J (2001) Network identification and flux quantification in the central metabolism of *Saccharomyces cerevisiae* under different conditions of glucose repression. J Bacteriol 183:1441–1451.

Hansen EH, Møller BL, Kock GR, Bünner CM, Kristensen C, Jensen OR, Okkels FT, Olsen CE, Motawia MS, Hansen J (2009) De novo biosynthesis of vanillin in fission yeast (*Schizosaccharomyces pombe*) and baker's yeast (*Saccharomyces cerevisiae*). Appl Environ Microbiol 75:2765–2774.

De Jong-Gubbels P, van Dijken JP, Pronk JT (1996) Metabolic fluxes in chemostat cultures of *Schizosaccharomyces pombe* grown on mixtures of glucose and ethanol. Microbiology 142 (Pt 6:1399–1407.

De Jong-Gubbels P, Vanrolleghem P, Heijnen S, van Dijken JP, Pronk JT (1995) Regulation of carbon metabolism in chemostat cultures of *Saccharomyces cerevisiae* grown on mixtures of glucose and ethanol. Yeast 11:407–418.

Klein T, Schneider K, Heinzle E (2012) A system of miniaturized stirred bioreactors for parallel continuous cultivation of yeast with online measurement of dissolved oxygen and off-gas. Biotechnol Bioeng 110:535–542.

Klement T, Dankmeyer L, Hommes R, van Solingen P, Buchs J, Büchs J (2011) Acetate-glycerol cometabolism: cultivating *Schizosaccharomyces pombe* on a non-fermentable carbon source in a defined minimal medium. J Biosci Bioeng 112:20–25.

Matsuyama A, Arai R, Yashiroda Y, Shirai A, Kamata A, Sekido S, Kobayashi Y, Hashimoto A, Hamamoto M, Hiraoka Y, Horinouchi S, Yoshida M (2006) ORFeome cloning and global analysis of protein localization in the fission yeast *Schizosaccharomyces pombe*. Nat Biotechnol 24:841–847.

Matsuzawa T, Fujita Y, Tohda H, Takegawa K (2011) Snf1-like protein kinase Ssp2 regulates glucose derepression in *Schizosaccharomyces pombe*. Eukaryot Cell 11:159–167.

Matsuzawa T, Hara F, Tohda H, Uemura H, Takegawa K (2012) Promotion of glycerol utilization using ethanol and 1-propanol in *Schizosaccharomyces pombe*. Appl Microbiol Biotechnol 95:441–449.

Matsuzawa T, Ohashi T, Hosomi A, Tanaka N, Tohda H, Takegawa K (2010) The *gld1+* gene encoding glycerol dehydrogenase is required for glycerol metabolism in *Schizosaccharomyces pombe*. Appl Microbiol Biotechnol 87:715–727.

Moreira dos Santos M, Raghevendran V, Kotter P, Olsson L, Nielsen J (2004) Manipulation of malic enzyme in *Saccharomyces cerevisiae* for increasing NADPH production capacity aerobically in different cellular compartments. Metab Eng 6:352–363.

Mukaiyama H, Tohda H, Takegawa K (2009) Overexpression of protein disulfide isomerases enhances secretion of recombinant human transferrin in *Schizosaccharomyces pombe*. Appl Microbiol Biotechnol 86:1135–1143.

Neunzig I, Göhring A, Drăgan C-A, Zapp J, Peters FT, Maurer HH, Bureik M (2012) Production and NMR analysis of the human ibuprofen metabolite 3-hydroxyibuprofen. J Biotechnol 157:417–420.

Rhind N, Chen Z, Yassour M, Thompson DA, Haas BJ, et al. (2011) Comparative functional genomics of the fission yeasts. Science 332:930–936.

Rodríguez-Ruiz J, Belarbi EH, J.L.G S, Alonso DL (1998) Rapid simultaneous lipid extraction and transesterification for fatty acid analyses. Biotechnol Tech 12:689 – 691.

Rumbold K, van Buijsen HJJ, Gray VM, van Groenestijn JW, Overkamp KM, Slomp RS, van der Werf MJ, Punt PJ (2010) Microbial renewable feedstock utilization: a substrate-oriented approach. Bioeng Bugs 1:359–366.

Schneider K, Krömer JO, Wittmann C, Alves-Rodrigues I, Meyerhans A, Diez J, Heinzle E (2009) Metabolite profiling studies in *Saccharomyces cerevisiae*: an assisting tool to prioritize host targets for antiviral drug screening. Microb Cell Fact 8:12.

Tarrío N, Becerra M, Cerdán ME, González Siso MI (2006) Reoxidation of cytosolic NADPH in *Kluyveromyces lactis*. FEMS Yeast Res 6:371–380.

Urk H, Bruinenberg PM, Veenhuis M, Scheffers WA, Dijken JP (1989) Respiratory capacities of mitochondria of *Saccharomyces cerevisiae* CBS 8066 and *Candida utilis* CBS 621 grown under glucose limitation. Anton van Leeuw 56:211–220.

Van Winden WA, Wittmann C, Heinzle E, Heijnen JJ (2002) Correcting mass isotopomer distributions for naturally occurring isotopes. Biotechnol Bioeng 80:477–479.

Wittmann C, Heinzle E (1999) Mass spectrometry for metabolic flux analysis. Biotechnol Bioeng 62:739–750.

Yang TH, Bolten CJ, Coppi M V, Sun J, Heinzle E (2009) Numerical bias estimation for mass spectrometric mass isotopomer analysis. Anal Biochem 388:192–203.

Yang TH, Frick O, Heinzle E (2008) Hybrid optimization for 13C metabolic flux analysis using systems parametrized by compactification. BMC Syst Biol 2:29.

Yu KO, Jung J, Ramzi AB, Kim SW, Park C, Han SO (2012) Improvement of ethanol yield from glycerol via conversion of pyruvate to ethanol in metabolically engineered *Saccharomyces cerevisiae*. Appl Biochem Biotech 166:856–865.

CHAPTER IV

Overcoming the Metabolic Burden of Protein Secretion in *Schizosaccharomyces pombe* – A Quantitative Approach using ^{13}C-based Metabolic Flux Analysis

Tobias Klein, Sabrina Lange, Nadine Wilhelm, Matthias Bureik, Tae-Hoon Yang, Elmar Heinzle and Konstantin Schneider

Abstract

Protein secretion in yeast is generally associated with a burden to cellular metabolism. To investigate this metabolic burden in *Schizosaccharomyces pombe*, we constructed a set of strains secreting the model protein maltase in different amounts. We quantified the influence of protein secretion on the metabolism applying ^{13}C-based metabolic flux analysis in chemostat cultures. Analysis of the macromolecular biomass composition revealed an increase in cellular lipid content at elevated levels of protein secretion and we observed altered metabolic fluxes in the pentose phosphate pathway, the TCA cycle, and around the pyruvate node including mitochondrial NADPH supply. Supplementing acetate to glucose or glycerol minimal media was found to improve protein secretion, accompanied by an increased cellular lipid content and carbon flux through the TCA cycle as well as increased mitochondrial NADPH production. Thus, systematic metabolic analyses can assist in identifying factors limiting protein secretion and in deriving strategies to overcome these limitations.

1. Introduction

Yeasts are attractive host systems for the production and secretion of recombinant proteins and have been the topic of different research efforts over the last decades (Mattanovich et al., 2012). Most of these studies have been conducted using the industrial workhorses *Pichia pastoris* and *Saccharomyces cerevisiae*, describing molecular engineering as well as process optimization strategies (Celik & Calik, 2011; Porro et al., 2005; Zhang et al., 2000). While many proteins have been successfully produced with these cell factories, production of mammalian proteins, e.g., for therapeutic purpose can potentially pose a problem because of low yields and hyperglycoslyation (Hamilton and Gerngross, 2007; Celik and Calik, 2011). Especially hyperglycoslation of recombinant proteins produced in yeasts has been extensively studied, leading to the successful development of glycoengineered yeasts with humanized glycosylation patterns (Chiba and Akeboshi, 2009). Another way to approach this topic can be the use of the fission yeast *Schizosaccharomyces pombe* as an alternative expression system. *S. pombe* shares several important properties with higher eukaryotes such as regulation of cell cycle, chromosomal organization and regulation of transcription and translation (Takegawa et al., 2009; Celik and Calik, 2011). In addition, glycoslyation patterns as well as mechanisms for quality control and folding of glycoproteins are considered to be more closely related to those of mammalian cells compared to other yeast species (Parodi, 1999). The production and functional secretion of an antibody fragment (scFv) linked to GFP has already been demonstrated in fission yeast with yields up to 5 mg/L, which is a higher value than all previously published yields for scFv–GFP fusion protein production in *S. cerevisiae*, but lower than that reported for *P. pastoris* (Naumann et al., 2010). Moreover, during the last decade, several approaches have been made to improve the production and secretion of recombinant proteins in *S. pombe*, including the construction of protease-deficient strains (Idiris et al., 2006), engineering of the secretory pathway (Mukaiyama et al., 2009), and addition of surfactants to the media (Mukaiyama et al., 2009).

Besides the molecular engineering of the cellular transport machinery and membrane composition, host cell physiology plays an important role for efficient production of recombinant proteins along with a proper process management. Recent publications focusing on these aspects in *P. pastoris* and *S. cerevisiae* have demonstrated the influence of carbon sources and oxygen supply (Baumann et al., 2010; Liu et al., 2013; Wong et al., 2002) as well as the metabolic burden of recombinant protein production and secretion itself (Heyland et al., 2011;

Jordà et al., 2012; Tyo et al., 2012). Systems level analyses based on transcriptome, proteome and metabolome data were applied to develop strategies for strain engineering and process design. In *S. pombe*, investigations concerning metabolic flux distributions and cofactor availability were so far limited to whole-cell biotransformations using strains expressing human cytochrome P450 enyzmes (Dragan et al., 2006; Zehentgruber et al., 2010). To the authors' knowledge no comparable studies concerning secretion of proteins in this yeast have been published so far.

In this study, we investigated the impact of increasing protein secretion on the central carbon metabolism of *S. pombe* using ^{13}C-based metabolic flux analysis. The α-glucosidase maltase, previously described by Jansen et al. (2006), was chosen as a model protein. Maltase, encoded by the *agl1* gene of *S. pombe,* is secreted in significant amounts up to 10 mg per g cells by the wild type strain. Expression of this gene is subject to glucose catabolite repression. Jansen et al. (2006) described a fed-batch process producing maltase in g/L scale, which proves that *S. pombe* is well-suited as a host for high-level protein secretion. We constructed strains exhibiting either an *agl1* deletion or an additional copy of the *agl1* gene located on an episomal plasmid. Using these strains, the impact of increasing maltase secretion on the central carbon metabolism was investigated. Analysis of the cellular macromolecular composition in combination with ^{13}C-based metabolic flux analysis was conducted to quantify major changes in cellular protein and lipid content and in key fluxes in the central metabolic pathways in response to elevated protein secretion. We aimed at understanding the metabolic perturbations caused by increased protein secretion in *S. pombe* and derived a strategy for feeding alternative substrate mixtures to improve maltase secretion.

2. Material and Methods

2.1 Vector design and strain construction

A new vector designated pREPura was cloned by substituting the expression cassette, the promotor, and the *LEU2* selection marker of pREP42GFP-C (Craven et al., 1998) by a fragment from pREP1 (Maundrell, 1993) that comprises both the strong *nmt1* promoter and the *ura4* gene. The *S. pombe agl1* gene (Okuyama et al., 2001) was amplified from genomic DNA by PCR with flanking primers that introduce restriction sites for *Nde*I (5') and *Bam*HI (3'), respectively. After restriction digest the amplified *agl1* gene was cloned into the expression vector to yield the new plasmid pREPura-agl1. For the generation of the engineered fission yeast strains, the parental strain NCYC 2036 (Losson and Lacroute, 1983) was transformed with pREPura andpREPura-agl1, yielding strain NW8 and NW9, respectively. For construction of the Δ*agl1* strain SL4, the regions 400 base pairs upstream and downstream of the *agl1* gene were amplified. Plasmid pUG25 (Goldstein and McCusker, 1999) was purchased from EUROSCARF and used for amplification of the natMX cassette. The three fragments were aligned using fusion PCR. The resulting DNA-Fragment was transformed into NCYC 2036 by electroporation (Suga and Hatakeyama, 2001). Selection of positive transformants was conducted using YE plates containing 100 µg/mL nourseothricin. Integration of the natMX cassette into the *agl1* locus was confirmed by PCR. The resulting Δ*agl1* strain was transformed with the PREPura plasmid yielding strain SL4. The strains investigated in the present work are listed in Table IV-1.

Table IV-1: Recombinant fission yeast strains used in this study

Strain	Genotype	Reference
NCYC 2036	*h-ura4.dl18*	(Losson and Lacroute, 1983)
NW8	*h-ura4.dl18 /pREPura*	This study
NW9	*h-ura4.dl18 /pREPura-agl1*	This study
Δ*agl1*	*h-ura4.dl18 /agl1::*natMX	This study
SL4	*h-ura4.dl18 /agl1::*natMX */pREPura*	This study

2.2 Media and growth conditions

The strains were cultivated using in a chemostat system of 10 mL scale parallel bioreactors applying minimal media (Klein et al., 2012) containing either 15 mM glucose or 10 mM glucose with additional supplement of 20 mM sodium acetate. Shake flask cultures were implemented for growth on glycerol/acetate mixtures. Cultivation details are described elsewhere (Klein et al., 2013)

2.3 Determination of cell growth and dry biomass

Cell growth was monitored via photometric measurement of optical density (OD) at 595 nm (Klein et al., 2012). A correlation between OD_{595nm} and cell dry weight (CDW) resulted in previously published values (Klein et al., 2013): Cell concentration on CDW basis equals $0.62 * OD_{595nm}$ on glucose and the glucose/acetate mixture and $0.60 * OD_{595nm}$ on the glycerol/acetate mixture.

2.4 Maltase activity assay

Maltase activity assay was performed as described by Jansen et al. (2006). Glucose produced from maltose hydrolysis was determined enzymatically (D-Glucose UV method, product code 10716251035, R-Biopharm, Germany). The amount of secreted maltase was determined using the specific enzyme activity described by Jansen et al. (2006).

2.5 Analysis of culture supernatants and off-gas

For the analysis of culture supernatants, bioreactors were run for at least five residence times to obtain metabolic steady-state. Afterwards, the entire liquid of the bioreactors was harvested on ice. During shake flask cultivations, multiple samples were taken during the balanced (exponential) growth phase, i.e., metabolic pseudo-steady-state. Cells were separated from culture supernatants by centrifugation, and the latter were analyzed by HPLC as described previously (Klein et al., 2012). Fermentation off gas analysis was conducted using mass spectrometry (Klein et al., 2012).

2.6 Determination of macromolecular cell composition

The analysis of cellular macromolecule composition was conducted in triplicates using the cells obtained under the balanced growth conditions. For the quantification of cellular protein content and its average amino acid composition, 1 mL of cell suspension was taken from chemostat or shake flask cultures. The cell pellet was resuspended in 100 µL of 6 M HCl and hydrolyzed for 24 h at 100°C. The suspension was neutralized, the cell debris was removed by filtration, and the remaining solution was lyophilized. The lyophilisate was resuspended in 500 µL of 200 µM α-butyric acid, which served as internal standard for HPLC analysis (Bolten and Wittmann, 2008). For the shake flask cultures, lipid content was quantified using 100 mL cell suspension, which corresponded to approximately 100 mg CDW. For chemostat cultures, multiple bioreactors were pooled to get an amount of biomass comparable to shake flask cultures. Extraction of lipids was performed as described for baker's yeast (Ejsing et al., 2009), and lipids extracted in the organic phase were dried on ice under nitrogen atmosphere. The remaining lipid fraction was used for gravimetrical determination of the cellular lipid content.

2.7 Analysis of ^{13}C enrichment in proteinogenic amino acids and fatty acids

Samples from shake flask cultures of *S. pombe* cells grown on [1,3-^{13}C] glycerol or [U-^{13}C] sodium acetate were taken during mid-exponential phase. To ensure isotopic steady state, samples were taken at three different biomass concentrations. Metabolic steady state was confirmed by constant rates for substrate uptake and product formation. In case of chemostat experiments, samples were taken after at least 5 residence times from the bioreactor outlets after switching to [1-^{13}C] glucose. A final sample was taken by harvesting the whole bioreactor content. Cells were harvested by centrifugation at 13.000 x g at 4°C for 3 min. For isolation of amino acids from the cellular proteins, the cell pellet was washed twice with distilled water, resuspended in 100 µL of 6 M HCl and incubated for 24 h at 100°C for hydrolysis of the cellular protein. GC-MS measurement of the proteinogenic amino acids was carried out as described by Frick and Wittmann (2005), ^{13}C-labeling analysis of fatty acids was conducted as described previously (Klein et al., 2013). The ^{13}C-labeling distribution of stearic acid was analyzed to determine the contribution of supplemented acetate to acetyl-CoA biosynthesis. The amino acid and fatty acid fragments chosen for the quantification of ^{13}C labeling enrichment are listed in Table IV-2.

Table IV-2: Fragments of amino acids and fatty acids analyzed by GC-MS for determination of ^{13}C enrichment.

Metabolite	Measured Fragments (m/z)	Carbon Atoms from Precursor
alanine	260	1-2-3
glycine	246	1-2
valine	288	1-2-3-4-5
leucine	274	2-3-4-5-6
isoleucine	274	2-3-4-5-6
serine	390	1-2-3
threonine	404	1-2-3-4
phenylalanine	336	1-2-3-4-5-6-7-8-9
aspartate	418	1-2-3-4
glutamate	432	1-2-3-4-5
stearic acid	143	2-3-4-5-6-7-8

2.8 ^{13}C Metabolic Flux Analysis

The metabolic network for *S. pombe* recently published was used for ^{13}C metabolic flux analysis (Klein et al., 2013). The metabolic network comprises glycolysis, pentose phosphate pathway (PPP), and the tricarboxylic acid cycle (TCA) including anabolic reactions for biomass formation and effluxes. In addition, a maltase secretion efflux was added by taking the corresponding intracellular precursor amino acids into account. The stoichiometric model and reaction reversibilities are depicted in Table IV-S1. The anabolic demand for biomass formation was adapted from the *Saccharomyces cerevisiae* model from Gombert et al. (2001). Hereto, the proteinogenic amino acid composition was corrected, lipid content was determined for the present strains, and dependency on growth conditions was taken into account (Table IV-S2). *In vivo* fluxes and their statistical properties were determined stochastically by numerically

optimizing the simulated mass isotopomer distributions to the corresponding measurements (Table IV-S3). The numerical optimization was implemented using MATLAB Version 7.7.0 (Mathworks, Inc., Nattick, USA) following the method of Yang et al. (2008) with 100 stochastic runs. The correction of naturally occurring isotopes in the analyzed amino acid and fatty acid fragments was performed as described previously (Wittmann and Heinzle, 1999; van Winden et al., 2002; Yang et al., 2009).

2.9 Balancing of reducing equivalents, ATP and combustion energies

The production and consumption rates for reducing equivalents were calculated from the flux estimates. Fixed values for the anabolic NADPH and NADH demands were adapted from Gombert et al. (2001). Surplus reducing equivalents were oxidized via the respiratory chain with a ratio of two electron pairs per O_2, as reported before (Klein et al., 2013). This redox balance was used for the calculation of specific O_2 consumption rates. Specific CO_2 production rates were calculated from the decarboxylation and carboxylation reactions. For ATP balancing, all the reactions producing and consuming ATP were taken into account and a P/O ratio of 1.5 for ATP production via the respiratory chain was assumed. We used a Y_{ATP} of 15.8 g mol^{-1} for biomass formation and a demand of 4 ATP per peptide bond for maltase formation (Verduyn et al., 1991; van Gulik and Heijnen, 1995). To estimate the efficiency of substrate utilization, the heats of combustion of glucose, acetate, glycerol, and biomass were employed (Villadsen et al., 2011). The heat of combustion from maltase was calculated from the respective amino acids and the peptide bonds were considered with an average of 12 kJ mol^{-1} (Domalski, 1972; Wu Yang et al., 1999). The surplus energy from substrate consumption was considered to dissipate as heat.

3. Results

3.1 Maltase secretion and physiology in chemostat cultivations on glucose

The strains NW8, NW9, and SL4 were grown in a 10 mL chemostat system under carbon limitation at a dilution rate D of 0.1 h^{-1} to ensure respiratory growth and full expression of the genomic *agl1* locus (Jansen et al., 2006). In Table IV-3, all physiological parameters for the strains are listed. Balancing of extracellular carbon led to closed balances (> 97%) for all strains, validating the completeness of the analytics. No maltase activity was detected in the supernatant of strain SL4. The strains NW8 and NW9 gave a secretion of 273 ± 28 U g CDW^{-1} and 907 ± 68 U g CDW^{-1}, respectively. Thus, maltase was produced with a selectivity of 7.8 mg g CDW^{-1} by NW8 and 25.9 mg g CDW^{-1} by NW9 with respect to biomass formation (Table IV-3 and Figure IV-1). The maximum of secreted maltase was 5.3% of the total cellular protein, indicating that *S. pombe* is a suitable host for high-level production and secretion of proteins.

Between strains biomass yields on glucose were comparable under the applied cultivation conditions, yet glucose uptake was reduced in NW9 compared to SL4: The specific glucose uptake rate was 1.12 ± 0.06 mmol g CDW^{-1} h^{-1} for SL4 and 1.02 ± 0.04 mmol g CDW^{-1} h^{-1} for NW9. The strains secreted low amounts of glycerol, acetate and pyruvate, in total 7% of the consumed carbon (Figure IV-2). Regarding the specific CO_2 production (q_{CO2}) and O_2 uptake rates (q_{O2}) obtained from off-gas analysis, a decrease of both q_{CO2} and q_{O2} with increasing maltase production was observed. The reduction of q_{CO2} was more pronounced, which led to a drop of the respiratory quotient (RQ) in NW9 compared to SL4 (0.91 vs. 1.02).

3.2 Changes of the macromolecular composition in response to increased protein secretion

The impact of elevated maltase secretion on the macromolecular composition of the cells was evaluated by analyzing the protein as well as the lipid content in the present strains. While the average amino acid composition of the cellular protein did not change significantly, protein content was increased in NW8 and NW9 compared to SL4: $42.5 \pm 2.3\%$ for strain SL4, $43.7 \pm 3.0\%$ NW8, and $46.6 \pm 2.1\%$ for NW9. Concerning the lipid fraction, the changes in NW8 and NW9 were $8.9 \pm 0.9\%$ and $9.7 \pm 0.8\%$, respectively, compared to $8.0 \pm 0.6\%$ in SL4.

Table IV-3: Physiological characteristics and selectivity of maltase secretion with respect to biomass formation of *S. pombe* strains SL4, NW8 and NW9 grown in chemostat cultures under respiratory growth conditions ($D = 0.1$ h^{-1}) using glucose as sole carbon source compared to NW9 grown on mixtures of glucose and acetate (Glc/Ac) in chemostat ($D = 0.1$ h^{-1}) or on glycerol and acetate (Gly/Ac) in shake flask ($\mu = 0.1$ h^{-1}). n.d. not detectable. The specific rate of carbon uptake q_{carbon} is given in [Cmmol g CDW^{-1} h^{-1}] and available energy from consumed substrates per g CDW ($Y_{\Delta H/X}$) is given in [kJ g CDW^{-1}], calculated from the heats of combustion per Cmol ($-\Delta H^0_c$). Specific rates of CO_2 production (q_{CO2}) and O_2 consumption (q_{O2}) determined experimentally from off gas analysis (EXP) are compared to values determined from the results of the metabolic flux analysis (MFA).

Strain	$Y_{X/S}$ [g CDW $Cmol^{-1}$]	q_s [mmol g CDW^{-1} h^{-1}]	q_{carbon} [Cmmol g CDW^{-1} h^{-1}]	$Y_{\Delta H/X}$ [kJ g CDW^{-1}]	q_{CO2} [mmol g CDW^{-1} h^{-1}] EXP	MFA	q_{O2} [mmol g CDW^{-1} h^{-1}] EXP	MFA	RQ	$Y_{maltase}$ [mg g CDW^{-1}]
SL4	14.7 ± 0.3	1.12 ± 0.06	6.72 ± 0.36	31.4	3.18 ± 0.10	3.18 ± 0.20	3.11 ± 0.11	3.18 ± 0.18	1.02	n.d.
NW8	14.8 ± 0.3	1.08 ± 0.04	6.48 ± 0.24	30.3	2.66 ± 0.08	2.79 ± 0.12	2.58 ± 0.06	2.55 ± 0.15	1.03	7.8 ± 0.8
NW9	14.6 ± 0.5	1.02 ± 0.03	6.12 ± 0.18	28.6	2.11 ± 0.06	2.18 ± 0.10	2.31 ± 0.04	2.40 ± 0.12	0.91	25.9 ± 1.9
NW9 (Glc/Ac)	14.8 ± 0.4	Glc: 0.90 ± 0.04 Ac: 0.65 ± 0.01	6.70 ± 0.04	30.9	2.85 ± 0.08	2.96 ± 0.18	2.75 ± 0.06	2.80 ± 0.17	1.04	39.7 ± 2.7
NW9 (Gly/Ac)	11.3 ± 0.2	Gly: 2.54 ± 0.08 Ac: 0.88 ± 0.03	9.38 ± 0.09	49.9	4.81 ± 0.24	5.05 ± 0.25	5.60 ± 0.38	5.80 ± 0.30	0.86	53.8 ± 3.0
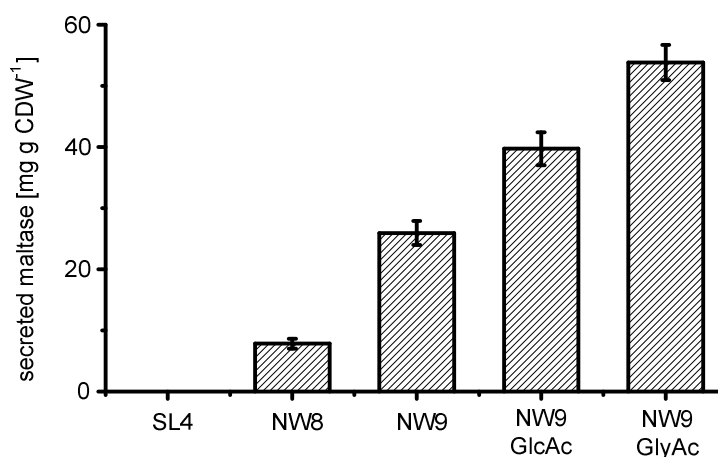
Figure IV-1: Selectivity of maltase secretion with respect to biomass formation for *S. pombe* strains SL4, NW8 and NW9 grown in chemostat cultures on glucose under respiratory growth conditions (D = 0.1 h^{-1}) and NW9 grown on mixtures of glucose and acetate (GlcAc) in chemostat and glycerol and acetate (GlyAc) in shake flask.

3.3 Metabolic flux distributions on glucose

^{13}C-based metabolic flux analysis was carried out to quantify the substrate distribution throughout the central carbon metabolism. The resulting flux distributions for the three strains are illustrated in Figure IV-2, and all fluxes are normalized to the specific glucose uptake rate (Table IV-3).

The increasing protein secretion caused a burden to the cells in terms of the anabolic demand for the amino acids required for cellular protein and secreted maltase as well as lipids. In response to this, we observed major redistributions of the metabolic fluxes with increasing maltase secretion. The flux through the oxidative PPP was significantly higher in NW9 than SL4, which was 54.1 ± 3.3% and 46.3 ± 3.0%, respectively. Accordingly, the flux through the glycolysis decreased with increasing protein secretion. Along with the increased anabolic demand this caused a decreased flux from glyceraldehyde-3-phosphate towards pyruvate, with 127.8 ± 3.4% in SL4 to 115.2 ± 2.5% in NW9.

The flux distribution between the pyruvate dehydrogenase (PDH) and the PDH bypass could not be resolved under the applied cultivation conditions. A minimum flux through the PDH bypass is necessary to meet the anabolic demand for cytosolic lipid biosynthesis. At the same time, a minimum import of pyruvate into the mitochondrial matrix is required since mitochondrial

pyruvate is a precursor for several amino acid biosyntheses, whereas surplus pyruvate is converted to acetyl-CoA by the PDH complex in the mitochondrial matrix. Acetyl-CoA molecules formed via both pathways have identical ^{13}C-labeling patterns, and, therefore, allow only a rough estimation of the *in vivo* flux distributions based on stoichiometry. This is reflected in the high standard deviations of these fluxes (between 30% to 85% of the calculated values). However, we could estimate a flux difference around the pyruvate node between SL4 and NW9: An elevated protein secretion increased pyruvate import into the mitochondria to meet the increased anabolic demand of pyruvate for amino acid biosynthesis. Along with the increased cytosolic oxaloacetate (OAA) production, the flux through the PDH bypass decreased. In accordance to this, the cytosolic acetyl-CoA production was reduced, while its anabolic demand increased at the same time due to the elevated lipid biosynthesis in NW9. The remaining cytosolic acetyl-CoA was imported into the mitochondria. The PDH flux also dropped with increasing protein secretion, resulting in decrease of acetyl-CoA availability and TCA cycle fluxes. In particular, we observed a decreased isocitrate dehydrogenase (IDH) flux in NW9 compared to SL4 with increasing maltase secretion, with 52.1 ± 2.6% vs.78.3 ± 5.7%. At the same time, cytosolic malic enzyme flux towards cytosolic pyruvate significantly increased in NW8 and NW9 from 2.6 ± 6.9% in SL4 to 9.4 ± 5.7% and 23.8 ± 5.8% in NW8 and NW9, respectively. Due to this, mitochondrial malate dehydrogenase flux replenishing mitochondrial OAA was the lowest in NW9 (16.7 ± 5.4%) and consequently cytosolic pyruvate carboxylase (PYC) converting pyruvate to OAA was the highest in this strain. PYC activity increased from 21.4 ± 6.7% in SL4 to 49.8 ± 5.6% in NW9. In all strains, more than 60% of this cytosolic OAA was transported into the mitochondria to replenish the TCA cycle. Aspartate was exclusively produced from cytosolic OAA, which could be determined from different labeling patterns of cytosolic and mitochondrial OAA. With increasing protein secretion, the anabolic flux increased accordingly to meet the anabolic demand of the cells for amino acids.
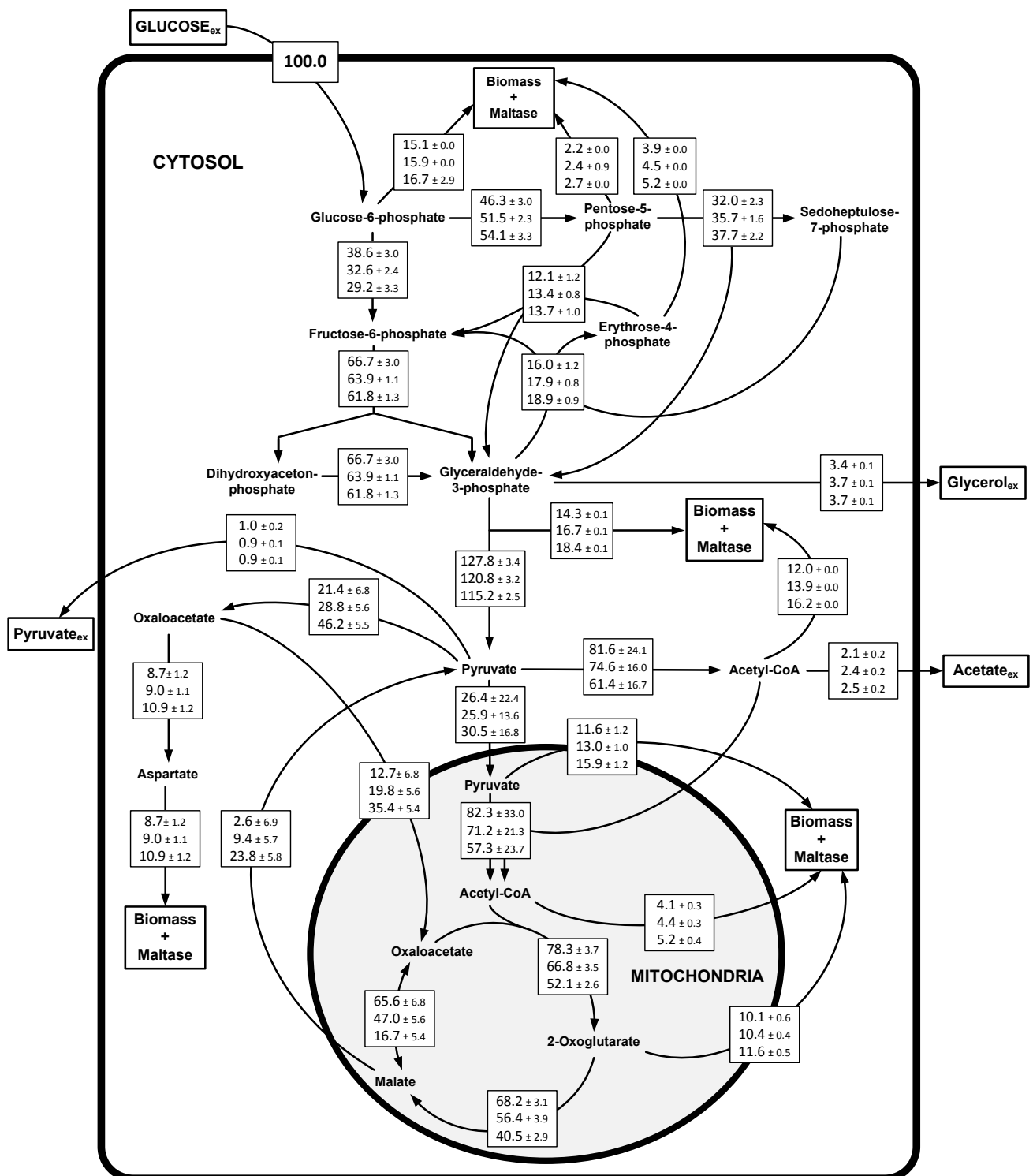
Figure IV-2: Metabolic flux distributions in *S. pombe* strains SL4, NW8 and NW9 are depicted from top to bottom. Cells were grown on [1-^{13}C] glucose in chemostat experiments under respiratory growth conditions with D = 0.1 h^{-1}. Fluxes are given as percentage of the molar glucose uptake rates (Table IV-3). For reversible reactions, net fluxes are depicted and arrows indicate the direction of the fluxes. Standard deviations were calculated to reflect the precision of the flux determination.

3.4 Cultivation on substrate mixtures increases maltase secretion

The increase in the lipid fraction of *S. pombe* associated with elevated protein secretion can be well due to the increased formation of membranes and transport vesicles. Based on this, we hypothesized that co-feeding of acetate as an additional carbon source might further increase the lipid fraction and, thus, improve maltase secretion. Further, the main redistributions of metabolic fluxes in response to an elevated protein secretion occurred in the TCA cycle and around the pyruvate node. Therefore, the additional feeding of acetate as second carbon source might also improve TCA cycle activity and precursor supply.

We performed chemostat experiments in which strain NW9 was cultivated on a mixture of glucose and acetate at D = 0.1 h^{-1}. The dilution rate was chosen to achieve respiratory growth and thus, circumvent glucose catabolite repression of acetate uptake. We also conducted shake flask batch cultures of NW9 on a mixture of glycerol and acetate. The specific growth rate μ on this mixture was 0.1 h^{-1}, which is identical to the dilution rate chosen for the chemostat experiments.

Acetate feeding led to significantly increased selectivity of maltase production with 1389 ± 94 U g CDW^{-1} on the glucose/acetate mixture and 1883 ± 106 U g CDW^{-1} on the glycerol/acetate mixture. The selectivity for secreted maltase was 39.7 and 53.8 mg g CDW^{-1} on glucose/acetate and glycerol/acetate, respectively, which corresponds to 1.5- and 2.1-fold higher protein secretion, respectively, compared to the glucose grown NW9 (Figure IV-1). Due to the acetate co-feeding, secreted maltase accounted for up to 10.4 % of the total cellular proteins.

3.5 Physiology of NW9 grown on substrate mixtures

We observed respiratory growth on both substrate mixtures that was characterized by a growth rate of 0.1 h^{-1}, high biomass yields of 15.7 g CDW Cmol^{-1} and 11.3 g CDW Cmol^{-1} for mixtures of glucose/acetate and glycerol/acetate, respectively and the absence of ethanol formation as main fermentative product. Small amounts of pyruvate were detectable in both supernatants, always below 0.02 mmol g CDW^{-1} h^{-1}. Cells grown on the glycerol/acetate mixture further produced 0.02 mmol g CDW^{-1} h^{-1} of succinate. Compared to growth on glucose as sole carbon source, the specific glucose uptake rate on the glucose/acetate mixture was lowered to 0.90 ± 0.04 mmol g CDW^{-1} h^{-1} and acetate uptake was observed at a specific rate of 0.65 ± 0.01 mmol g CDW^{-1} h^{-1}. Applying the glycerol/acetate mixture as substrate, specific uptake rates for glycerol and acetate were 2.54 ± 0.08 mmol g CDW^{-1} h^{-1} and

0.88 ± 0.03 mmol g CDW^{-1} h^{-1}, respectively. Off gas analysis of NW9 grown on both substrate mixtures yielded a q_{CO2} of 2.85 ± 0.08 mmol g CDW^{-1} h^{-1} and and a q_{O2} of 2.75 ± 0.06 mmol g CDW^{-1} h^{-1} respectively on the glucose/acetate mixture resulting in a RQ value of 1.04. On the glycerol/acetate mixture, a tremendous increase in respiratory activity was observed, with a specific oxygen uptake rate q_{O2} of 5.60 ± 0.38 mmol g CDW^{-1} h^{-1}. The specific CO_2 production rate q_{CO2} was 4.81 ± 0.24 mmol g CDW^{-1} h^{-1}, resulting in a RQ value of 0.86. All physiological parameters are summarized in Table IV-3. CO_2 production rates were used for carbon balancing, resulting in carbon balances of 104.6% and 99.0% for mixtures of glucose/acetate and glycerol/acetate, respectively.

3.6 Efficiency of carbon source utilization

With a specific uptake rate of 9.38 Cmmol g CDW^{-1} h^{-1}, the highest carbon uptake was observed for NW9 grown on the glycerol/acetate mixture (Table IV-3). On the glucose/acetate mixture, the specific carbon uptake rate was lower (6.70 Cmmol g CDW^{-1} h^{-1}) and the lowest uptake was observed for cells grown on glucose as sole carbon source, with 6.12 Cmmol g CDW^{-1} h^{-1}. However, regarding the biomass yields of strain NW9 on the different substrates, we observed the highest yield in cells grown on glucose and the glucose/acetate mixture with 14.6 ± 0.5 g Cmol^{-1} and 14.8 ± 0.4 g Cmol^{-1}, respectively (Table IV-3). In contrast, the biomass yield was lower on the glycerol/acetate mixture with 11.3 ± 0.2 g Cmol^{-1}. Thus, we conclude that substrate utilization of glucose and the glucose/acetate mixture was equally efficient but lower when glucose was exchanged for glycerol in the mixture.

To estimate the efficiency of substrate utilization, we calculated the amount of energy available to the cells [kJ g CDW^{-1}] from the assimilated substrates, using heats of combustion. These values were balanced against heats of combustion for biomass and maltase formation to calculate the amount of energy dissipation under the different conditions. The energy available to the cells slightly decreased from SL4 to NW9, due to the decreased specific glucose uptake rate (Table IV-3). However, for all cultivations using glucose as sole carbon source or the mixture of glucose/acetate, the energy input was in a comparable range, between 31.4 to 28.6 kJ g CDW^{-1}. In contrast, the amount of available energy from the substrates was 1.7 times higher when the cells were grown on the glycerol/acetate mixture, with 49.89 kJ g CDW^{-1} (Table IV-3).

We compared the distribution of this available energy from the consumed substrates between biomass, maltase and dissipation energy (Figure IV-3) under the applied conditions. Biomass yields for strain SL4, NW8 and NW9 were similar when cells were grown on glucose as sole carbon source but specific substrate uptake rates decreased from SL4 to NW9. Thus, we observed a slight increase in the efficiency of biomass formation with respect to the available energy from the substrate. While *S. pombe* strain SL4 used 78.6% of the available energy for biomass formation, strain NW9 used 86.3%. The energy demand for maltase formation increased from 0.62% of the available energy in strain NW8 to 2.15% in strain NW9 when glucose was the sole carbon source. Consequently, the dissipated energy decreased from SL4 to NW9 from 21.4% to 11.5% of the available energy from the consumed substrates. During growth on the glucose/acetate mixture, the available energy from the substrates increased again to 30.9 kJ g CDW^{-1} (Table IV-3) compared to growth on glucose as sole carbon source (28.6 kJ g CDW^{-1}) and the dissipation energy also increased again to 17.3% of the available energy from the substrates. When NW9 was grown on the glycerol/acetate mixture, the energy distribution towards biomass formation decreased to 49.5% of the available energy and consequently 47.9% of the available energy was lost as heat. Thus, in terms of energy formation, the difference in the efficiency of substrate utilization between glucose cultivations and the glycerol/acetate mixture was even more pronounced than observable from the differences in the biomass yields. Nonetheless, selectivity of maltase secretion with respect to biomass was highest on the glycerol/acetate mixture and thus we were interested to investigate which changes in the cellular composition and redistribution of metabolic fluxes compared to glucose cultivations allowed the cells to secrete higher amounts of the protein of interest.

3.7 Macromolecular composition of NW9 grown on glucose and on substrate mixtures

During growth of NW9 on the substrate mixtures, we did not observe any significant changes in the protein content or composition compared to cells grown on glucose as sole carbon source. However, we found a significant increase in the lipid fraction (Figure IV-4). When *S. pombe* strain NW9 was grown on glucose as sole carbon source, a lipid content of 9.7 ± 0.8 % was determined. Feeding of acetate increased the lipid fraction, resulting in a lipid content of 12.4 ± 1.2 % on the glucose/acetate mixture and 16.1 ± 1.2 % on the glycerol/acetate mixture. We found a positive linear correlation between the increased lipid fractions and the amount of

secreted maltase (Figure IV-4), indicating that the cellular lipid content significantly influences the secretory capacity of the cells.
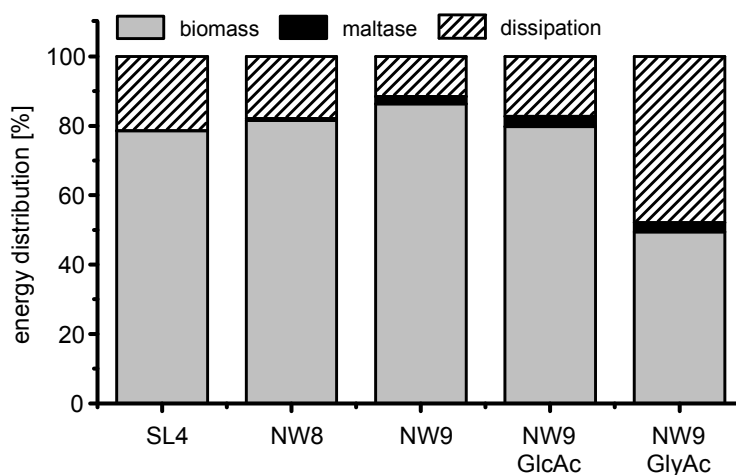
Figure IV-3: Distribution of the energy available from assimilated substrates between biomass, maltase and dissipated energy. Heats of combustion were used for these calculations (Domalski, 1972; Villadsen et al., 2011).. The surplus energy was considered lost to energy dissipation as heat.
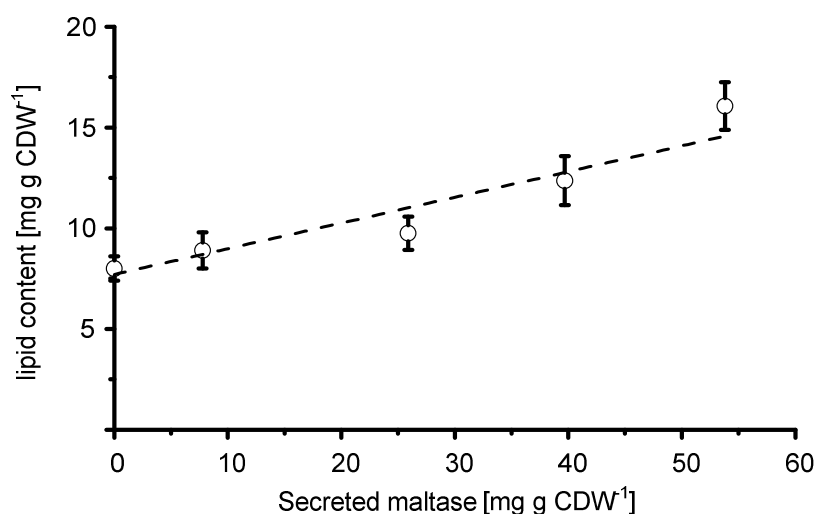
Figure IV-4: Correlation between increasing yield of secreted maltase and increasing cellular lipid content from strains SL4, NW8 and NW9 grown on glucose as sole carbon source and NW9 grown on substrate mixtures.

3.8 Metabolic flux distributions on glucose/acetate and glycerol/acetate mixtures

From an analytical point of view, adding acetate as second carbon source can further be used to resolve carbon fluxes around the pyruvate node by analyzing the ^{13}C enrichment of lipogenic fatty acids as shown in previous experiments (Klein et al., 2013). We cultivated *S. pombe* strain NW9 on the glucose/acetate mixture applying a combination of [1-^{13}C] glucose and [1,2-^{13}C] acetate as tracer substrates. On the glycerol/acetate mixture [1,3-^{13}C] glycerol and [1,2-^{13}C] acetate were applied as tracer substrates as described previously (Klein et al., 2013). The calculated metabolic flux distributions are depicted in Figure IV-5A and IV-5B.

We compared growth of this strain on both substrate mixtures to growth on glucose as sole carbon source, in order to estimate the metabolic changes which allowed the increased secretion of maltase. The key carbon fluxes are summarized in Table IV-4.

Table IV-4: Comparison of key carbon fluxes [mmol g CDW^{-1} h^{-1}] in NW9 grown on glucose as sole carbon source (Glc) compared to growth on mixtures of glucose/acetate (Glc/Ac) and glycerol/acetate (Gly/Ac).

Carbon flux	NW9 (Glc)	NW9 (Glc/Ac)	NW9 (Gly/Ac)
oxidative PPP (G6P-DH)	0.55 ± 0.03	0.49 ± 0.03	3.08 ± 0.11
Upper Glykolysis (G6P-isomerase)	0.30 ± 0.01	0.26 ± 0.03	-3.32 ± 0.03
TCA cycle (IDH)	0.53 ± 0.03	0.97 ± 0.02	0.94 ± 0.05
mitochondrial pyruvate import	0.31 ± 0.17	0.24 ± 0.02	0.27 ± 0.02
PDH	0.15 ± 0.17	0.09 ± 0.02	0.09 ± 0.02
PDH bypass (PDC/AADH)	0.63 ± 0.17	0.50 ± 0.02	0.32 ± 0.02
Anaplerosis (PYC)	0.47 ± 0.06	0.27 ± 0.01	0.30 ± 0.01
Anaplerosis (OAA import into mitochondria)	0.36 ± 0.06	0.15 ± 0.00	0.18 ± 0.01

The molar glucose uptake rate was 2.8 fold lower than the glycerol uptake rate (Table IV-3) and the flux through the oxidative PPP was about 6 times higher when cells were grown on the glycerol/acetate mixture. Glycerol was mostly channeled through the upper gluconeogenic pathway towards glucose-6-phosphate and from there towards the oxidative branch of the PPP. This created a high flux through the glucose-6-phosphate dehydrogenase and an accordingly increased back flux towards the non-oxidative reactions of the PPP to fructose-6-phosphate. Thus, glycerol circulated through the PPP and the upper gluconeogenesis, explaining the observed high CO_2 production rate (Table IV-3). In addition, the increased flux towards the oxidative PPP resulted in a tremendous increase in cytosolic NADPH generation from both glucose 6-phosphate dehydrogenase and 6-phosphogluconate dehydrogenase.

In contrast to these differences in carbon flux distributions in the upper part of the glycolysis and the PPP, fluxes around the pyruvate node and the TCA cycle were overall comparable on both substrate mixtures. Carbon fluxes from glyceraldehyde-3-phosphate towards pyruvate were slightly higher on the glucose/acetate mixture, with a flux of 1.00 ± 0.01 mmol g CDW^{-1} h^{-1} compared to 0.87 ± 0.02 mmol g CDW^{-1} h^{-1} on the glycerol/acetate mixture. Both substrate mixtures allowed a detailed resolution of the metabolic fluxes around the pyruvate node, especially the split between acetyl-CoA formation via PDH and the PDH bypass. The flux towards cytosolic OAA from pyruvate and the import of pyruvate into the mitochondria were both slightly larger on the glycerol/acetate mixture (Table IV-4), due to the increased anabolic demand for amino acid biosynthesis. The flux through the PDH was equally low on both substrate mixtures with 0.09 ± 0.01 mmol g CDW^{-1} h^{-1}. Under the chosen conditions, uptake of pyruvate into the mitochondrial matrix was just sufficient to meet the anabolic demand in this cellular compartment and mitochondrial acetyl-CoA for fueling the TCA cycle was exclusively provided by the import of cytosolic acetyl-CoA.

On the glycerol/acetate mixture the flux through the PDC and acetaldehyde dehydrogenase (AADH) was reduced by 0.18 mmol g CDW^{-1} h^{-1} compared to the glucose/acetate mixture. At the same time the anabolic demand for cytosolic acetyl-CoA was higher by a value of 0.08 mmol g CDW^{-1} h^{-1} in cells grown on the glycerol/acetate mixture due to the increased lipid content. This was also reflected by an increased acetate uptake of 0.88 mmol g CDW^{-1} h^{-1} compared to a specific uptake rate of 0.65 mmol g CDW^{-1} h^{-1} on the glucose/acetate mixture. The flux from cytosolic acetyl-CoA into the mitochondria was comparable on both substrate mixtures. Consequently, the flux through the IDH was similar on both substrates. Due to the increased anabolic demand and the small amount of secreted succinate, the subsequent TCA cycle fluxes were slightly reduced on the glycerol/acetate mixture. On both substrate mixtures

the flux through the malic enzyme was very low (0.03 ± 0.01 mmol g CDW^{-1} h^{-1}) and the import of cytosolic OAA was lower on both substrate mixtures than determined for NW9 grown on glucose as sole carbon source. As a result, the fluxes through the PYC were reduced to 0.27 ± 0.01 and 0.30 ± 0.01 mmol g CDW^{-1} h^{-1} on the glucose/acetate mixture and the glycerol/acetate mixture compared to cultivations with glucose as sole carbon source, where the cytosolic OAA formation rate was determined as 0.47 ± 0.06 mmol g CDW^{-1} h^{-1}. As already described for cultivations on glucose as sole carbon source, cytosolic OAA was the exclusive precursor for aspartate biosynthesis.

3.9 Influence of protein secretion on redox and energy metabolism

To investigate the influence of an increasing protein secretion on the energy metabolism of the strains, we calculated production and consumption rates for NADPH and ATP from the anabolic demand and the metabolic flux distributions.

Increasing protein production resulted in an increased NADPH consumption due to the increased demand for amino acids and lipids. In *S. pombe* the oxidative reactions of the PPP are the main source of cytosolic NADPH. Additional NADPH can be produced by the acetaldehyde dehydrogenase (AADH), which can use both NAD$^+$ and NADP$^+$ as cofactor (De Jong-Gubbels et al., 1996; Klein et al., 2013). There are two predicted AADH isoenzymes in *S. pombe*, encoded by the genes SPAC9E9.09c and SPBC21C3.15c, which are both assumed to be located in the cytosol (Matsuyama et al., 2006), thus acting as an additional source of cytosolic NADPH. When cells were grown on glucose as sole carbon source, the flux through the PPP increased from SL4 to NW9, while at the same time the flux through the NAD(P)$^+$ dependent AADH decreased. Assuming that AADHs used only NADPH as cofactor, we calculated the maximum cytosolic NADPH production rates, which decreased with increasing protein secretion. However, by balancing cytosolic NADPH we observed an overflow of cytosolic NADPH for all strains. The same was true for NW9 grown on the substrate mixtures. Especially the increased flux through the PPP on the glycerol/acetate mixture caused a tremendous overproduction of cytosolic NADPH with a value of 5.76 mmol g CDW^{-1} h^{-1} (Figure IV-6A).
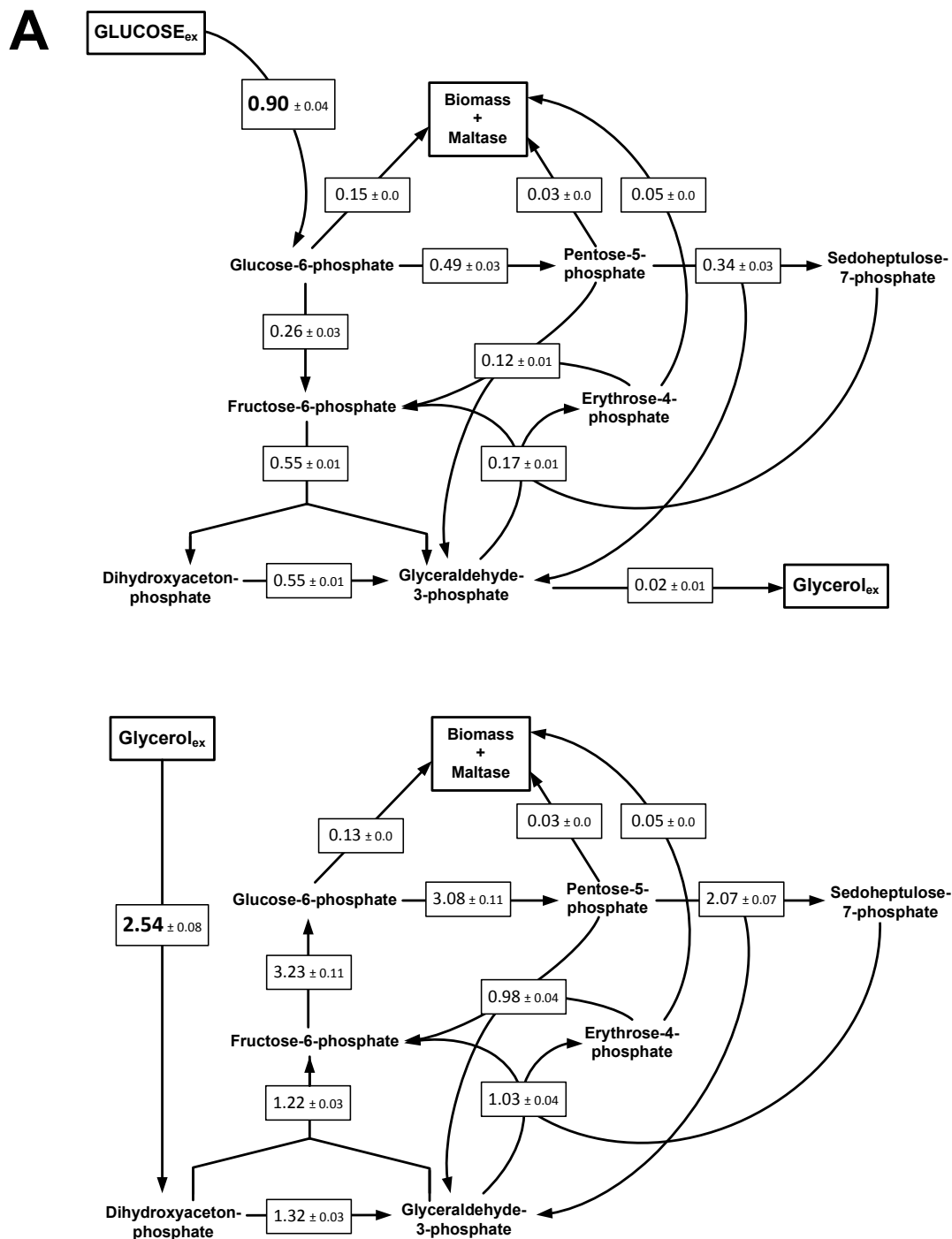
Figure IV-5A: Metabolic flux distributions in *S. pombe* strain NW9 grown on [1-^{13}C] glucose and [1,2-^{13}C] acetate in chemostat cultures under respiratory growth conditions with D = 0.1 h^{-1} (top) and grown on [1,3-^{13}C] glycerol and [1,2-^{13}C] acetate in shake flask with μ = 0.1 h^{-1} (bottom). Fluxes are given in mmol g CDW^{-1} h^{-1}. For reversible reactions, net fluxes are depicted and arrows indicate the direction of the fluxes. Flux distributions are shown for glycolysis, gluconeogenesis and PPP. Standard deviations were calculated to reflect the precision of the flux determination.
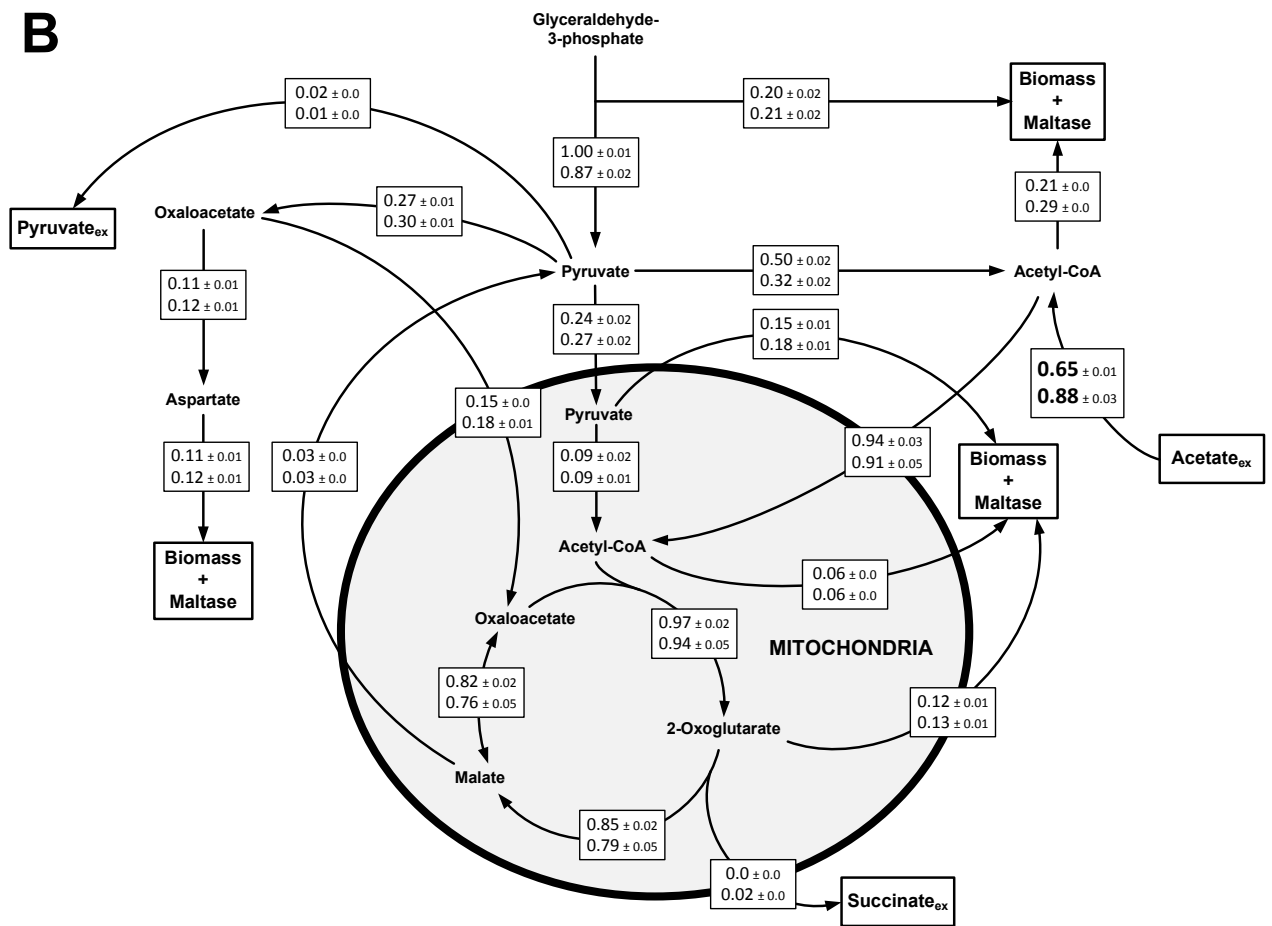
Figure IV-5B: Metabolic flux distributions in *S. pombe* strain NW9 grown on [1-^{13}C] glucose and [1,2-^{13}C] acetate in chemostat cultures under respiratory growth conditions with D = 0.1 h^{-1} (top) and grown on [1,3-^{13}C] glycerol and [1,2-^{13}C] acetate in shake flask with μ = 0.1 h^{-1} (bottom). Fluxes are given in mmol g CDW^{-1} h^{-1}. For reversible reactions, net fluxes are depicted and arrows indicate the direction of the fluxes. Flux distributions are shown around the pyruvate node and through the TCA cycle. Standard deviations were calculated to reflect the precision of the flux determination.

In *S. pombe* mitochondrial NADPH is exclusively produced by the reaction of the isoenzymes of isocitrate dehydrogenase (IDH), which can also use both cofactors under the applied cultivation conditions (Klein et al., 2013). In cells grown on glucose as sole carbon source the reduction of the TCA cycle activity also caused a reduction of the mitochondrial NADPH production. Assuming that IDH is only $NADP^+$ dependent, we observed an overflow of mitochondrial NADPH production for strains SL4 and NW8 of 0.35 mmol g CDW^{-1} h^{-1} and 0.18 mmol g CDW^{-1} h^{-1}. For strain NW9, mitochondrial NADPH production and consumption rates matched with values of 0.53 mmol g CDW^{-1} h^{-1} and 0.52 mmol g CDW^{-1} h^{-1} respectively. NW9 grown on the substrate mixtures showed significantly increased TCA cycle fluxes compared to growth on glucose as sole carbon source. Consequently we observed an overproduction of mitochondrial NADPH of 0.46 mmol g CDW^{-1} h^{-1} on the glucose/acetate mixture and 0.34 mmol g CDW^{-1} h^{-1} on the glycerol/acetate mixture (Figure IV-6B).

For redox balancing, the surplus NADPH present in all strains was considered to enter the respiratory chain eventually by transhydrogenase-like cycles (Boles et al., 1993; Klein et al., 2013). This was verified by comparing experimental and simulated q_{CO2} and q_{O2} values, which were in good agreement (< 10 % divergence) (Table IV-3).

The ATP demand increased with increasing protein secretion but at the same time, the ATP production decreased with increasing protein secretion when glucose was the sole carbon source (Figure IV-6C). However, balancing ATP production and consumption resulted in an ATP surplus for all strains which was lowest for NW9 grown on glucose as sole carbon source. Feeding of acetate as additional carbon source increased TCA cycle fluxes and consequently ATP production increased on the glucose/acetate mixture and the glycerol/acetate mixture and surplus formation of ATP increased in the same way (Figure IV-6C). In case of the glycerol/acetate mixture, the vast amount of NADPH entering the respiratory chain tremendously increased ATP production. These findings suggest that the availability of reducing equivalents as well as increased TCA cycle fluxes and ATP formation are possible bottlenecks for protein secretion in *S. pombe* during growth on glucose as sole carbon and energy source.
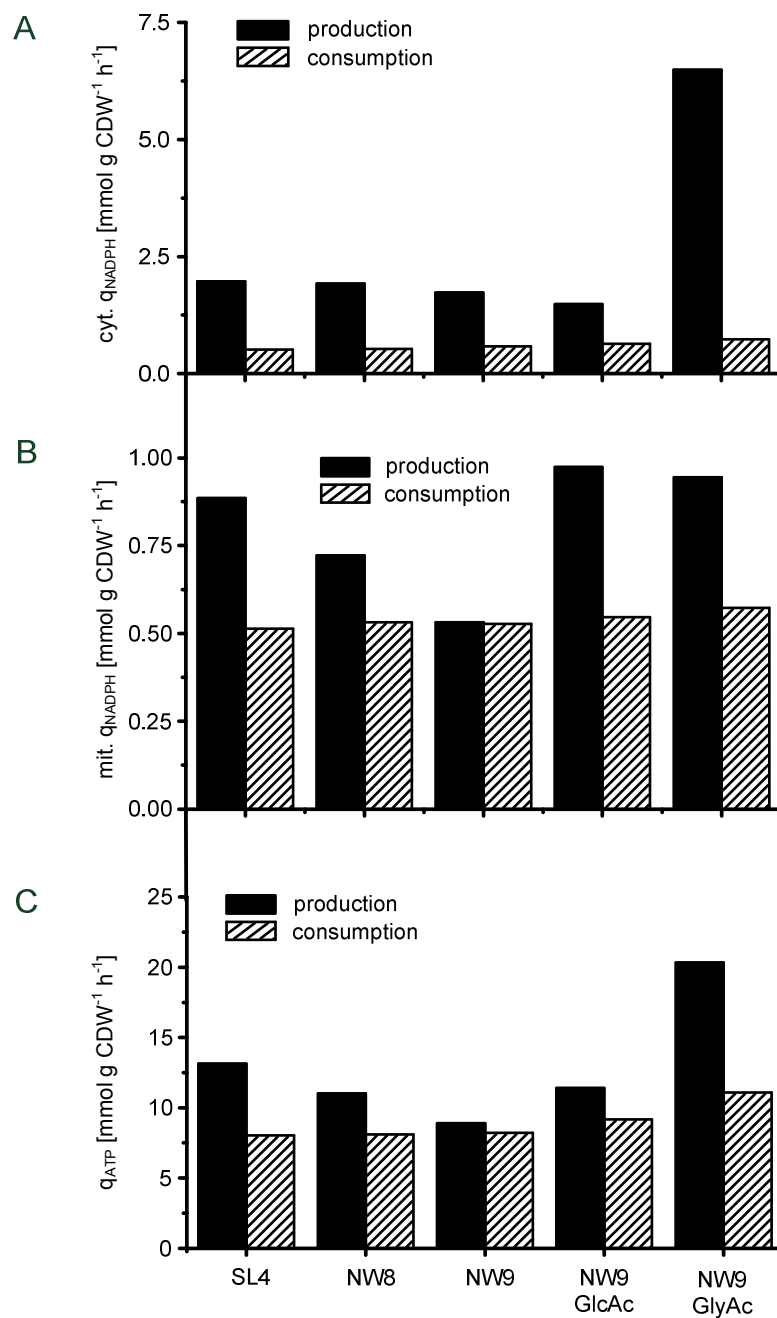
Figure IV-6: Specific production and consumption rates of A) cytosolic NADPH, B) mitochondrial NADPH and C) ATP for SL4, NW8 and NW9 grown on glucose as sole carbon source and NW9 grown on substrate mixtures. cyt: cytosolic. mit: mitochondrial. For NADPH calculations AADH and IDH were considered to only use NADP$^+$ as cofactor. For ATP calculations we assumed a P/O ratio of 1.5 and the cytosolic surplus production of NADPH was considered to enter the respiratory chain eventually via transhydrogenase-like cycles.

4. Discussion

This study aimed at understanding the influence of an increased protein secretion on the central carbon metabolism of *S. pombe*. We used the α-glucosidase maltase as a model protein for secretion (Jansen et al., 2006) and constructed mutant strains where the *agl1* gene was either deleted (SL4) or overexpressed (NW9). By comparing these mutant strains to a strain exhibiting the wild type secretion level of maltase (NW8) we could study the influence of varying levels of protein secretion on cellular physiology and metabolic flux distributions as well as the influence of different carbon sources in detail.

4.1 Strain construction and evaluation of maltase secretion

Maltase was first described in 2006 by Jansen et al. as an α-glucosidase encoded by the *agl1* gene of *S. pombe*. We chose maltase as model protein because of its high secretion rates under carbon-limited growth conditions. The *agl1* deletion strain SL4 exhibited no extracellular maltase activity, confirming the findings of Jansen *et al.* that maltase is encoded by the *agl1* gene and further confirming that its gene product is the only secreted α-glucosidase of *S. pombe*. In that work, strain CBS 356 was found to secrete 330 ± 15 U g CDW^{-1} in glucose-limited chemostat cultures, corresponding to 9.4 mg g CDW^{-1} (Jansen et al., 2006). In the present study, strain NW8 containing only the wild type copy of the maltase gene exhibited a comparable maltase secretion of 273 ± 28 U g CDW^{-1} corresponding to 7.8 mg g CDW^{-1} under comparable cultivation conditions. By overexpression of the *agl1* gene using the strong *nmt1* promotor of fission yeast we could increase secretion up to 907 ± 68 U g CDW^{-1}, corresponding to 25.9 mg g CDW^{-1}. This corresponds to a 3.3-fold increased maltase secretion compared to the wild type and a 1.3-fold increase compared to Jansen et al. (2006) after their evolutionary engineering approach for improved maltase production. From the analysis of the cellular composition and the *in vivo* metabolic flux distributions we concluded that additional feeding of acetate might help to overcome the observed limitations in the lipid and the energy metabolism (Figure IV-4 and Figure IV-6). In fact, cultivating strain NW9 on mixtures of glucose/acetate and glycerol/acetate further increased maltase secretion 6.9 fold compared to NW8 to up to 53.8 mg g CDW^{-1}. These data clearly show that secretion of maltase is not only depended on the gene copy number or promotor strength but also strongly on the physiology of the cell. The right choice of the carbon source can significantly improve protein secretion and detailed

metabolic studies can help to identify limitations in the central carbon metabolism and to derive strategies to overcome these limitations.

4.2 Physiology and metabolic flux distributions of maltase secreting strains using glucose as sole carbon source

Strains SL4, NW8 and NW9 exhibited similar biomass yields but the specific substrate uptake rate q_s decreased with increasing protein secretion. This is in accordance with results obtained for other yeast species like *Pichia pastoris*, where an improved production and secretion of a recombinant protein also decreased substrate uptake compared to the control strain (Baumann et al., 2010). However, *P. pastoris* is a Crabtree-negative yeast and is characterized by respiratory growth on glucose under aerobic conditions in the presence of high glucose concentrations in the media (Walker, 1998). In contrast, *S. pombe* is a Crabtree-positive yeast and increased glucose uptake rates lead to a mixed substrate utilization in respiratory and fermentative metabolism (De Jong-Gubbels et al., 1996). To the authors' knowledge no comparable chemostat experiments have been performed with *S. cerevisiae* up to now. However, comparing our data with literature data derived from respiratory fed-batch processes of *S. cerevisiae*, a reduction of glucose consumption in producer strains compared to non-producing control strains has also been observed (Calado et al., 2003). Further, usage of galactose as carbon source for these fed-batch processes improved recombinant protein secretion due to the reduced specific uptake rate of this sugar (Ferreira et al., 2003). It appears that yeasts are able to control glucose uptake to a certain extent and that reduced glucose uptake under producing conditions seems to improve protein secretion. The reduced carbon uptake might slow down metabolic processes, including protein biosynthesis which in turn has been shown to improve proper folding and secretion of recombinant proteins (Parekh and Wittrup, 1997).

We observed an increase in the cellular protein content of 4.1 percent points from SL4 to NW9, most likely reflecting the intracellularly retained maltase protein itself as well as an increased content of chaperones and transport proteins, which are induced in response to the increasing levels of protein secretion (unpublished data). The same is true for the increase in the lipid fraction of the cells which is most likely linked to an increasing demand for membranes and transport vesicles in the secretory pathway. A macromolecular analysis of *P. pastoris* strains secreting an antibody fragment did not reveal such changes in the cellular composition (Carnicer et al., 2009). However, the selectivity of antibody secretion per cell was more than 100-fold lower compared to the secretion level of our model protein. The same changes may

occur in *P. pastoris* when higher amounts of the secreted protein are reached. A comparable change of the cellular composition concerning the lipid fraction in response to high levels of secreted protein has recently been described for *S. cerevisiae* secreting α-amylase (Tyo et al., 2012; Liu et al., 2013) as well as the mammalian cell line AGE1.HN (Niklas et al., 2013).

We observed major redistributions of the *in vivo* carbon fluxes of strains SL4, NW8 and NW9 concerning the PPP, glycolysis, the TCA cycle and the pyruvate node, which were consistent over all three strains. The TCA cycle fluxes were strongly reduced upon an increased maltase secretion due to the accordingly increased precursor demand and a significant increase of cytosolic formation of OAA from pyruvate. While a decrease of the TCA cycle fluxes has been reported in producer strains of *P. pastoris* and *A. niger* previously (Baumann et al., 2010; Driouch et al., 2011), no increased cytosolic OAA formation has been observed in these strains. The increasing drain of precursors from the TCA cycle with increasing protein secretion caused an increased flux through the PYC to refill the TCA cycle. An efficient anaplerosis can strongly impact the secretory capacity of cells, as shown e.g in CHO cells, where overexpression of the PYC of *S. cerevisiae* could increase recombinant erythropoietin secretion 2-fold (Irani et al., 2002).

4.3 Physiology of strain NW9 grown on substrate mixtures

When the different *S. pombe* strains were grown on glucose as sole carbon source, we observed an increase in the cellular lipid content with increasing maltase secretion, which we linked to increasing membranes and transport vesicles in the secretory pathway of the cell. We hypothesized that feeding of acetate as second carbon source might facilitate lipid formation for the cell, thus improving protein secretion. The uptake of acetate strongly increased the lipid content of the cells on both substrate mixtures, as did the selectivity of maltase secretion. Since lipid content and maltase secretion directly correlate (Figure IV-4) we concluded that lipid metabolism can be one bottleneck of protein secretion and improving lipid biosynthesis may also improve secretion of other proteins than maltase in *S. pombe*.

The specific glucose uptake rate of cells grown on the glucose/acetate mixture was reduced to 0.90 ± 0.04 mmol g CDW^{-1} h^{-1} compared to cells grown on glucose as sole carbon source. A similar behavior has been described for *S. pombe* grown on mixtures of glucose and ethanol (De Jong-Gubbels et al., 1996) and for *P. pastoris*, when grown on mixtures of glucose and methanol (Jordà et al., 2012). Acetate taken up from the media is converted to cytosolic

acetyl-CoA, which in turn allows the cells to reduce the acetyl-CoA production from pyruvate. Under these conditions a high glycolytic flux can cause an accumulation of pyruvate, due to the limited capacity of the subsequent TCA cycle and the respiratory chain that would usually lead to ethanol production. However, we did not observe any production of ethanol or other fermentative products when cells were grown on the glucose/acetate mixture, indicating that any accumulated pyruvate did not further stimulate fermentative pathways. Rather, *S. pombe* seems to be able to reduce the glucose uptake rate to adapt to the maximum capacity of the TCA cycle and the respiratory chain. In cells grown on the glycerol/acetate mixture, uptake of the glycolytic substrate glycerol was significantly increased compared to glucose uptake of NW9 grown on glucose as sole carbon source or in combination with acetate. Nonetheless, growth on this mixture was respiratory and fluxes around the pyruvate pool and in the TCA cycle were in the same range on both substrate mixtures. This supports the suggested limitation of the pyruvate converting pathways. Consequently, most of the glycerol was channeled through the gluconeogenesis and the PPP, producing CO_2 and NADPH, thus allowing fast substrate metabolization, without using fermentative pathways.

On glucose/acetate mixtures the specific acetate uptake rate was determined at 0.65 ± 0.03 mmol g CDW^{-1} h^{-1}. De Jong-Gubbels et al. described cultivations of *S. pombe* on mixtures of glucose and ethanol (De Jong-Gubbels et al., 1996). In these experiments, an increase of the ethanol fraction in the media increased ethanol uptake. However, fractions of more than 0.30 Cmol ethanol per Cmol glucose resulted in acetate formation. The authors concluded that ethanol uptake and oxidation to acetate are performed efficiently but acetyl-CoA synthetase is limiting the ethanol assimilation, thus causing acetate secretion with increasing ethanol uptake. In our experiments increasing the acetate concentration in media containing either glucose or glycerol did not increase acetate uptake by the cells (data not shown). Thus, we observed a constant uptake ratio of 0.24 Cmol acetate per Cmol glucose and 0.23 Cmol acetate per Cmol glycerol, respectively. Both values are in a comparable range to the ratio described by De Jong-Gubbels et al. (1996) before acetate production occurred. While uptake ratios were similar, the uptake rate of acetate was higher on the glycerol/acetate mixture. At the same time the flux through the PDH bypass was lower on this mixture and calculating the total acetyl-CoA forming flux from the acetate uptake and the flux through the PDH bypass gave a total acetyl-CoA forming flux of 1.15 mmol g CDW^{-1} h^{-1} and 1.20 mmol g CDW^{-1} h^{-1} on glycerol/acetate and glucose/acetate mixtures, respectively. Taken together, these findings support the view of acetyl-CoA synthetase acvtivity being the limiting step in acetate and ethanol assimilation by *S. pombe* (De Jong-Gubbels et al., 1996).

4.4 Efficiency of substrate utilization

Comparing carbon uptake and biomass yields, the efficiency of substrate utilization was worst on the glycerol/acetate mixture (Table IV-3). To estimate the efficiency of substrate utilization of the different carbon sources, we investigated the substrate utilization from a thermodynamic point of view (Figure IV-3). Surprisingly, using glucose as sole carbon source the efficiency of substrate utilization for biomass and maltase formation increased from strain SL4 to NW9, from 78.6% to 88.5% of the energy available from the substrates. These findings suggest that the burden of an elevated protein secretion forces the cells to optimize the substrate utilization, in order to maintain the high biomass yield in the presence of increasing demands of energy and carbon for the formation and secretion of maltase.

When NW9 was grown on the glucose/acetate mixture 82.7% of the available energy was used for biomass and maltase formation, which was well within the range of cultivations using glucose as sole carbon source (Table IV-3). In contrast, utilization of glycerol and acetate was far less efficient. Only 52.1% of the available energy was used for biomass and maltase formation (Figure IV-3). The remaining energy was lost as heat of reaction accompanied by a high CO_2 production, explaining the decrease of the biomass yield to 11.3 ± 0.2 g CDW Cmol^{-1} (Table IV-3). In summary, these data demonstrate that the efficiency of substrate utilization can differ severely in *S. pombe* and that glucose utilization is far more efficient than growth on glycerol. However, on the glycerol/acetate mixture, maltase was produced with the highest selectivity with respect to biomass formation. Thus, the relationship between the efficiency of substrate utilization and efficiency of protein secretion per cell is not straightforward but also strongly influenced by others factors, e.g. lipid metabolism and precursor availability, as shown in this study.

4.5 Metabolic flux distributions in NW9 grown on substrate mixtures

A proper quantification of the fluxes around the pyruvate node is not possible in *S. pombe* when glucose is the sole carbon source. In *S. cerevisiae,* mitochondrial pyruvate formed by the malic enzyme reaction and the acetyl-CoA formed by the mitochondrial PDH exhibit a different labeling pattern than acetyl-CoA formed in the cytosol via the PDH bypass. Due to the cytosolic localization of malic enzyme in *S. pombe*, acetyl-CoA formed via either pathway exhibit an identical labeling pattern and thus cannot be distinguished. Since we observed major redistributions of metabolic fluxes around the pyruvate node, we concluded that a proper resolution of this node might further increase our understanding of the metabolic response to the

burden of increased protein secretion. We recently demonstrated that feeding of acetate and analysis of ^{13}C enrichment in fatty acids can be used to resolve the split between PDH and PDH bypass very well in *S. pombe* grown on a mixture of glycerol and acetate (Klein et al., 2013). This worked equally well when *S. pombe* strain NW9 was grown on a mixture of glucose and acetate or glycerol and acetate, respectively. We did only observe small differences in the carbon fluxes around the pyruvate node on both substrate mixtures. Most of the acetyl-CoA produced from extracellular acetate entered the TCA cycle. This significantly increased the TCA cycle fluxes compared to NW9 grown on glucose as sole carbon source. The flux through the IDH almost doubled from 0.53 mmol g CDW^{-1} h^{-1} to 0.97 mmol g CDW^{-1} h^{-1} and 0.94 mmol g CDW^{-1} h^{-1} on the glucose/acetate and the glycerol/acetate mixture, respectively. The similarity of the TCA cycle fluxes points at an upper limitation of TCA cycle fluxes, most likely due to a limitation of the respiratory capacity of the cells and this limitation of the TCA cycle activity may in turn be limiting protein secretion, as discussed in the following paragraph (4.6). A limiting influence of TCA cycle fluxes has already been described for intracellular recombinant protein production in *P. pastoris* (Heyland et al., 2011), but to the authors' knowledge a limiting influence of the TCA cycle on secretion of proteins in yeasts has not been described before. Taken together, these results indicate that, besides the lipid biosynthesis, an increased TCA cycle flux, providing precursors and energy is important for efficient secretion of proteins in *S. pombe*.

4.6 Redox and energy metabolism in protein secreting strains

With increasing protein production, consumption rates for NADPH and ATP increased due to the increased anabolic demand of the cells. Balancing mitochondrial NADPH production and consumption rates, we observed a decrease in production due to decreased TCA cycle fluxes in the producer strains. For NW9, production and consumption rates were similar, indicating a limitation of the protein secretion by mitochondrial NADPH. This assumption was further supported by the observation of an increase of protein secretion with increased mitochondrial NADPH supply on the substrates mixtures. These findings suggest that formation of mitochondrial NADPH can be one bottleneck of high-level protein secretion in *S. pombe*.

Concerning cytosolic NADPH, the oxidative reactions of PPP are the most important source in *S. pombe* and a redirection of the metabolic fluxes towards the oxidative branch of the PPP was observed with increasing protein secretion. Comparable results have been obtained for protein secreting strains of *P. pastoris* and *A. niger* (Baumann et al., 2010; Driouch et al., 2011).

Further *S. pombe* AADHs can use both NAD$^+$ and NADP$^+$ as co-substrates (De Jong-Gubbels et al., 1996; Klein et al., 2013) and can thus serve as an additional supply of cytosolic NADPH in *S. pombe* by switching between both cofactors. When cells were grown on glucose we observed that total cytosolic NADPH production was decreasing due to a decrease of the estimated flux through the PDC and AADH. Thus the increase of the PPP fluxes is most likely a response to this decreased flux and the resulting decreased cytosolic NADPH production. The yield of NADPH per mol glucose produced through the PPP was equal in NW9 grown on glucose as sole carbon source and grown on the glucose/acetate mixture, with 54.1% and 54.4%, respectively. However, specific molar rates were lower on the glucose/acetate mixture compared to cells grown on glucose as sole carbon source, due to the reduced glucose uptake rate on the mixture. Nonetheless during growth on all substrates a surplus production of cytosolic NADPH by the oxidative PPP was observable which was highest on the glycerol/acetate mixture with 3.08 ± 0.11 mmol g CDW^{-1} h^{-1}, producing 6.16 mmol g CDW^{-1} h^{-1} of cytosolic NADPH. The surplus was assumed to enter the respiratory chain by transhydrogenase-like cycles, as described recently (Klein et al., 2013).

Protein biosynthesis is an energy intensive process consuming 4 ATP per peptide bond formed. When cells were grown on glucose, the TCA cycle was the main source of energy, providing ATP and NADH. Cells grown on glucose as sole carbon source showed a decreasing ATP production with increasing protein secretion. A surplus of ATP was observable for all strains but was very low in NW9 grown on glucose as sole carbon source. Cultivating NW9 on the glucose/acetate mixture increased TCA cycle fluxes and thus energy formation which appeared to be one key element to increase secretion of proteins. ATP and NADPH are also required for secretion and folding of proteins (Freedman et al., 1994; Graham, 2004). We did not consider ATP and NADPH needed for these processes in our balancing, since these values are in the best case rough estimations. However, the low ATP surplus in NW9 grown on glucose as sole carbon source and the increase of protein secretion with an increasing ATP surplus by additional feeding of acetate, indicate a possible limitation of the energy metabolism regarding protein secretion under the applied conditions. Finally, the highest maltase secretion was reached on the glycerol/acetate substrate mixture where both the NADPH and ATP production were highest. The increased ATP production compared to the glucose/acetate mixture was due to the high cytosolic NADPH surplus, which we considered to enter the respiratory chain to produce ATP. These data show that high production rates of NADPH and ATP both strongly improve protein secretion in *S. pombe* and that redox and energy metabolism can be bottlenecks in high-level protein secretion in this yeast.

5. Conclusions

In this study we could clearly show that *S. pombe* is able to secrete high amounts of proteins, up to 53.8 mg g CDW^{-1}. This protein secretion is a burden to the cells that is reflected in the central carbon metabolism. We demonstrated that lipid biosynthesis and the TCA cycle activity can limit protein secretion as well as the supply of NADPH and ATP. These findings can be used to identify targets for metabolic engineering approaches to improve protein secretion in *S. pombe*. As one example of such an approach, we could show that additional feeding of acetate and change of the carbon source from glucose to glycerol could efficiently increase maltase secretion by improving the precursor supply to overcome these metabolic bottlenecks. Finally we hypothesize that the observed links of the central carbon metabolism to protein secretion are not maltase-specific but rather generally connected to the amount of secreted protein itself and the corresponding induced transport processes. Future experiments will, however, have to proof that this hypothesis is transferable to improve secretion of other, also recombinant, proteins in *S. pombe*.

6. References

Baumann, K., Carnicer, M., Dragosits, M., Graf, A.B., Stadlmann, J., Jouhten, P., Maaheimo, H., Gasser, B., Albiol, J., Mattanovich, D., Ferrer, P., 2010. A multi-level study of recombinant *Pichia pastoris* in different oxygen conditions. BMC Syst Biol 4, 141.

Boles, E., Lehnert, W., Zimmermann, F.K., 1993. The role of the NAD-dependent glutamate dehydrogenase in restoring growth on glucose of a *Saccharomyces cerevisiae* phosphoglucose isomerase mutant. Eur J Biochem 217, 469–477.

Bolten, C.J., Wittmann, C., 2008. Appropriate sampling for intracellular amino acid analysis in five phylogenetically different yeasts. Biotechnol Lett 30, 1993–2000.

Calado, C.R.C., Almeida, C., Cabral, J.M.S., Fonseca, L.P., 2003. Development of a Fed-Batch Cultivation Strategy for the Enhanced production and Secretion of Cutinase by a Recombinant *Saccharomyces cerevisiae* SU50 Strain. J Biosci Bioeng 96, 141–148.

Carnicer, M., Baumann, K., Töplitz, I., Sánchez-Ferrando, F., Mattanovich, D., Ferrer, P., Albiol, J., 2009. Macromolecular and elemental composition analysis and extracellular metabolite balances of *Pichia pastoris* growing at different oxygen levels. Microb Cell Fact 8, 65.

Celik, E., Calik, P., 2011. Production of recombinant proteins by yeast cells. Biotechnol Adv 30, 1108–1118.

Chiba, Y., Akeboshi, H., 2009. Glycan engineering and production of "humanized" glycoprotein in yeast cells. Biol Pharm Bull 32, 786–795.

Craven, R.A., Griffiths, D.J., Sheldrick, K.S., Randall, R.E., Hagan, I.M., Carr, A.M., 1998. Vectors for the expression of tagged proteins in *Schizosaccharomyces pombe*. Gene 221, 59–68.

Domalski, E.S., 1972. Selected Values of Heats of Combustion and Heats of Formation of Organic Compounds Containing the Elements C, H, N, O, P, and S. J Phys Chem Ref Data 1, 221.

Dragan, C.A., Blank, L.M., Bureik, M., 2006. Increased TCA cycle activity and reduced oxygen consumption during cytochrome P450-dependent biotransformation in fission yeast. Yeast 23, 779–794.

Driouch, H., Melzer, G., Wittmann, C., 2011. Integration of *in vivo* and *in silico* metabolic fluxes for improvement of recombinant protein production. Metab Eng 14, 47–58.

Ejsing, C.S., Sampaio, J.L., Surendranath, V., Duchoslav, E., Ekroos, K., Klemm, R.W., Simons, K., Shevchenko, A., 2009. Global analysis of the yeast lipidome by quantitative shotgun mass spectrometry. Proc Natl Acad Sci USA 106, 2136–2141.

Ferreira, B.S., Calado, C.R.C., Van Keulen, F., Fonseca, L.P., Cabral, J.M.S., Da Fonseca, M.M.R., 2003. Towards a cost effective strategy for cutinase production by a recombinant *Saccharomyces cerevisiae*: strain physiological aspects. Appl Microbiol Biotechnol 61, 69–76.

Freedman, R.B., Hirst, T.R., Tuite, M.F., 1994. Protein disulphide isomerase: building bridges in protein folding. Trends Biochem Sci 19, 331–336.

Frick, O., Wittmann, C., 2005. Characterization of the metabolic shift between oxidative and fermentative growth in *Saccharomyces cerevisiae* by comparative 13C flux analysis. Microb Cell Fact 4, 30.

Goldstein, A.L., McCusker, J.H., 1999. Three new dominant drug resistance cassettes for gene disruption in *Saccharomyces cerevisiae*. Yeast 15, 1541–1553.

Gombert, A.K., Moreira dos Santos, M., Christensen, B., Nielsen, J., 2001. Network identification and flux quantification in the central metabolism of *Saccharomyces cerevisiae* under different conditions of glucose repression. J Bacteriol 183, 1441–1451.

Graham, T.R., 2004. Flippases and vesicle-mediated protein transport. Trends Cell Biol 14, 670–677.

Van Gulik, W.M., Heijnen, J.J., 1995. A metabolic network stoichiometry analysis of microbial growth and product formation. Biotechnol Bioeng 48, 681–698.

Hamilton, S.R., Gerngross, T.U., 2007. Glycosylation engineering in yeast: the advent of fully humanized yeast. Curr Opin Microbiol 18, 387–392.

Heyland, J., Fu, J., Blank, L.M., Schmid, A., 2011. Carbon metabolism limits recombinant protein production in *Pichia pastoris*. Biotechnol Bioeng 108, 1942–1953.

Idiris, A., Bi, K., Tohda, H., Kumagai, H., Giga-Hama, Y., 2006. Construction of a protease-deficient strain set for the fission yeast *Schizosaccharomyces pombe*, useful for effective production of protease-sensitive heterologous proteins. Yeast 23, 83–99.

Irani, N., Beccaria, A.J., Wagner, R., 2002. Expression of recombinant cytoplasmic yeast pyruvate carboxylase for the improvement of the production of human erythropoietin by recombinant BHK-21 cells. J Biotechnol 93, 269–282.

Jansen, M.L., Krook, D.J., De Graaf, K., Van Dijken, J.P., Pronk, J.T., De Winde, J.H., 2006. Physiological characterization and fed-batch production of an extracellular maltase of *Schizosaccharomyces pombe* CBS 356. FEMS Yeast Res 6, 888–901.

De Jong-Gubbels, P., Van Dijken, J.P., Pronk, J.T., 1996. Metabolic fluxes in chemostat cultures of *Schizosaccharomyces pombe* grown on mixtures of glucose and ethanol. Microbiology 142 (Pt 6, 1399–1407.

Jordà, J., Jouhten, P., Cámara, E., Maaheimo, H., Albiol, J., Ferrer, P., 2012. Metabolic flux profiling of recombinant protein secreting *Pichia pastoris* growing on glucose:methanol mixtures. Microb Cell Fact 11, 57.

Klein, T., Heinzle, E., Schneider, K., 2013. Metabolic fluxes in *Schizosaccharomyces pombe* grown on glucose and mixtures of glycerol and acetate. Appl Microbiol Biotechnol 97, 5013–5026.

Klein, T., Schneider, K., Heinzle, E., 2012. A system of miniaturized stirred bioreactors for parallel continuous cultivation of yeast with online measurement of dissolved oxygen and off-gas. Biotechnol Bioeng 110, 535–542.

Liu, Z., Osterlund, T., Hou, J., Petranovic, D., Nielsen, J., 2013. Anaerobic α-amylase production and secretion with fumarate as the final electron acceptor in yeast. Appl Environ Microbiol 79, 2962–2967.

Losson, R., Lacroute, F., 1983. Plasmids carrying the yeast OMP decarboxylase structural and regulatory genes: transcription regulation in a foreign environment. Cell 32, 371–377.

Matsuyama, A., Arai, R., Yashiroda, Y., Shirai, A., Kamata, A., Sekido, S., Kobayashi, Y., Hashimoto, A., Hamamoto, M., Hiraoka, Y., Horinouchi, S., Yoshida, M., 2006. ORFeome cloning and global analysis of protein localization in the fission yeast *Schizosaccharomyces pombe*. Nat Biotechnol 24, 841–847.

Mattanovich, D., Branduardi, P., Dato, L., Gasser, B., Sauer, M., Porro, D., 2012. Recombinant protein production in yeasts. Meth Mol Biol 824, 329–358.

Maundrell, K., 1993. Thiamine-repressible expression vectors pREP and pRIP for fission yeast. Gene 123, 127–130.

Mukaiyama, H., Giga-Hama, Y., Tohda, H., Takegawa, K., 2009. Dextran sodium sulfate enhances secretion of recombinant human transferrin in *Schizosaccharomyces pombe*. Appl Microbiol Biotechnol 85, 155–164.

Mukaiyama, H., Tohda, H., Takegawa, K., 2009. Overexpression of protein disulfide isomerases enhances secretion of recombinant human transferrin in *Schizosaccharomyces pombe*. Appl Microbiol Biotechnol 86, 1135–1143.

Naumann, J.M., Kuttner, G., Bureik, M., 2010. Expression and secretion of a CB4-1 scFv-GFP fusion protein by fission yeast. Appl Biochem Biotechnol 163, 80–89.

Niklas, J., Priesnitz, C., Rose, T., Sandig, V., Heinzle, E., 2013. Metabolism and metabolic burden by α1-antitrypsin production in human AGE1.HN cells. Metab Eng 16C, 103–114.

Okuyama, M., Okuno, A., Shimizu, N., Mori, H., Kimura, A., Chiba, S., 2001. Carboxyl group of residue Asp647 as possible proton donor in catalytic reaction of alpha-glucosidase from *Schizosaccharomyces pombe*. Euro J Biochem 268, 2270–2280.

Parekh, R.N., Wittrup, K.D., 1997. Expression level tuning for optimal heterologous protein secretion in *Saccharomyces cerevisiae*. Biotechnol Prog 13, 117–122.

Parodi, A.J., 1999. Reglucosylation of glycoproteins and quality control of glycoprotein folding in the endoplasmic reticulum of yeast cells. Biochim Biophys Acta 1426, 287–295.

Porro, D., Sauer, M., Branduardi, P., Mattanovich, D., 2005. Recombinant protein production in yeasts. Mol Biotechnol 31, 245–259.

Suga, M., Hatakeyama, T., 2001. High efficiency transformation of *Schizosaccharomyces pombe* pretreated with thiol compounds by electroporation. Yeast 18, 1015–1021.

Takegawa, K., Tohda, H., Sasaki, M., Idiris, A., Ohashi, T., Mukaiyama, H., Giga-Hama, Y., Kumagai, H., 2009. Production of heterologous proteins using the fission-yeast (*Schizosaccharomyces pombe*) expression system. Biotechnol Appl Biochem 53, 227–235.

Tyo, K.E.J., Liu, Z., Petranovic, D., Nielsen, J., 2012. Imbalance of heterologous protein folding and disulfide bond formation rates yields runaway oxidative stress. BMC Biol 10, 16.

Verduyn, C., Stouthamer, A.H., Scheffers, W.A., Van Dijken, J.P., 1991. A theoretical evaluation of growth yields of yeasts. A van Leeuw 59, 49–63.

Villadsen, J., Nielsen, J., Gunnar, L., 2011. Bioreaction Engineering Principles, Third Edit. Springer.

Walker, G.M., 1998. Yeast Physiology & Biotechnology. Wiley.

Van Winden, W.A., Wittmann, C., Heinzle, E., Heijnen, J.J., 2002. Correcting mass isotopomer distributions for naturally occurring isotopes. Biotechnol Bioeng 80, 477–479.

Wittmann, C., Heinzle, E., 1999. Mass spectrometry for metabolic flux analysis. Biotechnol Bioeng 62, 739–750.

Wong, D., Batt, S., Lee, C., Robertson, G., 2002. Increased expression and secretion of recombinant alpha-amylase in *Saccharomyces cerevisiae* by using glycerol as the carbon source. J Protein Chem 21, 419–425.

Wu Yang, X., Rui Liu, J., Li Gao, S., Dong Hou, Y., Zhen Shi, Q., 1999. Determination of combustion energies of thirteen amino acids. Thermochim Acta 329, 109–115.

Yang, T.H., Bolten, C.J., Coppi, M. V, Sun, J., Heinzle, E., 2009. Numerical bias estimation for mass spectrometric mass isotopomer analysis. Anal Biochem 388, 192–203.

Yang, T.H., Frick, O., Heinzle, E., 2008. Hybrid optimization for 13C metabolic flux analysis using systems parametrized by compactification. BMC Syst Biol 2, 29.

Zehentgruber, D., Dragan, C., Bureik, M., Luetz, S., 2010. Challenges of steroid biotransformation with human cytochrome P450 monooxygenase CYP21 using resting cells of recombinant *Schizosaccharomyces pombe*. J Biotechnol 146, 179–185.

Zhang, W., Inan, M., Meagher, M.M., 2000. Fermentation strategies for recombinant protein expression in the methylotrophic yeast *Pichia pastoris*. Biotechnol Bioproc E 5, 275–287.

CHAPTER V

Growth on acetate-containing substrate mixtures increases secretion of heterologous proteins in the fission yeast *Schizosaccharomyces pombe*

Abstract

Heterologous secretion of proteins in yeast poses a burden to the cellular metabolism and in turn can be strongly influenced by host physiology. Recently, we demonstrated that high level secretion of the α-glucosidase maltase in *Schizosaccharomyces pombe* is limited by bottlenecks in the lipid biosynthesis and energy metabolism. A rational media optimization approach improved maltase production through addition of acetate and the change of the carbon source from glucose to glycerol. In this work we investigated if these strategies were specific for maltase secretion or rather applicable to protein secretion in general. We used *S. pombe* strain NCYC 2036 carrying plasmids for secretion of either green fluorescent protein (GFP) or a fluorescent single-chain antibody fragment (CB4-1 scFv-GFP). The strains were grown in minimal media under fermentative and respiratory conditions on glucose as sole carbon source and on mixtures of glucose/acetate and glycerol/acetate. We observed an increase in the secretion of both proteins on the acetate-containing substrate mixtures, showing that the application of these mixtures as carbon source has in general a beneficial effect on protein secretion in *S. pombe*.

1. Introduction

Secretion of heterologous proteins in yeasts is a fast and efficient way to produce the protein of interest while minimizing expensive downstream processing at the same time. The metabolism of the production host can hereby strongly influence product quality and product yields (Mattanovich et al. 2012; Porro et al. 2005). At the same time, protein secretion itself is a burden to the cellular metabolism and several studies deal with the influence of recombinant protein secretion on host physiology in *Pichia pastoris* and *Saccharomyces cerevisiae* (Jordà et al. 2012; Tyo et al. 2012; Baumann et al. 2010). Consequently changes in process conditions and alterations in the applied carbon sources can have a tremendous influence on host physiology and thereby on product yields (Holmes et al. 2009; Liu et al. 2012; Wong et al. 2002).

We recently investigated the influence of high level protein secretion on the metabolism of *Schizosaccharomyces pombe*. The α-glucosidase maltase, which naturally encoded in the genome of *S. pombe*, was used as model protein and the gene locus either deleted or overexpressed via an episomal plasmid. Analyses of the macromolecular cell composition and the metabolic flux distributions indicated that energy metabolism and precursor supply as well as lipid biosynthesis were the major metabolic bottlenecks for high-level protein secretion. Applying mixtures of mixtures of glucose and acetate or glycerol and acetate as feed enabled the cells to overcome these limitations and could increase maltase secretion 5-fold compared to the wild type strain. In the present study we wanted to investigate, whether these results were specific for the secretion of maltase or generally applicable to improve heterologous protein secretion in *S. pombe*.

2. Material and Methods

2.1 Strain construction

We transformed *S. pombe* strain NCYC 2036 (*h-ura4.dl18*) with the plasmid pTZsp-GFP, kindly provided by the group of Prof. Manfred Schmitt. This plasmid carries the viral secretion signal from K28 killer virus fused to green fluorescent protein (GFP) under control of the *nmt1* promoter, which allows the secretion of yeast enhanced GFP in *S. pombe* (Eiden-Plach et al. 2004; Heintel et al. 2001). Further, NCYC 2036 was transformed with the plasmid pJMN6, kindly provided by Dr. Matthias Bureik. This plasmid allows the secretion of the fluorescent single-chain antibody fragment CB4-1 scFv-GFP using the Cpy1 secretion signal in *S. pombe* (Naumann et al. 2010). All strains are listed in Table 1.

Table 1: Recombinant strains of *Schizosaccharomyces pombe* used in this study

Strain	Genotype	Reference
NCYC 2036	*h-ura4.dl18*	(Losson and Lacroute 1983)
pTZ-spGFP	*h-ura4.dl18 /pTZ-GFP*	(Eiden-Plach et al. 2004)
pJMN6	*h-ura4.dl18 /pJMN6*	(Naumann et al. 2010)

2.2 Cultivation conditions

Cells were grown in shake flasks or in the previously published chemostat system at $D = 0.1$ h^{-1} allowing respiratory growth (Klein et al. 2012). In chemostat experiments 15 mM glucose or a mixture of 10 mM glucose and 10 mM acetate served as carbon sources using the previously described minimal media (Klein et al. 2013). In the shake flask cultivations, we used either 100 mM of glucose as sole carbon source or a mixture of 100 mM glycerol and 50 mM of acetate (Klein et al. 2013).

2.3 Analytics of cell growth and fluorescence measurements

Determination of optical density at 595 nm (OD_{595}) and cell dry weight (CDW) was performed as described previously (Klein et al. 2013). Quantification of secreted GFP and the fluorescent single-chain antibody fragment was performed by fluorescence measurement in a Fluoroskan Ascent Microplate Reader (Thermo Scientific) as describe by Naumann et al. (2010).

3. Results and Discussion

Both strains were cultivated in shake flask cultivations with 100 mM glucose as sole carbon source and the amount of secreted proteins quantified by fluorescence measurement at the end of the glucose growth phase. These values were compared to yields of secreted GFP and CB4-1-scFv-GFP obtained from cells grown in chemostat cultures at $D = 0.1$ h^{-1} on glucose and on the glucose/acetate mixture as well as to shake flask cultivations using the mixture of glycerol/acetate as carbon sources (Figure 1).

Comparing GFP secretion between cells grown in shake flasks (fermentative growth) and chemostat cultivations (respiratory growth) using glucose as sole carbon source, we observed no difference in the selectivity of GFP secretion with respect to biomass, yielding 0.13 ± 0.01 mg g CDW^{-1} (Fig. 1). However, changing the carbon source to the mixture of glucose and acetate, increased the selectivity of GFP secretion by a factor of 1.3 to 0.18 ± 0.00 mg g CDW^{-1}. The best results were achieved applying the glycerol/acetate mixture. Cultivation of *S. pombe* strain pTZ-spGFP on this mixture further increased GFP secretion 1.9-fold compared to cultivations using glucose as sole carbon source, with a selectivity of 0.25 ± 0.01 mg g CDW^{-1} (Figure 1).

To estimate the impact on the secretion of the single-chain antibody fragment, we cultivated *S. pombe* strains pJMN6 on the different substrates. Since we had not observed any differences in the selectivity of GFP secretion during fermentatitve growth (shake flask) and respiratory growth (chemostat) on glucose as sole carbon source, we did not perform this comparison for the secretion of the antibody fragment.

Cultivation of *S. pombe* strain pJMN6 on glucose in shake flasks resulted in a selectivity of CB4-1 scFv-GFP secretion of 0.13 ± 0.02 mg g CDW^{-1} (Fig. 1). Again, using the acetate containing substrate mixtures improved heterologous protein secretion. In case of the antibody fragment the increase was even more pronounced compared to GFP secretion. On the

glucose/acetate mixture the selectivity of secreted CB4-1 scFv-GFP increased 3.1-fold to 0.40 ± 0.04 mg g CDW^{-1} and applying the glycerol/acetate mixture, a further increase of antibody secretion was observed up to 0.50 ± 0.04 mg g CDW^{-1} (3.8-fold), compared to cultivations using glucose as sole carbon source (Figure 1).
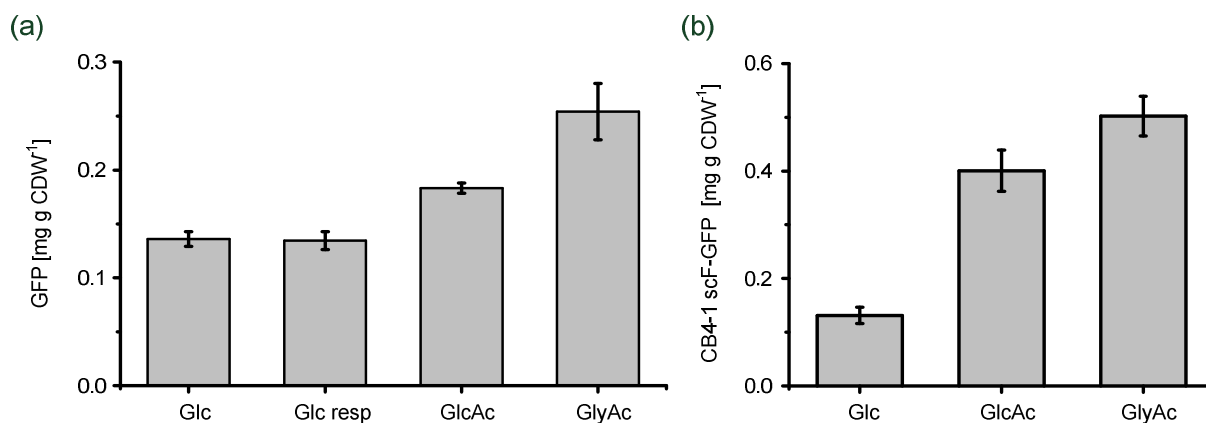
Figure 1: Secretion of (a) GFP and (b) CB4-1-scFv-GFP in *S. pombe* under different cultivation conditions: Glc: in shake flask using glucose as sole carbon source; Glc resp.: in chemostat using glucose as sole carbon source under respiratory growth conditions (D = 0.1 h^{-1}). GlcAc: in chemostat using a mixture of glucose and acetate as carbon source. GlyAc: in shake flask, using a mixture of glycerol and acetate as carbon source.

For secretion of both recombinant proteins in *S. pombe*, we observed similarly increasing yields of secreted product from glucose as sole carbon source to the mixture of glucose/acetate with a maximum secretion level reached during growth on the mixture of glycerol/acetate. In contrast, changing between respiratory and fermentative growth conditions did not influence selectivity of protein secretion with respect to biomass for GFP and the single-chain antibody fragment, respectively. Respiratory growth allows the cell to metabolize the substrate more efficiently regarding energy formation per mol glucose. The TCA cycle and the respiratory chain are the main sources of energy for the cell and during high-level secretion of maltase we could identify TCA cycle activities and mitochondrial NADPH supply as bottlenecks limiting protein secretion However, selectivities of secretion of GFP and the CB4-1 antibody fragment were both 100-fold lower than for maltase. Consequently, a limitation of the central carbon metabolism in

terms of NADPH and energy metabolism does most likely not occur, even under fermentative growth conditions.

Providing acetate as additional carbon and energy source increased secretion of both recombinant proteins. An intracellular accumulation in the endoplasmic reticulum and the Golgi apparatus during the production phase has been reported for both GFP and the antibody fragment (Eiden-Plach et al. 2004; Naumann et al. 2010). Further, Hou et al. (2012) could recently demonstrate that increasing vesicle formation can efficiently improve recombinant protein secretion in *S. cerevisiae.* In our previous study, we could show that the lipid content of maltase secreting *S. pombe* cells increased significantly when acetate was added to the media. Thus, we propose that addition of acetate and the resulting increased cellular lipid content may allow an increased membrane and vesicle formation, thus improving transport and secretion of otherwise retained proteins.

Changing the carbon source from glucose to glycerol further increased the secretion of both proteins. Tyo et al. (2012) recently reported an increase of oxygen consumption levels in *S. cerevisiae* cells secreting α-amylase. They linked this increased O_2 demand to futile cycles of protein folding and refolding, consuming O_2 as final electron acceptor. In these cycles NADPH is most important as electron carrier for the regeneration of glutathione. Previously, we could show that growth of *S. pombe* on glycerol/acetate mixtures results in a tremendous cytosolic NADPH formation, which is eventually regenerated via the respiratory chain (Klein et al. 2013). The increased lipid formation consumes additional cytosolic NADPH and futile cycles of protein folding may also be a constant drain from the cytosolic NADPH pool. Consequently, using a substrate like glycerol providing high amounts of cytosolic NADPH might allow the cells to synthesize lipids and regenerate glutathione in a more efficient way. Thus we propose that the switch from glucose to glycerol/acetate improved membrane formation for vesicular transport of proteins and as well as folding of proteins, explaining the increase of recombinant protein secretion.

We demonstrated that the results obtained in the previous study with the model protein maltase could be transferred to improve heterologous secretion of both GFP and CB4-1 scFv-GFP. This demonstrates that these previous findings were not specific for maltase secretion but can be applied in general to improve secretion of recombinant proteins in *S. pombe*. In the maltase study, secreted protein yields were much higher than those for the two recombinant proteins we used in the present study. Thus, the underlying mechanisms which enable an improved heterologous protein secretion may partially differ between different proteins, depending on the

amount of secreted protein. Further work is necessary to investigate in detail how, upon changing the carbon source, redistributions of the *in vivo* carbon fluxes influence secretion of recombinant proteins with low specific yields. However, this study is a good starting point for future metabolic and biochemical studies regarding the improvement of recombinant protein secretion in *S. pombe*.

4. Acknowledgements

5. References

Baumann K, Carnicer M, Dragosits M, Graf AB, Stadlmann J, Jouhten P, Maaheimo H, Gasser B, Albiol J, Mattanovich D, Ferrer P (2010) A multi-level study of recombinant *Pichia pastoris* in different oxygen conditions. BMC Syst Biol 4:141.

Eiden-Plach A, Zagorc T, Heintel T, Carius Y, Breinig F, Schmitt MJ (2004) Viral Preprotoxin Signal Sequence Allows Efficient Secretion of Green Fluorescent Protein by Candida glabrata, Pichia pastoris, Saccharomyces cerevisiae, and *Schizosaccharomyces pombe*. Appl Environ Microbiol 70:961–966.

Heintel T, Zagorc T, Schmitt MJ (2001) Expression, processing and high level secretion of a virus toxin in fission yeast. Appl Microbiol Biotechnol 56:165–172.

Holmes WJ, Darby RA, Wilks MD, Smith R, Bill RM (2009) Developing a scalable model of recombinant protein yield from *Pichia pastoris*: the influence of culture conditions, biomass and induction regime. Microb Cell Fact 8:35.

Hou J, Tyo K, Liu Z, Petranovic D, Nielsen J (2012) Engineering of vesicle trafficking improves heterologous protein secretion in *Saccharomyces cerevisiae*. Metab Eng 14:120–127.

Jordà J, Jouhten P, Cámara E, Maaheimo H, Albiol J, Ferrer P (2012) Metabolic flux profiling of recombinant protein secreting *Pichia pastoris* growing on glucose:methanol mixtures. Microb Cell Fact 11:57.

Klein T, Heinzle E, Schneider K (2013) Metabolic fluxes in *Schizosaccharomyces pombe* grown on glucose and mixtures of glycerol and acetate. Appl Microbiol Biotechnol 97:5013–5026.

Klein T, Schneider K, Heinzle E (2012) A system of miniaturized stirred bioreactors for parallel continuous cultivation of yeast with online measurement of dissolved oxygen and off-gas. Biotechnol Bioeng 110:535–542.

Liu Z, Tyo KEJ, Martínez JL, Petranovic D, Nielsen J (2012) Different expression systems for production of recombinant proteins in *Saccharomyces cerevisiae*. Biotechnol Bioeng 109:1259–1268.

Losson R, Lacroute F (1983) Plasmids carrying the yeast OMP decarboxylase structural and regulatory genes: transcription regulation in a foreign environment. Cell 32:371–377.

Mattanovich D, Branduardi P, Dato L, Gasser B, Sauer M, Porro D (2012) Recombinant protein production in yeasts. Meth Mol Biol 824:329–358.

Naumann JM, Kuttner G, Bureik M (2010) Expression and secretion of a CB4-1 scFv-GFP fusion protein by fission yeast. Appl Biochem Biotechnol 163:80–89.

Porro D, Sauer M, Branduardi P, Mattanovich D (2005) Recombinant protein production in yeasts. Mol Biotechnol 31:245–259.

Tyo KEJ, Liu Z, Petranovic D, Nielsen J (2012) Imbalance of heterologous protein folding and disulfide bond formation rates yields runaway oxidative stress. BMC Biol 10:16.

Wong D, Batt S, Lee C, Robertson G (2002) Increased expression and secretion of recombinant alpha-amylase in *Saccharomyces cerevisiae* by using glycerol as the carbon source. J Protein Chem 21:419–425.

CHAPTER VI

Concluding Remarks and Outlook

1. Summary

This work focuses on the complex metabolism of the fission yeast *Schizosaccharomyces pombe* and addresses in particular the metabolic burden of homologous and heterologous protein secretion. ^{13}C-based metabolic flux analysis (MFA) was applied as central method for the quantitative description of *in vivo* carbon fluxes under the different cultivation conditions. Most experiments were performed in continuous culture, as it allows keeping the cells in a stable steady state over the whole cultivation time.

To perform a large number of experiments, a system of 10 mL scale bioreactors for parallel continuous cultivation was constructed in the first place. In **Chapter II**, construction and validation of this system is described. Online measurement of dissolved oxygen served as indicator for the metabolic steady state of the yeast culture and off gas analysis via mass spectrometry was implemented into the system for quantifying oxygen uptake rates and carbon balancing. Comparison of cultivation data generated with this bioreactor system to literature data was in good agreement, showing that this system is applicable for metabolic studies in continuous culture.

This bioreactor system was used in **Chapter III** to compare *in vivo* carbon flux distributions in *S. pombe* during respiratory growth on glucose with growth on mixtures of glycerol and acetate. Quantifying ^{13}C incorporation into lipogenic fatty acids allowed to distinguish the carbon flux distribution between pyruvate dehydrogenase (PDH) and the PDH bypass. While TCA cycle fluxes were similar on both substrates, a much higher flux through the pentose phosphate pathway (PPP) was observed on the glycerol/acetate mixture. This resulted in an increased CO_2 production rate compared to glucose cultivations and generated a surplus of cytosolic NADPH. CO_2 production and O_2 consumption rates derived from MFA were in good agreement with experimental data generated by gas balancing using mass spectrometry. This supports the supposed terminal regeneration of the cytosolic NADPH surplus via the respiratory chain. It was assumed that transhydrogenase-like cycles of glutamate dehydrogenases as described for *S. cerevisiae* might mediate the electron transfer from NADPH to NADH. Activity for glutamate dehydrogenase with both cofactors was demonstrated in cells grown on the substrate mixture, indicating that such electron transfer cycles can take place in *S. pombe*.

In **Chapter IV** the response of the central carbon metabolism of *S. pombe* to elevated levels of protein secretion was investigated. Strains SL4, NW8 and NW9 were constructed, expressing

the model protein maltase in varying amounts. In carbon-limited chemostat cultures using glucose as sole carbon source a selectivity of maltase secretion with respect to biomass of up to 27 mg per g cells was observed, corresponding to approximately 5.3% of the total cellular protein. A redirection of carbon fluxes towards the PPP occurred with increasing protein secretion while the flux through glycolysis and the TCA cycle fluxes decreased at the same time. Analysis of the macromolecular cell composition showed an increase in the lipid content and balancing of redox cofactors indicated a limitation of protein secretion due to a limited supply of mitochondrial NADPH. To overcome these bottlenecks, the cultivation media was optimized in a rational, directed way and the best producer NW9 was cultivated on mixtures of glucose/acetate and glycerol/acetate. Feeding of acetate improved lipid formation and this correlated with an increased maltase secretion. TCA cycle activity on the mixtures was higher compared to glucose as sole carbon source, providing additional mitochondrial NADPH and ATP, which was beneficial for protein secretion. Using the glycerol/acetate mixture as substrate, maltase secretion of NW9 was improved 1.8-fold up to 53.8 mg per g cells, corresponding to 10.4% of the total cellular protein.

In **Chapter V** the question was addressed, whether the strategies for improving protein secretion developed in the previous chapter were specific for maltase secretion or rather applicable in general. Two *S. pombe* strains expressing either GFP or a GFP-coupled single-chain antibody fragment were cultivated on glucose as sole carbon source and mixtures of glucose/acetate or glycerol/acetate. Using these substrate mixtures, an increased selectivity of secretion of both heterologous proteins was observed, especially using the glycerol/acetate mixture. The underlying mechanisms improving the heterologous protein secretion might partially differ from those observed for maltase secretion, since the amounts of secreted recombinant proteins (0.06% and 0.13% of the total cellular protein for GFP and CB4-1-scFv-GFP, respectively) and thus the metabolic loads were much lower than for maltase. Nonetheless, applying mixtures containing acetate increased protein secretion in *S. pombe* compared to glucose as sole carbon source in general and demonstrated that this is a feasible strategy to improve heterologous protein secretion in this yeast.

2. Engineering of *S. pombe* as versatile cell factory: current state and future prospects

The present work could demonstrate that *S. pombe* is a promising host for high-level protein secretion. Physiology and metabolic flexibility of the producer strain play an important role in this context and systematic metabolic studies on this yeast yielded information to derive metabolic engineering strategies for improving the secretion of homologous and heterologous proteins. Nonetheless, the *S. pombe* expression system must be further developed to compete with the leading yeast cell factories *Pichia pastoris* and *Saccharomyces cerevisiae*.

As model organism for cell biology, the toolbox for genetic engineering of *S. pombe* is well developed. Systems for gene deletion are available using Cre/lox mediated recycling of auxothrophic and resistance markers (Iwaki and Takegawa 2004; Sato et al. 2005; Watson et al. 2008). Plasmids for episomal expression of proteins as well as integration into the genome have been available for a long time, providing different auxothropic markers and promoters (Sabatinos and Forsburg 2010). Recent publications describe an update of these vector systems, presenting smaller vectors with higher copy numbers and increased mitotic stability as well as the application of dominant resistance markers for use in complex media (Ahn et al. 2013; Verma and Singh 2012). These developments aim towards the right direction but there is still a lot of work ahead on the level of molecular and metabolic engineering in order to to establish *S. pombe* as a compatible host system besides cell factories like *S. cerevisiae* and *P. pastoris* (Celik and Calik 2011).

2.1 Promoters for recombinant protein expression

For expression of recombinant proteins, several promoters have been evaluated in the past. There are constitutive variants like the *adh1* and the recombinant *CAMsv40* promoter (Forsburg 1993). With the *nmt1* promoter and its derivates *nmt41* and *nmt81* a set of controllable promoters with different strengths of expression for homologous and heterologous proteins is available (Basi et al. 1993; Maundrell 1993).

Since recombinant proteins can have toxic effects on the cell and strong overexpression of secreted proteins can lead to an overload of the secretory pathway, protein production processes with yeasts are often separated into an initial growth phase, where biomass is formed followed

by a production phase, where expression of heterologous proteins is induced. The most commonly applied promoters are *nmt1* and its derivates, which are repressed in the presence of thiamine and induced upon its removal. Thus, induction of gene expression is always coupled to a media change, which is impractical for large-scale processes. For *S. cerevisiae*, galactose-inducible promoters are commonly applied, using the switch from glucose to galactose as carbon source upon glucose depletion (Mendoza-Vega et al. 1994; Park et al. 1993). In *P. pastoris*, induction of heterologous protein secretion is in general achieved by methanol feeding (Hellwig et al. 2001; Zhang et al. 2003). However, methanol is volatile and flammable and thus connected to certain safety hazards in industrial processes. Lately, methanol-independent inducible promoters for *P. pastoris* have been described, showing repression in the presence of glycerol and induction in the carbon-limited production phase (Prielhofer et al. 2013). A related, carbon source inducible system has been recently described for *S. pombe*, using the promoter region of *gld1*, a glycerol-dehydrogenase, which is subject to glucose catabolite repression (Klein et al. 2013; Matsuzawa et al. 2012). Upon glucose depletion and addition of glycerol and C_2 bodies like acetate or ethanol, induction of gene expression takes place in less than an hour. Applying this system, secretion of GFP was 1.8-fold higher compared to the expression via the *nmt1* promoter under the same cultivation conditions (Matsuzawa et al. 2013). Also, the application of the *agl1* promoter might be a likely alternative to the existing expression systems. Expression of the maltase wild type locus is also subject to glucose catabolite repression (Jansen et al. 2006) which would allow its application as inducible promoter. An approach using the *agl1* promoter in carbon-limited fed-batch processes for production of maltase in g/L scale has already been described by Jansen et al. (2006). Nonetheless, very few information is available on *gld1* and *agl1* promoter regions yet. A thorough characterization of both promoter loci as well as comparison of their promoter strengths with the nmt* promoter family is obligatory prior to their possible application as expression systems.

2.2 Influence of leader peptides on heterologous protein secretion

The choice of the leader peptide can heavily influence the secretion rate of the protein of interest. The α-factor leader peptide *of S. cerevisiae* is up to now the most commonly applied secretory leader in both *S. cerevisiae* and *P. pastoris* (Hou et al. 2012). However, using this leader peptide in *S. pombe* for GFP secretion resulted in intracellular accumulation rather than secretion of the recombinant protein (Kjaerulff and Jensen 2005). Moreover, it is not possible to

predict which leader is best suited for efficient secretion of a given protein (Hou et al. 2012). There are a number of leader peptides described in literature for efficient secretion of recombinant proteins, with the *Cpy1* leader peptide and the P3-factor as most commonly applied examples (Giga-Hama and Kumagai 1998; Kjaerulff and Jensen 2005). Moreover, Eiden-Plach et al. (2004) could demonstrate the application of the viral K28-leader peptide for secretion of GFP in various yeasts, including *S. pombe*. Regarding the present work, the *agl1* leader peptide could also confer high-level secretion of maltase up to 50 mg per g cells. Thus, it is a promising leader signal for *S. pombe* and its application for secretion of recombinant proteins should be investigated in the future.

.

2.3 Metabolic engineering targets for heterologous protein secretion

Engineering of genetic elements and the secretory transport machinery are often studied targets in order to improve recombinant protein production in yeasts. The connection between recombinant protein secretion and central metabolic pathway activities is less straightforward and evaluation and rational engineering of metabolic targets can prove more difficult than molecular engineering of the secretory pathway. Thus studies focusing on the metabolic burden of recombinant protein secretion only slowly emerged over the last decade. Moreover, most of the studies so far are descriptive, demonstrating metabolic changes in response to secretion of heterologous proteins and defining metabolic targets but lacking application of the generated data yet (Baumann et al. 2010; Celik et al. 2009; Jordà et al. 2012).

In mammalian cell culture, metabolic engineering approaches are much more popular, with the aim of improving cell viability and selectivity of product formation. Genetic manipulation of the producer cell line is one approach but creating stable mammalian cells lines is difficult and time-consuming (Kim et al. 2012). Instead, rational approaches targeting media composition are often applied and the development of new screening techniques enabled high-throughput testing of a variety of parameters in a short time (Wurm 2004). Variation of substrate concentrations is a common strategy with the aim of redirecting central carbon fluxes towards elevated product formation, as shown by Niklas et al. (2012b) for the human producer cell line AGE1.HN. Another approach is the addition of media components which indirectly cause metabolic flux redistributions by acting upon molecular targets. For instance, addition of the inhibitor quercetin improved culture longevity and α_1-antitrypsin production in AGE1.HN, improving mitochondrial pyruvate import and decreasing waste product formation by reducing the glucose uptake rate (Niklas et al. 2012a).

Regarding yeast biotechnology, systematic approaches were so far restricted to evolutionary engineering and subsequent metabolic analysis of the adapted producer strains (Kazemi Seresht et al. 2013) and the recently reported optimization of *S. cerevisiae* α-amylase production under anaerobic growth conditions by supplementing the media with fumarate as final electron acceptor (Liu et al. 2013). However, more and more publications are emerging in this field, describing interactions between metabolism and heterologous protein secretion. In this context, the first genome-scale model of the protein secretory pathway of *S. cerevisiae* has just been published (Feizi et al. 2013). In the present work, a systematic analysis of macromolecular cell composition and *in vivo* metabolic flux distributions of maltase-secreting strains of *S. pombe* pointed out energy metabolism and lipid biosynthesis as limiting factors of high-level protein secretion. In the AGE1.HN cell line, an increase of the lipid content was also observable with increased productivity (Niklas et al. 2013). Thus, the observed limitations are at least partially species-spanning which may enable the development of generic approaches for both analysis and overcoming of common metabolic bottlenecks. In case of *S. pombe*, overcoming these limitations was achieved by rational media design, feeding acetate to fuel the TCA cycle and providing precursors for an improved lipid biosynthesis. Most important, acetate feeding could improve protein secretion in *S. pombe* in general, as demonstrated by the elevated heterologous secretion of GFP and CB4-1scFv-GFP. Thus, a transfer of this acetate feeding strategy, at least to other yeasts and fungi appears reasonable and could be easily tested.

On the basis of these systematic studies in **Chapter IV** a variety of further strategies for improving the production of recombinant proteins in *S. pombe* can be derived. Some selected examples will be discussed in the following sections with emphasis on genetic modifications in the central carbon metabolism.

2.3.1 Engineering of mitochondrial NADPH supply

Energy metabolism, especially mitochondrial NADPH supply, was identified as one of the bottlenecks in maltase secretion. In *S. pombe*, isocitrate dehydrogenase is the sole source of mitochondrial NADPH (Klein et al. 2013), while e.g. in *S. cerevisiae*, the mitochondrial malic enzyme can provide additional NADPH (Boles et al. 1998). Relocating the malic enzyme from the mitochondria to the cytosol in *S. cerevisiae* resulted in major flux redistributions as well as changes in the $NADP^+/NADPH$ ratio, indicating the strong influence of this enzyme on redox homeostasis and NADPH supply (Moreira dos Santos et al. 2004). Consequently, expression of *S. cerevisiae MAE1* gene with its mitochondrial leader sequence in *S. pombe* might provide a

second mitochondrial source of NADPH and thus represent a strategy to overcome the limitation in mitochondrial NADPH supply. Additional deletion of the mitochondrial malate transporter *mae1* and the cytosolic malic enzyme *mae2* (Boles et al. 1998; Grobler et al. 1995) should result in mitochondrial accumulation of malate and enhance the flux through the mitochondrial, NADP$^+$ dependent malic enzyme from *S. cerevisiae* providing additional mitochondrial NADPH (Figure VI-1A).
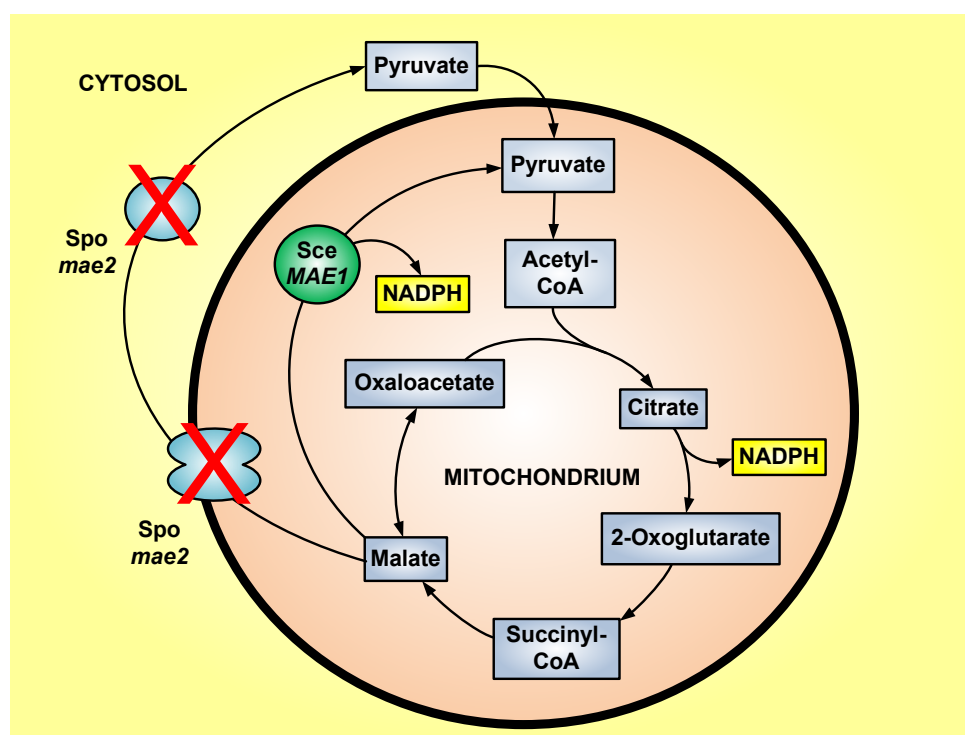
Figure VI-1A: Improving supply of mitochondrial NADPH by expression of *S. cerevisiae* NADP$^+$ dependent malic enzyme (*Sce MAE1*) with mitochondrial localization in *S. pombe*. Further deletion of *S. pombe* malate transporter (*Spo mae1*) and cytosolic malic enzyme (*Spo mae2*) should lead to mitochondrial accumulation of malate and enhance the flux through the recombinant mitochondrial malic enzyme.

2.3.2 Improving cytosolic acetyl-CoA supply

Since mitochondrial NADPH production and lipid biosynthesis are both dependent on efficient precursor supply, provision of cytosolic acetyl-CoA is a promising target for metabolic engineering of *S. pombe* towards improved secretion of proteins. Chen et al. (2013) reported engineering of *S. cerevisiae* cytosolic acetyl-CoA metabolism to improve its supply for biofuel

and steroid production in this yeast. They used a push-pull-block strategy, first channeling carbon from ethanol towards acetyl-CoA. This was achieved by overexperession of *ADH2* and *ALD6* encoding an alcohol dehydrogenase and an aldehyde dehydrogenase, respectively, followed by a feed-back resistant acetyl-CoA synthetase variant for cytosolic acetyl-CoA formation. To ensure pulling cytosolic acetyl-CoA towards steroid biosynthesis, *ERG10*, encoding acetyl-CoA acetyltransferase was overexpressed, forming acetoacetyl-CoA. Additionally, both enzymes of the glyoxylate cycle were deleted to block acetyl-CoA conversion via this pathway.

Transferring this approach to *S. pombe* would likely be possible, providing more acetyl-CoA as precursor for lipid biosynthesis and for fueling the TCA cycle activity, with the additional benefit that no functional glyoxylate cycle is present in *S. pombe*. Acetyl-CoA synthetase emerged as limiting factor in acetate assimilation during the cultivation of *S. pombe* wild type and maltase-producing strain NW9 on acetate-containing substrate mixtures. Thus, overexpression of the enzyme might be especially important in combination with the above described genetic modifications to achieve a redistribution of the carbon flux towards cytosolic acetyl-CoA. The first and rate-limiting step of lipid biosynthesis in yeast is the reaction catalyzed by the acetyl-CoA carboxylase. The expression of this gene is tightly regulated in *S. cerevisiae* at the transcriptional level (Hasslacher et al. 1993). Further studies will be necessary to investigate the regulation of the *S. pombe* enzyme (*cut6*) and to design a deregulated enzyme variant to channel the carbon flux towards lipid biosynthesis. Finally, this pathway engineering approach might achieve results comparable to feeding of acetate with respect to lipid formation and probably also TCA cycle activities. At the same time, engineering of *S. pombe* in this manner would increase the metabolic flexibility of the organism, allowing improved protein secretion without addition of acetate and under fermentative growth conditions (Figure VI-1B).

2.3.3 Construction of a respiratory *S. pombe* strain

Finally, protein production is directly related to biomass formation and most fed-batch processes with Crabtree-positive yeasts are performed under carbon-limited conditions, inducing respiratory growth without byproduct formation and a high biomass yield. Alternatively, Ferndahl et al. (2010) could show improved GFP secretion using *S. cerevisiae* strain TM6*, which exhibited respiratory growth also under glucose-excess conditions. The application of such a strain would facilitate process design considerably. *S. cerevisiae* TM6*

was generated by exchanging wild type sugar transporters against a mutant variant, conferring reduced glucose uptake, which resulted in a complete respiratory metabolism of the strain (Otterstedt et al. 2004). Since sugar transport of *S. pombe* is thoroughly investigated and strains impaired in glucose uptake are available (Heiland et al. 2000; Peinado et al. 2005), construction of a respiratory *S. pombe* strain could likely be performed with minor effort. To elucidate if the metabolic activity and secretory efficiency of the resulting strain is comparable to strains with normal sugar uptake, the studies concerning maltase overexpression described in this work could be repeated with a respiratory *S. pombe* strain.
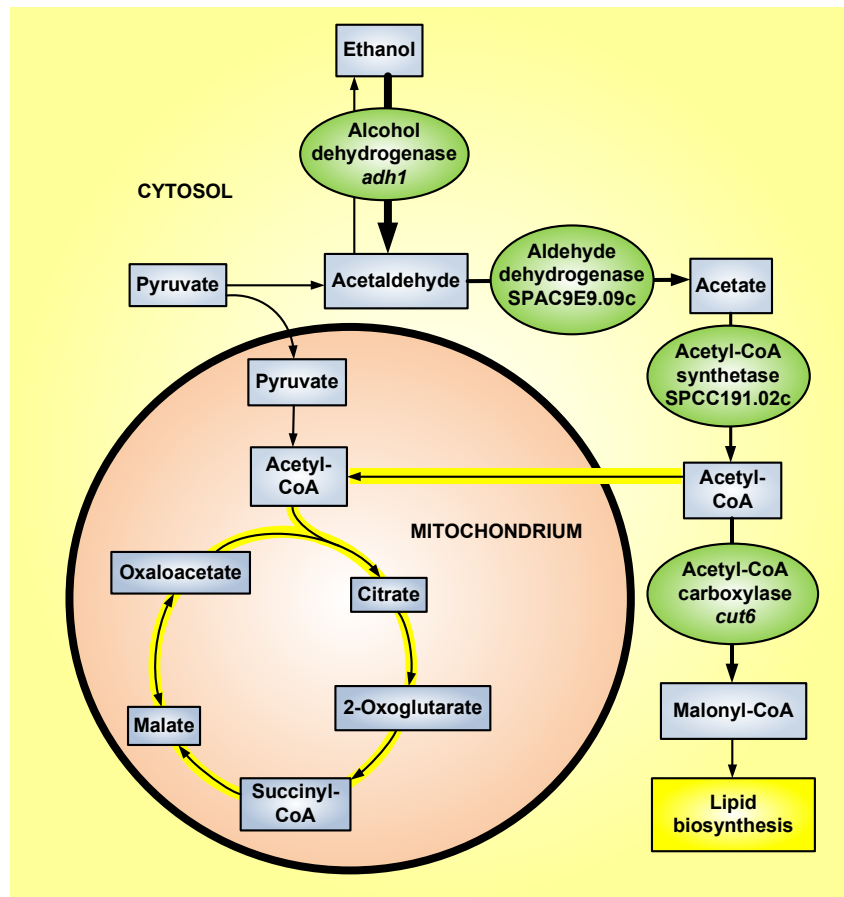
Figure VI-1B: Engineering of cytosolic acetyl-CoA supply for improved lipid biosynthesis and TCA cycle activity in *S. pombe*: Overexpression of alcohol-dehydrogenase *adh1* and aldehyde dehydrogenase SPAC9E9.09c will channel the carbon flux from cytosolic pyruvate towards cytosolic acetate. Overexpression of acetyl-CoA synthetase SPCC191.02c will provide a large cytosolic acetyl-CoA pool. Feedback inhibition can be avoided by a constant depletion of this pool by transport of acetyl-CoA into the mitochondria or conversion to malonyl-CoA via a deregulated, overexpressed variant of acetyl-CoA carboxylase *cut6*.

2.4 Process design and carbon source utilization

Production processes using the yeasts *P. pastoris* and *S. cerevisiae* are the topic of various research articles, describing fed-batch processes on different substrates with different strategies for feeding and process control (Cereghino et al. 2002; Mendoza-Vega et al. 1994). Moreover, systematic studies with the yeast *P. pastoris* investigated the influence of temperature, osmotic stress as well as anaerobic growth conditions (Baumann et al. 2010; Dragosits et al. 2009; Shi et al. 2003).

Comparable studies for high-density fermentations of *S. pombe* have not been performed yet. Thus, developing reasonable fed-batch processes for heterologous protein production in *S. pombe* is required, investigating feeding strategies and carbon sources. So far, a single publication describes a carbon-limited fed-batch strategy with glucose as substrate for the g/L scale production of maltase (Jansen et al. 2006). Following this strategy, vector systems using the *agl1* promoter sequence and maltase secretory leader peptide might be employed for the high-level production of recombinant proteins, as discussed above. Evaluation of different feeding strategies and carbon sources requires a great experimental effort. To save time and costs, systems with small working volumes enabling parallel cultivations are preferable. Bioreactor systems, either commercially available ones or the system described in **Chapter II** can be extremely useful for such studies.

Few data is available concerning utilization of different carbon sources of *S. pombe* regarding recombinant protein production. Recent publications deal with the regulation of growth on glycerol (Matsuzawa et al. 2012; Matsuzawa et al. 2010) on the protein level and the construction of an expression vector induced upon growth on glycerol and ethanol has been reported (Matsuzawa et al. 2013). However, few is known from a physiological point of view. In the present work, quantitative analysis of the carbon fluxes upon growth on mixtures of glycerol and acetate were performed. Growth on this mixture is completely respiratory, which is a good basis for fed-batch cultivations, since high biomass yields can be achieved without the accumulation of useless or even toxic byproducts. Moreover, using this mixture for homologous and heterologous protein could increase selectivity of protein secretion with respect to biomass compared to glucose cultivations. These results indicate a high potential for heterologous protein production processes using *S. pombe* and further work will be necessary to develop feasible fed-batch strategies using glucose or alternative substrates like glycerol.

3. Final thoughts

While our understanding of the whole process of protein secretion in yeast increases, it becomes more and more obvious how complex and prone to intra- and extracellular disturbances this system is. More and more systematic studies emerge that try to take various aspects into consideration at the same time to draw a greater picture. Understanding of the complex interactions and synergistic effects for the benefit of improved production is a must for developing successful processes. This is especially true for the development and establishment of an uncommon yeast cell factory like *S. pombe*.

As already indicated in this work, there is a huge potential for improving heterologous protein secretion in *S. pombe* by studying the response of the central carbon metabolism to elevated levels of protein secretion. Mathematical tools can be used for the quantitative description of metabolic flux distributions (Yang et al. 2008) and the first genome-scale network of *S. pombe* as well as a genome-scale secretory network of *S. cerevisiae* are now publicly available (Feizi et al. 2013; Sohn et al. 2012). This facilitates metabolic studies and enables the application of prediction tools, e.g. elementary modes, for identification of targets for metabolic and molecular engineering. For an efficient improvement of heterologous protein secretion with *S. pombe* a combination of all three approaches will be necessary: (I) identification and engineering of metabolic targets, (II) molecular engineering of expression systems (vectors, promoters, secretory leader peptides) and of the secretory pathway and (III) adaptation of the respective production processes to host requirements and reverse. With constant feedback between these three areas it will be possible to develop a versatile and competitive cell factory as well as practicable production processes. Such an attempt will be time and cost intensive but it will be necessary in the long run to serve the purpose of establishing *S. pombe* besides the existing cell factories *S. cerevisiae* and *P. pastoris*.

4. References

Ahn J, Won M, Kyun M-L, Kim YS, Jung C-R, Im D-S, Song K-B, Chung K-S (2013) Development of episomal vectors carrying a nourseothricin-resistance marker for use in minimal media for *Schizosaccharomyces pombe*. Yeast 30:219–227.

Basi G, Schmid E, Maundrell K (1993) TATA box mutations in the *Schizosaccharomyces pombe nmt1* promoter affect transcription efficiency but not the transcription start point or thiamine repressibility. Gene 123:131–136.

Baumann K, Carnicer M, Dragosits M, Graf AB, Stadlmann J, Jouhten P, Maaheimo H, Gasser B, Albiol J, Mattanovich D, Ferrer P (2010) A multi-level study of recombinant *Pichia pastoris* in different oxygen conditions. BMC Syst Biol 4:141.

Boles E, de Jong-Gubbels P, Pronk JT (1998) Identification and characterization of *MAE1*, the *Saccharomyces cerevisiae* structural gene encoding mitochondrial malic enzyme. J Bacteriol 180:2875–2882.

Celik E, Calik P (2011) Production of recombinant proteins by yeast cells. Biotechnol Adv 30:1108–1118.

Celik E, Calik P, Oliver SG (2009) Metabolic flux analysis for recombinant protein production by *Pichia pastoris* using dual carbon sources: Effects of methanol feeding rate. Biotechnol Bioeng 105:317–329.

Cereghino GPL, Cereghino JL, Ilgen C, Cregg JM (2002) Production of recombinant proteins in fermenter cultures of the yeast *Pichia pastoris*. Curr Opin Biotechnol 13:329–332.

Chen Y, Daviet L, Schalk M, Siewers V, Nielsen J (2013) Establishing a platform cell factory through engineering of yeast acetyl-CoA metabolism. Metab Eng 15:48–54.

Dragosits M, Stadlmann J, Albiol J, Baumann K, Maurer M, Gasser B, Sauer M, Altmann F, Ferrer P, Mattanovich D (2009) The effect of temperature on the proteome of recombinant *Pichia pastoris*. J Proteome Res 8:1380–1392.

Eiden-Plach A, Zagorc T, Heintel T, Carius Y, Breinig F, Schmitt MJ (2004) Viral Preprotoxin Signal Sequence Allows Efficient Secretion of Green Fluorescent Protein by *Candida glabrata*, *Pichia pastoris*, *Saccharomyces cerevisiae*, and *Schizosaccharomyces pombe*. Appl Environ Microbiol 70:961–966.

Feizi A, Osterlund T, Petranovic D, Bordel S, Nielsen J (2013) Genome-scale modeling of the protein secretory machinery in yeast. PloS one 8:e63284.

Ferndahl C, Bonander N, Logez C, Wagner R, Gustafsson L, Larsson C, Hedfalk K, Darby RAJ, Bill RM (2010) Increasing cell biomass in *Saccharomyces cerevisiae* increases recombinant protein yield: the use of a respiratory strain as a microbial cell factory. Microb Cell Fact 9:47.

Forsburg SL (1993) Comparison of *Schizosaccharomyces pombe* expression systems. Nucleic Acids Res 21:2955–2956.

Giga-Hama Y, Kumagai H (1998) Foreign gene expression in fission yeast *S. pombe*. Seikagaku 70:300–304.

Grobler J, Bauer F, Subden RE, Van Vuuren HJ (1995) The *mae1* gene of *Schizosaccharomyces pombe* encodes a permease for malate and other C4 dicarboxylic acids. Yeast 11:1485–1491.

Hasslacher M, Ivessa AS, Paltauf F, Kohlwein SD (1993) Acetyl-CoA carboxylase from yeast is an essential enzyme and is regulated by factors that control phospholipid metabolism. J Biol Chem 268:10946–10952.

Heiland S, Radovanovic N, Hofer M, Winderickx J, Lichtenberg H (2000) Multiple hexose transporters of *Schizosaccharomyces pombe*. J Bacteriol 182:2153–2162.

Hellwig S, Emde F, Raven NP, Henke M, van Der Logt P, Fischer R (2001) Analysis of single-chain antibody production in *Pichia pastoris* using on-line methanol control in fed-batch and mixed-feed fermentations. Biotechnol Bioeng 74:344–352.

Hou J, Tyo KEJ, Liu Z, Petranovic D, Nielsen J (2012) Metabolic engineering of recombinant protein secretion by *Saccharomyces cerevisiae*. FEMS Yeast Res 12:491–510.

Iwaki T, Takegawa K (2004) A set of loxP marker cassettes for Cre-mediated multiple gene disruption in *Schizosaccharomyces pombe*. Biosci Biotechnol Biochem 68:545–550.

Jansen ML, Krook DJ, De Graaf K, van Dijken JP, Pronk JT, de Winde JH (2006) Physiological characterization and fed-batch production of an extracellular maltase of *Schizosaccharomyces pombe* CBS 356. FEMS Yeast Res 6:888–901.

Jordà J, Jouhten P, Cámara E, Maaheimo H, Albiol J, Ferrer P (2012) Metabolic flux profiling of recombinant protein secreting *Pichia pastoris* growing on glucose:methanol mixtures. Microb Cell Fact 11:57.

Kazemi Seresht A, Cruz AL, de Hulster E, Hebly M, Palmqvist EA, van Gulik W, Daran J-M, Pronk J, Olsson L (2013) Long-term adaptation of *Saccharomyces cerevisiae* to the burden of recombinant insulin production. Biotechnol Bioeng *in press*.

Kim JY, Kim Y-G, Lee GM (2012) CHO cells in biotechnology for production of recombinant proteins: current state and further potential. Appl Microbiol Biotechnol 93:917–930.

Kjaerulff S, Jensen MR (2005) Comparison of different signal peptides for secretion of heterologous proteins in fission yeast. Biochem Biophys Res Commun 336:974–982.

Klein T, Heinzle E, Schneider K (2013) Metabolic fluxes in *Schizosaccharomyces pombe* grown on glucose and mixtures of glycerol and acetate. Appl Microbiol Biotechnol 97:5013–5026.

Liu Z, Osterlund T, Hou J, Petranovic D, Nielsen J (2013) Anaerobic α-amylase production and secretion with fumarate as the final electron acceptor in yeast. Appl Environ Microbiol 79:2962–2967.

Matsuzawa T, Hara F, Tohda H, Uemura H, Takegawa K (2012) Promotion of glycerol utilization using ethanol and 1-propanol in *Schizosaccharomyces pombe*. Appl Microbiol Biotechnol 95:441–449.

Matsuzawa T, Ohashi T, Hosomi A, Tanaka N, Tohda H, Takegawa K (2010) The *gld1+* gene encoding glycerol dehydrogenase is required for glycerol metabolism in *Schizosaccharomyces pombe*. Appl Microbiol Biotechnol 87:715–727.

Matsuzawa T, Tohda H, Takegawa K (2013) Ethanol-inducible gene expression using *gld1 (+)* promoter in the fission yeast *Schizosaccharomyces pombe*. Appl Microbiol Biotechnol 97:6835-6843

Maundrell K (1993) Thiamine-repressible expression vectors pREP and pRIP for fission yeast. Gene 123:127–130.

Mendoza-Vega O, Sabatié J, Brown SW (1994) Industrial production of heterologous proteins by fed-batch cultures of the yeast *Saccharomyces cerevisiae*. FEMS Microbiol Lett 15:369–410.

Moreira dos Santos M, Raghevendran V, Kotter P, Olsson L, Nielsen J (2004) Manipulation of malic enzyme in *Saccharomyces cerevisiae* for increasing NADPH production capacity aerobically in different cellular compartments. Metab Eng 6:352–363.

Niklas J, Nonnenmacher Y, Rose T, Sandig V, Heinzle E (2012a) Quercetin treatment changes fluxes in the primary metabolism and increases culture longevity and recombinant α_1-antitrypsin production in human AGE1.HN cells. Appl Microbiol Biotechnol 94:57–67.

Niklas J, Priesnitz C, Rose T, Sandig V, Heinzle E (2012b) Primary metabolism in the new human cell line AGE1.HN at various substrate levels: increased metabolic efficiency and α1-antitrypsin production at reduced pyruvate load. Appl Microbiol Biotechnol 93:1637–1650.

Niklas J, Priesnitz C, Rose T, Sandig V, Heinzle E (2013) Metabolism and metabolic burden by α1-antitrypsin production in human AGE1.HN cells. Metab Eng 16C:103–114.

Otterstedt K, Larsson C, Bill RM, Ståhlberg A, Boles E, Hohmann S, Gustafsson L (2004) Switching the mode of metabolism in the yeast *Saccharomyces cerevisiae*. EMBO Rep 5:532–537.

Park YS, Shiba S, Lijima S, Kobayashi T, Hishinuma F (1993) Comparison of three different promoter systems for secretory alpha-amylase production in fed-batch cultures of recombinant *Saccharomyces cerevisiae*. Biotechnol Bioeng 41:854–861.

Peinado RA, Moreno JJ, Medina M, Mauricio JC (2005) Potential application of a glucose-transport-deficient mutant of *Schizosaccharomyces pombe* for removing gluconic acid from grape must. J Agric Food Chem 53:1017–1021.

Prielhofer R, Maurer M, Klein J, Wenger J, Kiziak C, Gasser B, Mattanovich D (2013) Induction without methanol: novel regulated promoters enable high-level expression in *Pichia pastoris*. Microb Cell Fact 12:5.

Sabatinos SA, Forsburg SL (2010) Molecular genetics of *Schizosaccharomyces pombe*. Meth Enzymol 470:759–795.

Sato M, Dhut S, Toda T (2005) New drug-resistant cassettes for gene disruption and epitope tagging in *Schizosaccharomyces pombe*. Yeast 22:583–591.

Shi X, Karkut T, Chamankhah M, Alting-Mees M, Hemmingsen SM, Hegedus D (2003) Optimal conditions for the expression of a single-chain antibody (scFv) gene in Pichia pastoris. Protein Expr Puri 28:321–330.

Sohn SB, Kim TY, Lee JH, Lee SY (2012) Genome-scale metabolic model of the fission yeast *Schizosaccharomyces pombe* and the reconciliation of in silico/in vivo mutant growth. BMC Syst Biol 6:49.

Verma HK, Singh J (2012) New multi-purpose high copy number vector with greater mitotic stability for diverse applications in fission yeast *Schizosaccharomyces pombe*. Plasmid 68:186–194.

Watson AT, Garcia V, Bone N, Carr AM, Armstrong J (2008) Gene tagging and gene replacement using recombinase-mediated cassette exchange in *Schizosaccharomyces pombe*. Gene 407:63–74.

Wurm FM (2004) Production of recombinant protein therapeutics in cultivated mammalian cells. Nat Biotechnol 22:1393–1398.

Yang TH, Frick O, Heinzle E (2008) Hybrid optimization for 13C metabolic flux analysis using systems parametrized by compactification. BMC Syst Biol 2:29.

Zhang W, Hywood Potter KJ, Plantz BA, Schlegel VL, Smith LA, Meagher MM (2003) *Pichia pastoris* fermentation with mixed-feeds of glycerol and methanol: growth kinetics and production improvement. J Ind Microbiol Biot 30:210–215.

SUPPLEMENTARY

1. Mass isotopomer distributions used for ^{13}C-based metabolic flux analysis in Chapter III

Table III-S1: Mass isotopomer distributions of amino acids from cell hydrolysates of *S. pombe* cultivated on :[1-^{13}C] glucose under respirative growth conditions (D = 0.1 h^{-1}) in chemostat; [1,3-^{13}C] glycerol and [1,2-^{13}C] acetate in a mixture of glycerol and acetate. Shown are experimentally determined labeling patterns (exp.) and simulated patterns from metabolic flux analysis (sim.). For metabolic flux analysis on glycerol/acetate, flux simulations were performed with labeling of either glycerol or acetate and a simulation combining both labeling patterns.

| | | glucose | | glycerol | | acetate | | glycerol and acetate | | | |
| | | | | | | | | glycerol | | acetate | |
		sim.	exp..	sim.	exp.	sim.	exp.	sim.	exp.	sim.	exp.
alanine	m+0	0.684	0.683	0.038	0.038	0.945	0.94	0.041	0.038	0.944	0.94
(m/z 260)	m+1	0.299	0.307	0.028	0.028	0.038	0.038	0.032	0.028	0.038	0.038
	m+2	0.016	0.01	0.924	0.924	0.011	0.01	0.917	0.924	0.011	0.01
	m+3	0	0	0.011	0.01	0.007	0.013	0.01	0.01	0.007	0.013
glycine	m+0	0.952	0.952	0.052	0.051	0.962	0.962	0.054	0.051	0.96	0.962
(m/z 246)	m+1	0.047	0.048	0.936	0.936	0.026	0.03	0.935	0.936	0.027	0.03
	m+2	0.001	0	0.012	0.012	0.012	0.008	0.011	0.012	0.014	0.008
valine	m+0	0.487	0.487	0.016	0.017	0.903	0.911	0.028	0.017	0.902	0.911
(m/z 288)	m+1	0.405	0.406	0.024	0.024	0.069	0.065	0.015	0.024	0.069	0.065
	m+2	0.101	0.101	0.05	0.05	0.02	0.017	0.054	0.05	0.021	0.017

Table III-S1 continued

	m+3	0.007	0.006	0.883	0.886	0.007	0.006	0.882	0.886	0.008	0.006
	m+4	0	0	0.022	0.022	0	0	0.021	0.022	0	0
	m+5	0	0	0.005	0.002	0	0	0	0.002	0	0
isoleucine	m+0	0.41	0.414	0.019	0.02	0.619	0.619	0.028	0.02	0.618	0.619
(m/z 200)	m+1	0.42	0.413	0.067	0.067	0.306	0.301	0.055	0.067	0.305	0.301
	m+2	0.149	0.149	0.516	0.517	0.054	0.054	0.517	0.517	0.054	0.054
	m+3	0.02	0.022	0.378	0.382	0.02	0.024	0.388	0.382	0.021	0.024
	m+4	0.001	0.002	0.013	0.013	0.001	0.001	0.01	0.013	0.001	0.001
	m+5	0	0.001	0.007	0.002	0	0.001	0	0.002	0	0.001
serine	m+0	0.705	0.708	0.022	0.022	0.95	0.951	0.029	0.022	0.949	0.951
(m/z 390)	m+1	0.282	0.285	0.071	0.071	0.043	0.043	0.067	0.071	0.044	0.043
	m+2	0.013	0.007	0.898	0.898	0.007	0.006	0.893	0.898	0.007	0.006
	m+3	0	0	0.009	0.008	0	0	0.01	0.008	0	0
phenylalanine	m+0	0.374	0.374	0.015	0.015	0.908	0.899	0.026	0.015	0.908	0.899
(m/z 336)	m+1	0.424	0.41	0.003	0.003	0.088	0.092	0.003	0.003	0.088	0.092
	m+2	0.171	0.174	0.001	0.002	0.004	0.007	0	0.002	0.004	0.007
	m+3	0.029	0.032	0.01	0.01	0	0	0	0.01	0	0
	m+4	0.002	0.002	0.03	0.03	0	0	0.012	0.03	0	0
	m+5	0	0.001	0.227	0.227	0	0.001	0.258	0.227	0	0.001
	m+6	0	0.002	0.681	0.685	0	0	0.678	0.685	0	0
	m+7	0	0.003	0.025	0.025	0	0	0.022	0.025	0	0
	m+8	0	0.001	0.001	0.001	0	0	0	0.001	0	0
	m+9	0	0.001	0.006	0.001	0	0	0	0.001	0	0

Table III-S1 continued

aspartate	m+0	0.546	0.551	0.051	0.052	0.632	0.633	0.055	0.052	0.632	0.633
(m/z 418)	m+1	0.377	0.374	0.055	0.055	0.289	0.289	0.055	0.055	0.288	0.289
	m+2	0.073	0.071	0.498	0.498	0.038	0.037	0.499	0.498	0.038	0.037
	m+3	0.004	0.004	0.387	0.389	0.027	0.026	0.387	0.389	0.027	0.026
	m+4	0	0	0.009	0.005	0.014	0.016	0.004	0.005	0.014	0.016
glutamate	m+0	0.405	0.403	0.269	0.28	0.102	0.096	0.264	0.28	0.092	0.096
(m/z 432)	m+1	0.42	0.408	0.397	0.397	0.092	0.096	0.409	0.397	0.08	0.096
	m+2	0.152	0.16	0.243	0.251	0.248	0.249	0.26	0.251	0.247	0.249
	m+3	0.022	0.028	0.063	0.066	0.239	0.229	0.063	0.066	0.239	0.229
	m+4	0.001	0.002	0.005	0.005	0.195	0.19	0.004	0.005	0.206	0.19
	m+5	0	0	0.023	0.001	0.124	0.139	0	0.001	0.137	0.139
threonine	m+0	0.553	0.55	0.052	0.053	0.637	0.634	0.052	0.053	0.638	0.634
(m/z 404)	m+1	0.373	0.373	0.053	0.053	0.288	0.288	0.054	0.053	0.287	0.288
	m+2	0.071	0.073	0.503	0.503	0.039	0.036	0.507	0.503	0.038	0.036
	m+3	0.004	0.004	0.385	0.388	0.024	0.026	0.383	0.388	0.025	0.026
	m+4	0	0	0.007	0.004	0.012	0.016	0.004	0.004	0.013	0.016
leucine	m+0	0.378	0.383	0.018	0.019	0.317	0.315	0.028	0.019	0.283	0.315
(m/z 200)	m+1	0.427	0.417	0.046	0.046	0.62	0.612	0.037	0.046	0.649	0.612
	m+2	0.168	0.171	0.673	0.677	0.05	0.05	0.656	0.677	0.053	0.05
	m+3	0.026	0.027	0.241	0.249	0.013	0.015	0.273	0.249	0.014	0.015
	m+4	0.001	0.001	0.008	0.008	0	0.004	0.007	0.008	0.001	0.004

2. Supplementary Information for Chapter IV

Table IV-S1: Stoichiometric network used for metabolic flux analysis. cyt: cytosolic. mit: mitochondrial.ext: external. P: phosphate residue.MTF: unbalanced pool of methyltetrahydrofolate. Arrows indicate direction of reaction and reversible reactions. vb = precursor demand for biomass formation. vm = precursor demand for maltase formation with respect to the amino acid composition of the protein.

Name	Reaction Stoichiometry		
	Educts		**Products**
v1	glucose-6-P	←→	fructose-6-P
v2	fructose-6-P	←→	glyceraldehyde-3-P + dihydroxyacetone-P
v3	glyceraldehyde-3-P	←→	dihydroxyacetone-P
v4	glyceraldehyde-3-P	→	3-Phosphoglycerate
v5	3-phosphoglycerate	→	Phosphoenolpyruvate
v6	phosphoenolpyruvate	→	cyt. pyruvate
v7	cyt. pyruvate	→	mit. pyruvate
v8	cyt. oxaloacetate	←→	mit. oxaloacetate
v9	cyt. acetyl-CoA	→	mit. acetyl-CoA
v10	mit. pyruvate	→	mit. acetyl-CoA + CO_2
v11	mit. malate	→	cyt. malate
v12	cyt. malate	→	cyt. pyruvate + CO_2
v13	cyt. pyruvate	→	cyt. oxaloacetate
v14	glucose-6-P	→	pentose-P + CO_2
v15	2 pentose-P	←→	sedoheptulose-5-P + glyceraldehyde-3-P
v16	sedoheptulose-5-P +	←→	fructose-6-P + erythrose-4-P
v17	pentose-P + erythrose-4-P	←→	fructose-6-phosphate + glyceraldehyde-3-P
v18	mit. oxaloacetate + mit. acetyl-CoA	→	mit. isocitrate
v19	isocitrate	→	2-oxoglutarate + CO_2
v20	2-oxoglutarate	→	succinate + CO_2
v21	succinate	→	fumarate
v22	fumarate	→	mit. malate
v23	mit. malate	→	mit. oxaloacetate
v24	cyt. pyruvate	→	acetaldehyde
v25	acetaldehyde	→	acetate
v26	acetate	→	cyt. acetyl-CoA

Table IV-S1 continued

v27	3-Phosphoglycerate	→	serine
v28	serine	←→	glycine + MTF
v29	cyt. oxaloacetate	→	cyt. aspartate
v30	mit. oxaloacetate	→	mit. aspartate
v31	cyt. asparate	→	threonine
v32	threonine	←→	glycine + acetaldehyde
v33	mit. pyruvate	→	oxoisovalerate
v34	phosphoenolpyruvate + erythrose-4-P	→	shikimate-5-P
v35	cyt. pyruvate	→	alanine
v36	mit. pyruvate	→	alanine
v37	2-oxisovalerate	→	valine
v38	phosphoenolpyruvate + shikimate-5-P	→	phenylalanine + CO_2
v39	2-oxoglutarate	→	glutamate
v40	threonine + mit. pyruvate	→	isoleucine + CO_2
v41	cyt. asparate + MTF	→	methionine
v42	2-oxoisovalerate + mit. acetyl-CoA	→	mit.2- oxoisocaproate + CO_2
v43	mit.2- oxoisocaproate	→	leucine
v44	pentose-P + CO_2	→	histidine
v45	glutamate + CO_2	→	arginine
v46	pentose-5-P + PEP + erythrose-4-P	→	tryptophane
v47	mit. 2-oxoglutarate + mit. acetyl-CoA	→	mit. oxaloglutarate
v48	mit. oxaloglutarate	→	mit. 2-oxoadipate + CO_2
v49	mit. 2-oxoadipate	→	lysine
v50	mit. aspartate	→	aspartate
v51	cyt. aspartate	→	aspartate
vext1	cyt. pyruvate	→	ext. pyruvate
vext2	mit. succinate	→	ext. succinate
vext3	cyt. acetate	→	ext. acetate
vinp	ext. glucose	→	glucose-6-P
vinp	ext. glycerol	→	dihydroxyacetone-P
vinp	ext. acetate	→	cyt. acetate
vb1	glucose-6-P	→	biomass
vb2	pentose-P	→	biomass
vb3	erythrose-4-P	→	biomass
vb4	glyceraldehyde-3-P	→	biomass
vb5	3-phosphoglycerate	→	biomass
vb6	phosphoenolpyruvate	→	biomass

Table IV-S1 continued

vb7	cyt. acetyl-CoA	→	biomass
vb8	mit. 2-oxoglutarate	→	biomass
vb9	alanine	→	biomass
vb10	glutamate	→	biomass
vb11	asparate	→	biomass
vb12	serine	→	biomass
vb13	glycine	→	biomass
vb14	threonine	→	biomass
vb15	phenylalanine	→	biomass
vb16	valine	→	biomass
vb17	isoleucine	→	biomass
vb18	methionine	→	biomass
vb19	leucine	→	biomass
vb20	lysine	→	biomass
vb21	histidine	→	biomass
vb22	arginine	→	biomass
vb23	tryptophane	→	biomass
vm1	glycine	→	maltase
vm2	aspartate	→	maltase
vm3	threonine	→	maltase
vm4	alanine	→	maltase
vm5	valine	→	maltase
vm6	phenylalanine	→	maltase
vm7	glutamate	→	maltase
vm8	isoleucine	→	maltase
vm9	methionine	→	maltase
vm10	leucine	→	maltase
vm11	lysine	→	maltase
vm12	serine	→	maltase
vm13	histidine	→	maltase
vm14	arginine	→	maltase
vm15	trytophane	→	maltase

Table IV-S2: Anabolic demands taken from Gombert et al. and adapted for the measured cellular compositions of *S. pombe* strains SL4, NW8 and NW9 grown on glucose as sole carbon source and on mixtures of glucose and acetate (GlcAc) or glycerol and acetate [GlyAc]. Values are given in [mmol g CDW^{-1}]. P = phosphate residue. cyt: = cytosolic. mit. = mitochondrial.

metabolite	SL4	NW8	NW9	NW9 GlcAc	NW9 GlyAc
glucose-6-P	1.73	1.73	1.73	1.50	1.40
pentose-5-P	0.26	0.26	0.27	0.27	0.27
erythrose-4-P	0.22	0.22	0.23	0.18	0.18
glyceraldehyde-3-P	0.06	0.06	0.07	0.08	0.11
3-phosphoglycerate	0.56	0.56	0.56	0.56	0.56
phosphoenolpyruvate	0.30	0.30	0.30	0.30	0.30
cyt. acetyl-CoA	1.36	1.50	1.65	2.08	2.72
mit. oxoglutarate	0.29	0.29	0.29	0.29	0.29
alanine	0.31	0.33	0.33	0.38	0.35
glutamate	0.61	0.63	0.65	0.63	0.65
aspartate	0.34	0.38	0.40	0.42	0.43
serine	0.22	0.24	0.28	0.31	0.29
glycine	0.22	0.27	0.27	0.31	0.27
threonine	0.20	0.20	0.22	0.22	0.21
phenylalanine	0.23	0.26	0.26	0.25	0.26
valine	0.16	0.18	0.23	0.21	0.23
isoleucine	0.16	0.17	0.16	0.18	0.16
methionine	0.05	0.05	0.06	0.06	0.06
leucine	0.27	0.27	0.29	0.32	0.29
lysine	0.21	0.20	0.22	0.24	0.24

Table IV-S3: Comparison of simulated (sim.) and experimentally determined (exp.) mass isotopomer distributions of amino acids and stearic acid used for ^{13}C-based metabolic flux analysis. *S. pombe* strains SL4, NW8 and NW9 were grown [1-^{13}C] glucose as sole carbon source in chemostat cultivations at D = 0.1 h^{-1}. Strain NW9 was also grown on mixtures of [1-^{13}C] glucose and [1,2-^{13}C] acetate (NW9-GlcAc) in a single labeling experiment in chemostat (D = 0.1 h^{-1}) and mixtures of glycerol/acetate in two independent experiments in shake flask using either [1,3-^{13}C] glycerol and unlabeled acetate (NW9-[13]GlyAc) or unlabeled glycerol and [1,2-^{13}C] acetate (NW9-Gly[13]Ac).

		SL4		NW8		NW9		NW9-GlcAc		NW9-[13]GlyAc		NW9-Gly[13]Ac	
		sim	exp	sim	exp	sim	exp	sim	exp	sim	exp	sim	exp
Ala	m+0	0.665	0.665	0.673	0.673	0.667	0.666	0.672	0.668	0.042	0.038	0.942	0.935
(m/z 260)	m+1	0.320	0.323	0.310	0.315	0.316	0.323	0.301	0.304	0.038	0.030	0.039	0.047
	m+2	0.014	0.011	0.017	0.012	0.017	0.010	0.022	0.020	0.907	0.913	0.012	0.012
	m+3	0.000	0.000	0.000	0.000	0.000	0.000	0.005	0.009	0.013	0.020	0.008	0.006
Gly	m+0	0.943	0.944	0.941	0.942	0.944	0.946	0.934	0.932	0.058	0.055	0.956	0.955
(m/z 246)	m+1	0.055	0.055	0.057	0.056	0.055	0.054	0.054	0.056	0.923	0.923	0.028	0.037
	m+2	0.002	0.001	0.002	0.002	0.001	0.000	0.012	0.011	0.019	0.022	0.016	0.008
valine	m+0	0.461	0.466	0.474	0.478	0.466	0.471	0.471	0.469	0.028	0.015	0.897	0.902
(m/z 288)	m+1	0.419	0.416	0.409	0.409	0.416	0.418	0.401	0.398	0.016	0.026	0.071	0.071
	m+2	0.114	0.111	0.110	0.107	0.111	0.107	0.113	0.115	0.061	0.055	0.023	0.020
	m+3	0.006	0.006	0.007	0.006	0.007	0.004	0.013	0.015	0.867	0.869	0.008	0.007
	m+4	0.000	0.000	0.000	0.000	0.000	0.000	0.002	0.002	0.028	0.032	0.000	0.000
	m+5	0.000	0.000	0.000	0.000	0.000	0.000	0.000	0.000	0.000	0.003	0.000	0.000
Ile	m+0	0.401	0.406	0.408	0.411	0.403	0.401	0.303	0.297	0.029	0.018	0.601	0.603
(m/z 274)	m+1	0.422	0.418	0.415	0.413	0.422	0.423	0.398	0.402	0.060	0.072	0.313	0.312

Table IV-S3 continued

	m+2	0.156	0.153	0.155	0.153	0.154	0.154	0.223	0.222	0.508	0.504	0.060	0.056
	m+3	0.020	0.021	0.021	0.022	0.020	0.021	0.066	0.068	0.389	0.385	0.024	0.027
	m+4	0.001	0.001	0.001	0.001	0.001	0.001	0.010	0.010	0.014	0.018	0.001	0.001
	m+5	0.000	0.000	0.000	0.000	0.000	0.000	0.000	0.002	0.000	0.003	0.000	0.000
Ser	m+0	0.682	0.686	0.689	0.692	0.686	0.688	0.700	0.704	0.030	0.022	0.947	0.949
(m/z 390)	m+1	0.301	0.305	0.293	0.297	0.299	0.302	0.278	0.282	0.073	0.073	0.044	0.045
	m+2	0.017	0.010	0.017	0.010	0.015	0.009	0.020	0.014	0.882	0.883	0.008	0.006
	m+3	0.001	0.000	0.001	0.000	0.000	0.000	0.002	0.001	0.015	0.022	0.000	0.000
Phe	m+0	0.347	0.349	0.364	0.362	0.353	0.350	0.382	0.384	0.026	0.013	0.908	0.897
(m/z 336)	m+1	0.413	0.415	0.409	0.411	0.423	0.420	0.409	0.410	0.003	0.001	0.088	0.092
	m+2	0.194	0.191	0.185	0.183	0.187	0.185	0.172	0.171	0.000	0.001	0.004	0.006
	m+3	0.041	0.038	0.038	0.035	0.034	0.035	0.034	0.031	0.001	0.008	0.000	0.000
	m+4	0.004	0.003	0.004	0.003	0.002	0.003	0.003	0.002	0.015	0.031	0.000	0.000
	m+5	0.000	0.002	0.000	0.002	0.000	0.003	0.000	0.001	0.259	0.226	0.000	0.001
	m+6	0.000	0.001	0.000	0.001	0.000	0.001	0.000	0.000	0.666	0.687	0.000	0.001
	m+7	0.000	0.001	0.000	0.001	0.000	0.002	0.000	0.000	0.030	0.030	0.000	0.001
	m+8	0.000	0.000	0.000	0.001	0.000	0.001	0.000	0.000	0.000	0.003	0.000	0.001
	m+9	0.000	0.000	0.000	0.000	0.000	0.000	0.000	0.000	0.000	0.000	0.000	0.001
Asp	m+0	0.548	0.552	0.538	0.543	0.541	0.545	0.403	0.404	0.058	0.052	0.613	0.615
(m/z 418)	m+1	0.376	0.375	0.377	0.376	0.381	0.383	0.392	0.391	0.063	0.067	0.297	0.298
	m+2	0.072	0.067	0.080	0.074	0.075	0.069	0.142	0.136	0.488	0.490	0.043	0.040
	m+3	0.004	0.005	0.005	0.006	0.004	0.003	0.045	0.044	0.385	0.380	0.031	0.029

Table IV-S3 continued

	m+4	0.000	0.001	0.000	0.001	0.000	0.000	0.017	0.025	0.006	0.011	0.016	0.018
Glu	m+0	0.341	0.336	0.377	0.368	0.395	0.407	0.097	0.092	0.248	0.241	0.098	0.091
(m/z 432)	m+1	0.416	0.417	0.413	0.416	0.422	0.411	0.138	0.139	0.404	0.388	0.086	0.097
	m+2	0.200	0.199	0.177	0.178	0.159	0.155	0.249	0.250	0.272	0.277	0.253	0.243
	m+3	0.041	0.043	0.031	0.033	0.023	0.026	0.258	0.254	0.071	0.086	0.240	0.233
	m+4	0.003	0.004	0.002	0.003	0.001	0.002	0.180	0.175	0.005	0.008	0.199	0.193
	m+5	0.000	0.001	0.000	0.001	0.000	0.000	0.078	0.091	0.000	0.000	0.124	0.143
Thr	m+0	0.555	0.551	0.549	0.544	0.547	0.544	0.408	0.405	0.056	0.053	0.621	0.617
(m/z 404)	m+1	0.374	0.378	0.372	0.377	0.378	0.384	0.391	0.391	0.062	0.063	0.294	0.298
	m+2	0.068	0.068	0.074	0.074	0.072	0.069	0.140	0.136	0.496	0.491	0.042	0.039
	m+3	0.004	0.004	0.004	0.005	0.003	0.003	0.044	0.045	0.380	0.385	0.029	0.029
	m+4	0.000	0.000	0.000	0.000	0.000	0.000	0.017	0.023	0.006	0.008	0.015	0.017
Leu	m+0	0.341	0.347	0.361	0.368	0.357	0.365	0.196	0.191	0.028	0.016	0.301	0.311
(m/z 274)	m+1	0.426	0.426	0.420	0.419	0.428	0.430	0.436	0.447	0.039	0.051	0.630	0.623
	m+2	0.199	0.193	0.187	0.182	0.184	0.177	0.295	0.286	0.632	0.644	0.054	0.052
	m+3	0.034	0.033	0.031	0.030	0.030	0.027	0.069	0.071	0.291	0.277	0.014	0.015
	m+4	0.001	0.001	0.001	0.001	0.001	0.001	0.004	0.005	0.010	0.012	0.001	0.000
	m+5	0.000	0.000	0.000	0.000	0.000	0.000	0.000	0.000	0.000	0.001	0.000	0.000
Stearic acid	m+0	-	-	-	-	-	-	0.040	0.055	0.301	0.354	0.031	0.055
(m/z 143)	m+1	-	-	-	-	-	-	0.030	0.049	0.397	0.392	0.015	0.011
	m+2	-	-	-	-	-	-	0.074	0.093	0.227	0.185	0.039	0.044

Table IV-S3 continued

m+3	-	-	-	-	-	-	0.152	0.131	0.064	0.040	0.106	0.100
m+4	-	-	-	-	-	-	0.190	0.180	0.009	0.007	0.122	0.103
m+5	-	-	-	-	-	-	0.250	0.207	0.001	0.003	0.292	0.306
m+6	-	-	-	-	-	-	0.144	0.153	0.000	0.008	0.128	0.129
m+7	-	-	-	-	-	-	0.119	0.132	0.000	0.010	0.268	0.252

3. Vector maps

3.1 Vectors pREPura and pREPura-agl1 described in Chapter IV
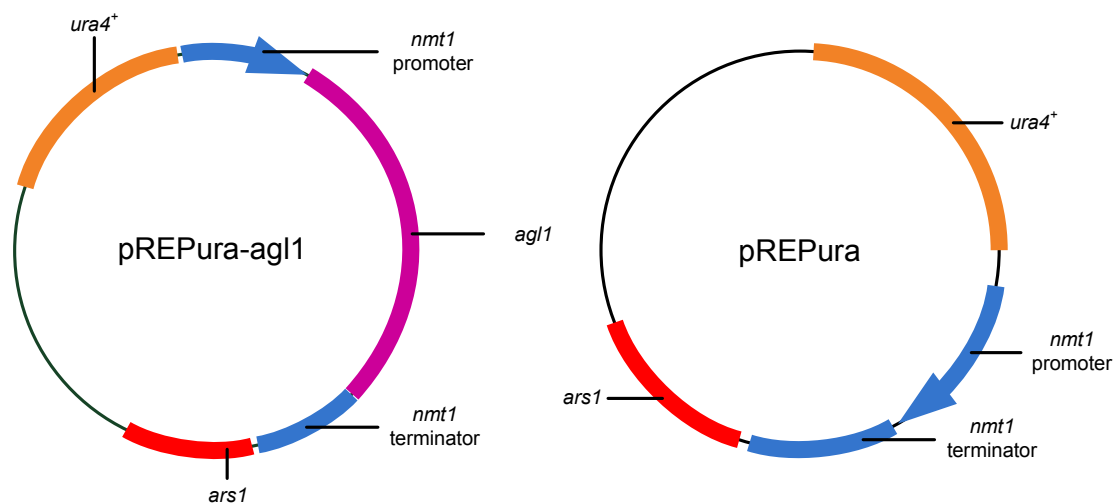
3.2 Vectors pJMN6 and pTZsp-GFP described in Chapter V
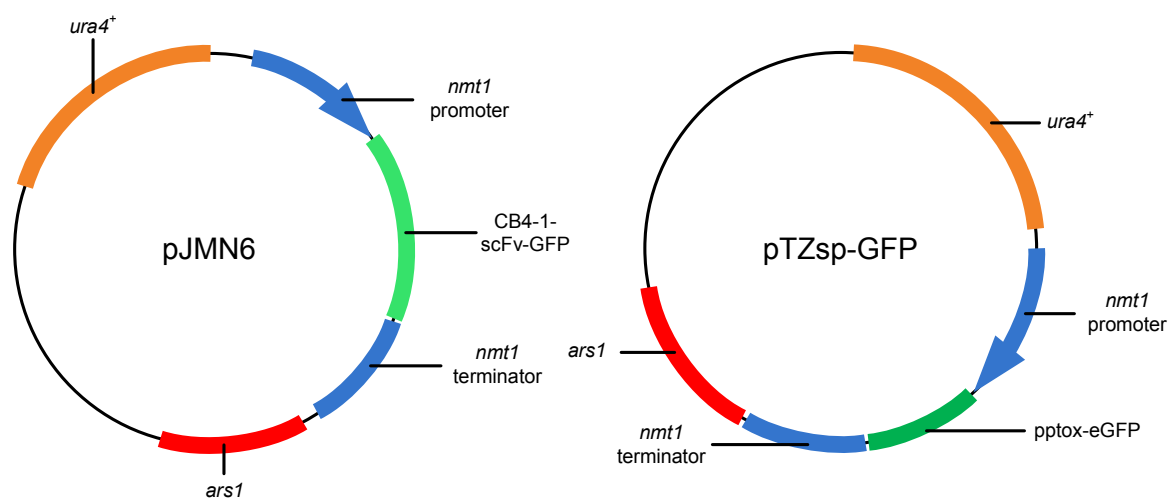
4. Acknowledgements

Lebenslauf

Tobias Klein

Diplom-Biologe, geboren am 23.09.1984 in Ottweiler

Akademische Ausbildung

von 2009 bis 2013 **wissenschaftlicher Mitarbeiter** an der Universität des Saarlandes am Lehrstuhl für Technische Biochemie im Rahmen der Dissertation

Promotion **11/2009 bis 08/2013**	Institut für Technische Biochemie, Universität des Saarlandes *Titel*: **Metabolic studies on *Schizosaccharomyces pombe* for improved protein secretion**
Diplomarbeit **01/2009 bis 09/2009**	Institut für Angewandte Mikrobiologie, Universität des Saarlandes *Titel*: **Molekularbiologische Optimierung einer Sorbitol-Dehydrogenase aus *Rhodobacter sphaeroides* Si4 zum Einsatz in elektroenzymatischen Reaktionen**
Studium **10/2004 bis 09/2009**	Diplomstudium der Human – und Molekularbiologie an der Universität des Saarlandes
Schulische Ausbildung	1995 bis 2004 Illtalgymnsium Illingen mit Abschluss Abitur 1990 bis 1995 Grundschule Illingen

Weitere Qualifikationen

Weiterbildungen	2010: Teilnahme am einwöchigen Workshop **„Biosystems Engineering- Bioreactors and Cell Factories"** in Braunwald, Schweiz
	2013: Workshop **"Qualtiätsmanagment im Unternehmen"** im Rahmen des Graduiertenkollegs der Universität des Saarlandes

Publikationsliste

Klein T, Schneider K, Heinzle E. **(2012)**. A system of miniaturized stirred bioreactors for parallel continuous cultivation of yeast with online measurement of dissolved oxygen and off-gas. **Biotechnology and Bioengineering** 110:535–42.

Klein T, Heinzle E, Schneider K. **(2013)**. Metabolic fluxes in *Schizosaccharomyces pombe* grown on glucose and mixtures of glycerol and acetate. **Applied Microbiology and Biotechnology** 97: 5013-26

Urbanova V, Kohring GW, **Klein T**, Wang Z, Mert O, Emrullahoglu M , Buran K, Demir AS, Etienne M, Walcarius A **(2013)**. Sol-gel Approaches for Elaboration of Polyol Dehydrogenase-Based Bioelectrodes. **Zeitschrift für Physikalische Chemie** 227: 667-89

Konferenzbeiträge

Klein T, Schneider K, Heinzle E. New insights into acetate and glycerol metabolism of *Schizosaccharomyces pombe*. **Jahrestagung der VAAM 2012**

Klein T, Schneider K, Heinzle E. A miniaturized parallel bioreactor system for continuous cultivation studies on yeast. **Jahrestagung der VAAM 2012**

Klein T, Schneider K, Heinzle E. *In vivo* carbon fluxes in *Schizosaccharomyces pombe*: Applying ^{13}C metabolic flux analysis in parallel small-scale continuous cultivations. **Metabolic Engineering IX 2012**

Klein T, Hung CW, Lange S, Bureik M, Tholey A, Heinzle E, Schneider K. Proteome analysis in *Schizosaccharomyces pombe*: amino acid biosynthesis and membrane composition as targets for improved protein secretion. **RPP7 conference 2013**

Klein T, Lange S, Bureik M, Heinzle E, Schneider K. *In vivo* metabolic flux redistributions in the central carbon metabolism of the yeast *Schizosaccharomyces pombe* in response to increased protein secretion. **RPP7 conference 2013**

Klein T, Hung CW, Lange S, Bureik M, Tholey A, Heinzle E, Schneider K. Proteome analysis in *Schizosaccharomyces pombe*: amino acid biosynthesis and membrane composition as targets for improved protein secretion. **Jahrestagung der VAAM 2013**

Eingereichte Manuskripte und geplante Veröffentlichungen

Klein T, Lange S, Wilhelm N, Yang TH, Bureik M, Heinzle E, Schneider K **(2013)**. Overcoming the metabolic burden of protein secretion in *Schizosaccharomyces pombe*- A quantitiative approach using ^{13}C based metabolic flux analysis**. eingereicht bei Metabolic Engineering**

Hung CW, **Klein T**, Lange S, Bureik M, Tholey A, Heinzle E, Schneider K. Proteome analysis in *Schizosaccharomyces pombe*: amino acid biosynthesis and membrane composition as targets for improved protein secretion. **in Vorbereitung**

Klein T, Heinzle E, Schneider K (**2013**): Growth on acetate-containing substrate mixtures increases secretion of heterologous proteins in the fission yeast *Schizosaccharomyces pombe***. in Vorbereitung**